Nagra
Nationale
Genossenschaft
für die Lagerung
radioaktiver Abfälle

Cédra
Société coopérative
nationale
pour l'entreposage
de déchets radioactifs

Cisra
Società cooperativa
nazionale
per l'immagazzinamento
di scorie radioattive

TECHNICAL REPORT 87-17

INTERPRETATION OF HYDRAULIC TESTING IN THE SEDIMENTS OF THE RINIKEN BOREHOLE

D.W. Belanger
T.L. Cauffman
J.L. Lolcama
D.E. Longsine
J.F. Pickens

INTERA Technologies, Inc., 6850 Austin

JANUARY 1989

Parkstrasse 23 5401 Baden / Schweiz Telephon 056 / 20 55 11

Nagra
Nationale
Genossenschaft
für die Lagerung
radioaktiver Abfälle

Cédra
Société coopérative
nationale
pour l'entreposage
de déchets radioactifs

Cisra
Società cooperativa
nazionale
per l'immagazzinamento
di scorie radioattive

TECHNICAL REPORT 87-17

INTERPRETATION OF HYDRAULIC TESTING IN THE SEDIMENTS OF THE RINIKEN BOREHOLE

D.W. Belanger
T.L. Cauffman
J.L. Lolcama
D.E. Longsine
J.F. Pickens

JANUARY 1989

INTERA Technologies, Inc., 6850 Austin

Parkstrasse 23 5401 Baden / Schweiz Telephon 056 / 20 55 11

Der vorliegende Bericht wurde im Auftrag der Nagra erstellt. Die Autoren haben ihre eigenen Ansichten und Schlussfolgerungen dargestellt. Diese müssen nicht unbedingt mit denjenigen der Nagra übereinstimmen.

Le présent rapport a été préparé sur demande de la Cédra.
Les opinions et conclusions présentées sont celles des auteurs et ne correspondent pas nécessairement à celles de la Cédra.

This report was prepared as an account of work sponsored by Nagra. The viewpoints presented and conclusions reached are those of the author(s) and do not necessarily represent those of Nagra.

ZUSAMMENFASSUNG

Die Resultate des in der Bohrung Riniken ausgeführten hydraulischen Versuchsprogramms werden in Form einer Zusammenfassung der Auswertungen der hydraulischen Durchlässigkeit, des Formationswasserdruckes und der äquivalenten Süsswasser-Druckspiegelhöhe präsentiert. In 22 Abschnitten in Perm-, Trias- und Jurasedimenten wurden hydraulische Versuche ausgeführt. Die Bohrung wurde bis 1800.5 m abgeteuft (Tiefenangaben als scheinbare Tiefe, d.h. als Bohrtiefe), die Versuche wurden mit einer Einfachpacker- oder einer Doppelpackeranordnung oder bei offenem Bohrloch ausgeführt. Die angewandten Versuchstechniken und die Auswertungsmethode, vervollständigt durch eine Darstellung des Vorgehens zur Abschätzung der mit der Versuchsanordnung zusammenhängenden Unsicherheiten in der Bestimmung der äquivalenten Süsswasser-Druckspiegelhöhe werden dargestellt.

Die Tests wurden als eine Kombination eines oder mehrerer der folgenden Versuchstypen ausgeführt: Slug-Injection- oder Slug-Withdrawal-Tests, Pulse-Injection- oder Pulse-Withdrawal-Tests, Pumpversuche. Zur Ermittlung der hydraulischen Durchlässigkeitsbeiwerte der untersuchten Formationen wurden analytische Lösungsansätze und graphische Techniken (Horner) angewandt. In jenen Fällen, in denen durch Störungen der Druckverhältnisse in der Bohrlochumgebung (Bohrloch-Druckgeschichte) und/oder thermische Effekte die Testresultate signifikant beeinflusst wurden, kam das Graph Theoretic Field Model (GFTM) von INTERA zur Simulierung der Druckverhältnisse zur Anwendung.

Der Ruhewasserdruck in den gestesteten Formationen wurde für 6 Testintervalls mittels einer Simulation des gemessenen Wiederanstieges des Druckes oder mit den Analysenmethoden von Horner für den Drill-Stem-Test ermittelt. Zwei weitere Formationswasserdrücke wurden aus der sich nach der Durchführung der hydraulischen Versuche im offenen Bohrloch einstellenden statischen Wasserspiegelhöhe bestimmt. Die äquivalenten Süsswasser-Druckspiegelhöhen, die aus dem im Zentrum des Versuchsabschnit-

tes oder in der Gesteinsformation herrschenden Formationswassserdruck berechnet wurden, befinden sich zwischen 460.4 m ü.M im Schilfsandstein (Bohrtiefe 515 m) und 360.6 m ü.M. im Perm (Bohrtiefe 1200 m). Die Ackersohle der Bohrung Riniken liegt bei 385.07 m ü.M.

In den acht Versuchen, in denen die Bestimmung der Druckspiegelhöhe möglich war, wurde zusätzlich die auf Messfehler an den verschiedenen Messgeräten zurückzuführende Unsicherheit in der Bestimmung der Druckspiegelhöhe analysiert. Bei zwei Versuchen rührt diese Unsicherheit hauptsächlich aus den Ungewissheiten über die Dichte der Bohrflüssigkeit her. In den anderen sechs Versuchen hängt sie hauptsächlich mit den Annahmen über die Messgenauigkeit des Drucknehmers zusammen. Wird die Unsicherheit als Bereich definiert, der zwischen der negativen und positiven doppelten Standardabweichung liegt, so beträgt im Bohrloch Riniken die mittlere Unsicherheit in der Bestimmung der Druckspiegelhöhe 3.1 m. Es ist zu betonen, dass die angeführte Unsicherheit lediglich die Messungenauigkeiten berücksichtigt und dass andere Quellen für Ungenauigkeiten wie z.B. die Abschätzung des repräsentativen Formationswasserdruckes aus den vorhandenden Daten, nicht miteinbezogen wurden.

Hydraulische Durchlässigkeitsbeiwerte konnten für 19 der 22 Versuchsabschnitte, die etwa 40 % der Bohrlochlänge der Bohrung Riniken abdecken, abgeschätzt werden. Die ermittelten hydraulischen Durchlässigkeitsbeiwerte liegen in einem Bereich von 2.0E-14 bis 1.5E-06 m/s. Durchlässigkeitsbeiwerte grösser als 1.0E-09 m/s wurden in fünf Zonen bestimmt (500.3-530.5 m, 617.3-696.0 m, 793.0-820.2 m, 958.4-972.5 und 977.0-1009.95 m). Die ersten drei Abschnitte liegen im Schilfsandstein, im Oberen Muschelkalk und im Buntsandstein, die restlichen zwei Zonen im Oberen Perm.

Der Variationsbereich des für die Auswertungen verwendeten spezifischen Speicherkoeffizienten liegt zwischen 9.4E-06 und 3.2E-07 m^{-1}. Niedrige Werte für den spezifischen Speicherkoeffizienten wurden gewählt für Versuche in den Karbonatgesteinen und im Anhydrit, die höheren Werte wurden im Sandstein und im Rotliegenden angewandt.

Die mit dem HTT (Hydrologic Test Tool) gemessenen Bohrlochtemperaturen liegen zwischen ungefähr 22°C in 217 m und 63°C in etwa 1513 m Tiefe. Die Temperatur am Bohrlochende konnte im Bottom Hole Test nicht bestimmt werden, da bei diesem Versuch der Temperaturfühler in einer Tiefe von 1500.5 m lag, also 300 m höher als das Bohrlochende. Der Gradient der Temperaturzunahme mit der Tiefe beträgt ungefähr 3.9°C/100 m und ist aus den während den hydraulischen Versuchen durchgeführten Temperaturmessungen und den Resultaten des Loggings der Bohrlochflüssigkeit mit einer HRT-Sonde (High Resolution Temperature) bestimmt worden.

RESUME

Les résultats du programme de tests hydrauliques réalisés dans le forage de Riniken (conductivité hydraulique, pression de formation, potentiel hydraulique calculé pour une colonne d'eau douce) sont présentés sous une forme résumée. On a conduit des tests hydrauliques dans 22 intervalles différents, situés dans les sédiments jurassiques, triassiques et permiens traversés par le forage. Ce dernier a atteint une profondeur apparente de 1800.5 m, et une profondeur vraie de 1800.2 m. Les intervalles testés ont été isolés soit par un obturateur unique plaçé au sommet de l'intervalle, soit par un double obturateur, soit encore par le casing au sommet de l'intervalle, le forage étant ouvert.

Le présent rapport donne une description succinte des techniques de test, et traite de manière plus approfondie la manière de les interpréter. Il décrit aussi l'approche utilisée pour estimer l'incertitude liée aux équipements sur les valeurs de potentiel hydraulique.

Les tests ont été conduits soit selon un mode de slug-test (injection ou soutirage d'eau à débit variable à partir d'une impulsion unique), soit selon un mode de pulse-test (rééquilibrage de pression dans la formation isolée par les obturateurs, à partir d'une impulsion unique), soit selon un mode de drill-stem-test (slug-test suivi de pulse-test sans impulsion additionnelle), soit encore par pompage continu.

La conductivité hydraulique des formations testées a été estimée par des solutions analytiques et des techniques graphiques (Horner). Lorsque les résultats se sont avérés soumis de manière significative à l'influence de pressions perturbatrices ou d'effets thermiques autour du forage, on a utilisé le code GTFM de INTERA (Graph Theoretic Field Model) pour simuler l'évolution des pressions mesurées.

Pour 6 intervalles de test, on a pu estimer la pression naturelle du fluide dans les formations, en simulant la séquence observée de rééquilibrage à la pression statique, ou, sur des tests de type drill-stem-test, en utilisant la méthode d'extrapolation de Horner. De plus, deux autres pressions de formation ont pu être déterminées à partir du niveau du fluide dans le forage en fin de test. Le potentiel, calculé pour une colonne d'eau douce à partir des pressions de formation au centre des intervalles de test, se situe entre 460.4 m.s.m à 515 m sous la surface du sol dans le Schilfsandstein, et 360.6 m.s.m à 1100 m sous la surface du sol dans le Permien. Au forage de Riniken, le sol se trouve à 385.07 m.s.m.

Pour les huit tests qui ont fourni des valeurs de potentiel, l'incertitude liée aux dispositifs de mesure a été soumise à un calcul d'erreur. Cette erreur ne prend pas en compte l'incertitude liée à l'estimation des pressions naturelles des formations à partir des pressions observées. Pour les deux tests où le potentiel a été déterminé à partir des niveaux du fluide dans le forage, l'incertitude calculée est en premier lieu due à une méconnaissance partielle de la densité du fluide dans la colonne de forage. Pour les six autres tests, l'incertitude calculée est due avant tout aux limites de précision des récepteurs de pression. Si l'on définit l'incertitude par un écart de ± 2 déviations standard, l'incertitude moyenne au forage de Riniken est de ± 3.1 m. Rappelons qu'il s'agit ici de l'incertitude liée aux dispositifs de mesure.

On a pu estimer la conductivité hydraulique pour 19 des 22 intervalles testés, soit pour 40% de la longueur totale du forage. Les valeurs se situent entre 2.0E-14 ms^{-1} et 1.5E-06 ms^{-1}. Cinq zones sont caractérisées par une conductivité hydraulique supérieure à 1.0E-09 ms^{-1}; elles se situent entre les profondeurs apparentes de 500.30 - 530.50 m, 617.30 - 696.00 m, 793.00 - 820.20 m, 958.40 - 972.50 m, et 977.00 - 1009.95 m. Les trois premières zones sont situées respectivement

dans le Schilfsandstein, le Muschelkalk supérieur et le Buntsandstein. Les deux dernières sont situées dans le Permien supérieur.

Les valeurs d'emmagasinement spécifique utilisées lors du calibrage se situent, pour les sédiments, entre 9.4E-06 m^{-1} et 3.2E-07 m^{-1}. On a attribué aux roches carbonatées et à l'anhydrite les valeurs inférieures, et aux grès du Rotliegendes les valeurs supérieures.

Les températures mesurées dans le forage à l'aide du dispositif de test se situent entre 22°C environ à 217 m, et 63°C à environ 1513 m de profondeur apparente. Les tests hydrauliques n'ont pas fourni de mesure de température au fond du forage. D'après les températures mesurées pendant les tests et la diagraphie thermique de haute résolution (HRT) exécutée séparément, l'accroissement de température avec la profondeur est d'environ 3.9°C / 100 m.

SUMMARY

The results of the hydraulic testing program in the Riniken borehole are presented as a summary of interpreted hydraulic conductivity, formation pressure, and equivalent freshwater head. Hydraulic tests were completed in 22 separate intervals in the Permian, Triassic and Jurassic sediments intersected by the borehole. Riniken was drilled to 1800.5 m apparent depth and tests were conducted in either single packer configuration, double packer configuration, or open borehole. A discussion of the testing techniques used in the borehole and the test interpretation approach is also presented along with estimates of equipment-related uncertainty on equivalent freshwater head values.

Testing was completed using either slug injection or withdrawal, pulse injection or withdrawal, drill-stem, or continuous pumping methods. Analytical solution and graphical (Horner) techniques were utilized for determining hydraulic conductivities of the tested formations. Where the test results were influenced significantly by a pressure disturbance around the borehole and/or thermal effects in the test interval, the INTERA Graph Theoretic Field Model (GTFM) was used to simulate the measured pressure responses.

Undisturbed fluid pressures in the tested formations were estimated for 6 test intervals by simulating the measured recovery to a static pressure or through the Horner method of drill-stem test analysis. Two additional formation pressures were determined from static water levels after testing in the open borehole. The equivalent freshwater heads, determined from formation pressure at the test interval or formation center, ranged from 460.4 m ASL at 515 m below ground surface in the Schilfsandstein to 360.6 m ASL at 1100 m below ground surface in the Permian. Ground surface datum at Riniken is 385.07 m.

The eight tests which provided freshwater heads were analyzed for uncertainty in head due to measurement errors of the various monitoring devices used. For two tests, the uncertainty of equivalent freshwater head for the water level tests is primarily caused by an uncertainty in fluid density. The head uncertainty for the other six tests is predominantly due to the accuracy specifications assumed for the pressure transducer P2. If the uncertainty range is defined by ±2 standard deviations, the average uncertainty at the Riniken borehole is 3.1 m. It should be emphasized that this uncertainty is based only on measurement error and that other sources of uncertainty such as estimation of representative formation pressures from data interpretation are not treated.

Hydraulic conductivities were estimated for 19 of the 22 intervals tested, covering about 40 percent of the Riniken borehole length. Interpreted hydraulic conductivities ranged from 2.0E-14 ms^{-1} to 1.5E-06 ms^{-1}. Hydraulic conductivities greater than 1.0E-09 ms^{-1} were obtained for 5 zones corresponding to the following tested apparent depths in the borehole: 500.99-530.50 m, 617.30-696.00 m, 793.00-820.20 m, 958.40-972.50 m, and 977.00-1009.95 m. The first three of these zones tested the Schilfsandstein, Upper Muschelkalk and Buntsandstein, respectively. The latter two zones were located in the upper Permian.

The range of specific storages used for the Riniken sediments was 9.4E-06 m^{-1} to 3.2E-07 m^{-1}. Lower specific storage values were chosen for carbonate rocks and anhydrite, and the higher storage values were used for sandstones of the Rotliegendes.

The measured borehole temperatures determined using the hydrologic test tool ranged from about 22°C at 217 m through 63°C at about 1513 m apparent depth. A bottom hole temperature was not available from hydraulic testing because the bottom hole testing configuration placed the temperature

sensor at 1500.5 m above the bottom of the borehole. The temperature increases with depth in the borehole at a gradient of about 3.9°C/100 m, based on measured temperatures during testing and high resolution temperature logging results.

TABLE OF CONTENTS

TABLE OF CONTENTS

(cont'd)

TABLE OF CONTENTS
(cont'd)

LIST OF FIGURES

LIST OF FIGURES
(cont'd)

LIST OF FIGURES
(cont'd)

LIST OF TABLES

1. INTRODUCTION

Nagra is currently conducting an investigation of the geologic and hydrogeologic characteristics of crystalline rock in Northern Switzerland. These investigations are intended to provide a high quality data base required to assess sites as potential repositories for radioactive waste.

As part of these investigations, Nagra has completed deep boreholes at six sites (Boettstein, Weiach, Riniken, Schafisheim, Kaisten and Leuggern). Twelve deep boreholes have been planned. The location of these boreholes is shown in Figure 1.1. This report addresses, for the Riniken borehole, the analysis and interpretation of hydraulic tests conducted in various zones.

The testing includes tests conducted both during and subsequent to the drilling of the borehole (total drilled depth of 1800.5 meters) during the period July, 1983 to June, 1985. A total of 19 tests were conducted with the Lynes 3.5 inch or 5 inch hydrologic tool. Other tests included a bottom-hole (1711.2P) test using a Lynes production-injection packer (PIP), a second bottom-hole test (1709.2D), and a Muschelkalk aquifer pumping test (654.4PV) in the open borehole using water-level measurements from surface. Two of the 22 tests were completed using a double packer configuration in perforated casing before installation of the long-term monitoring tools. The hydraulic testing has been conducted in the Riniken borehole by Gartner Lee AG in conjunction with Lynes personnel, with the exception of the pump test on the Muschelkalk aquifer which was conducted by Dr. H. Schmassmann.

In this report, depths below ground surface are referred to as either apparent depths or true vertical depths. The depth measured along the borehole length is referred to as the apparent depth. In general, all depths reported during

drilling and testing (i.e., drilling logs, testing field notes, geological and geophysical logs) are apparent depths. True vertical depths are needed for comparative analysis of formation pressure and equivalent freshwater head. True vertical depths used in this report have been calculated based on the results of an HDT Dipmeter Survey between ground surface and 900 m and an SHDT Dipmeter Survey between 900 m and the bottom of the borehole.

1.1 Objectives and Scope

The objectives of this interpretive report include the following components:

- Analysis and interpretation of the hydraulic tests completed in the Riniken borehole to derive the representative formation parameters: hydraulic conductivity, specific storage, formation pressure, equivalent freshwater head and temperature.
- A compilation and discussion of the interpreted formation parameters.

This report documents work completed by INTERA Technologies, Inc., under contract to Nagra. Contained within this report are brief descriptions of the borehole hydraulic test equipment, testing methods and analytical techniques, as well as, discussions of the hydraulic test results and interpretations. Several tests that were attempted had to be abandoned due to equipment related problems (e.g., packer slippage, packer failure). Two attempted interpretations did not provide confident results due to an anomalous pressure record and a poorly documented temperature record. A total of 22 hydraulic tests were analyzed for 19 different intervals in the borehole with three of the tests being of essentially the same zone. For three of the 22 hydraulic tests, a representative value of hydraulic conductivity could not be determined.

2. RINIKEN BOREHOLE DESCRIPTION

The Riniken borehole is located at coordinates 656'603.8/261'899.5 with a reference ground surface elevation of 385.07 m ASL. This location is about 12 km southwest of the confluence of the Rhine and Aare Rivers. The Riniken borehole intersected Jurassic and Triassic sediments overlying a trough of Permo- carboniferous sediments in the crystalline basement rocks of northern Switzerland. Drilling and testing of the borehole were suspended at 1800 m to assess the predicted depth of the crystalline basement from geophysical studies.

Drilling of the borehole began on 23 June, 1983 and finished on 12 January, 1984 at a total depth along the borehole of 1800.50 m. The borehole was set vertically but it deviates to the south between 50 m and 350 m and to the north from 400 m to 1800 m along the borehole. In the east-west direction deviation is minimal except between 1600 m and 1800 m apparent depth where the borehole trends to the west.

In this report, depths below ground surface are referred to as either apparent depths or true vertical depths. The depth measured along the borehole length is referred to as the apparent depth. In general, all depths reported during drilling and testing (i.e., drilling logs, testing field notes, geological and geophysical logs) are apparent depths. True vertical depths are needed for comparative analysis of formation pressure and equivalent freshwater head. True vertical depths used in this report have been calculated based on the results of an HDT Dipmeter Survey between ground surface and 900 m and an SHDT Dipmeter Survey between 900 m and the bottom of the borehole. The borehole deviation survey results are reported at 50 meter intervals along the borehole. The true vertical depth, for any selected apparent

depth, is derived from a linear approximation of the true vertical depths corresponding to the two nearest (one above and one below) measured apparent depths from the deviation survey.

The geology intersected by the Riniken borehole (Figure 2.1) is described in detail in the Nagra quarterly reports and only a brief description will be given here. The depths given in this section are apparent depths. The borehole intersects a thin layer of Quaternary sand, silt and gravel from ground surface to a depth of 25.1 m below surface. The surficial deposits are underlain by 463.4 m of Jurassic sediments consisting of limestone, marl and clay. Below the Jurassic are Triassic sediments consisting of the Keuper (127.5 m), Muschelkalk (177.90 m) and Buntsandstein (22.50 m) Groups. The Keuper is a mixture of marl, limestone, siltstone, and claystone lithologies. The Muschelkalk (Upper, Middle and Lower) is primarily composed of carbonates (dolomite and limestone) and evaporites (anhydrite and gypsum) with minor clay and siltstone layers. The Buntsandstein, found at 793.90 m, underlies the Muschelkalk and is composed of fine to coarse-grained sandstone and siltstone. The base of the Buntsandstein lies on the Rotliegendes Group of the Permian at 816.40 m. The lithologies within the Rotliegendes are primarily siltstone, sandstone and greywacke. The bottom of the borehole ends in the sedimentary Permian material at 1800.5 m.

The completed borehole to 1800.5 m telescoped from surface. Drilling of the borehole was completed with either a roller-cone or coring bit. By reaming the borehole, a diameter of 311 mm (12.25 in.) had been attained to 1618 m. Between 1618 m and 1800.5 m, the drilled diameter of the hole was 216 mm (8.5 in.).

The Riniken borehole was cased to 1618.00 m from 27 December to 30 December, 1983. The diameter of the installed casing was 245 mm (9.63 in.). A bottom casing shoe was cemented in fine grained sandstone and breccia. The casing isolates the Quaternary sediments and the Jurassic and Triassic units and extends 801.6 m into the Permian.

3. FIELD TESTING METHODS

3.1 Equipment Description

Hydraulic testing equipment used in the Riniken borehole was provided by Lynes GmbH and was operated by Lynes and Gartner Lee AG. The downhole equipment included the Lynes 3.5 inch and 5 inch hydrologic tools, and a production-injection packer assembly used in conjunction with a multiple sensor carrier. The Lynes Hydrologic Test Tool (HTT), is described in detail in Leech et al. (1985) and only a brief description will be provided here.

The hydraulic testing equipment for the HTT consists of the following major components:

- Hydraulically inflatable packers (single or double configurations) used to isolate the test interval from the rest of the borehole.
- J-Slot-controlled mandrel used to inflate the packers and open the test interval to the tubing string.
- Shut-in tool used to isolate (i.e. shut-in) the test interval from the tubing string.
- Multiple sensors used to measure downhole pressures and temperatures. Sensors consist of three pressure transducers to measure pressure below the bottom packer (P1), in the test interval (P2) and above the top packer in the annular space (P3). Temperature transducers (T1, T2, T3) measure the operational temperature of the respective pressure transducers within the sensor carrier. The sensors are located above the top packer and J-slot-controlled mandrel, i.e., approximately 4.7 m above the top of the test-interval. P1 and T1 sensors are located 0.25 m below P2 and T2 sensors, and P3 and T3 sensors are located 0.25 m above P2 and T2 sensors.

- Conductor cable to transmit pressure and temperature signals to the surface.
- Surface data collection equipment.

The simplified operation of the HTT is as follows. The packers and HTT are lowered to the test interval on the tubing string. At this point, the test tool is configured for a hydraulic connection between the tubing string and the packers. The tubing string is pressurized at the surface to inflate the packers. This inflation pressure is sealed in the packers by a movement of the mandrel assembly and the pressure in the tubing string is bled to the borehole annulus (equalization) above the top packer. The shut-in valve is then closed and the test interval is isolated from the tubing string. In this position the tubing string can be swabbed or pressurized without influencing the pressure in the test interval. To perform a slug test, the shut-in tool is opened causing an overpressure or underpressure on the test interval. To perform a pulse test, the shut-in valve is opened, the test interval is overpressured or underpressured and then the shut-in valve is quickly closed to trap the pressure pulse in the test interval. Section 3.2 gives a more detailed description of slug and pulse test methods.

With careful handling and frequent maintenance, the operation of the test equipment is generally trouble-free. The most frequent cause of abandoned tests is packer rupture or packer leakage. The equipment is known to be non-rigid or compliant due primarily to the use of flexible rubber packers (see Grisak et al., 1985, pp. 54-60 and 169-171). Packer readjustment or deformation during testing can affect the hydraulic test results, primarily in zones of lower hydraulic conductivity; however, testing methods that incorporate a compliance or waiting period after packer inflation are considered to greatly reduce compliance effects.

Non-Darcy flow conditions can have an effect on hydraulic testing results in two different manners. High flow rates through large aperture fractures in the formation or through the apertures in the Lynes HTT could result in turbulent flow conditions. This would cause a non-linear relationship between flow rate and measured pressure change in the test interval. The measured pressure response could be erroneously interpreted as a conventional formation response unless the non-Darcy flow condition is identified. High flow rates during hydraulic testing may be obtained while conducting slug or pump tests in test intervals with high hydraulic conductivity.

The reported accuracy of the pressure transducers for the HTT at full scale of 41370 kPa is ±0.05 percent with a resolution of 0.005 percent. This corresponds to an accuracy of about ±21 kPa or ±2 meters of water at full scale. The temperature transducers have a reported accuracy of about ±1°C with a resolution of 0.1°C.

Bottom hole testing at Riniken was completed with a Lynes 187 mm Production Injection Packer (PIP) isolating the test zone with 114 mm (4.5 in.) and 73 mm (2.875 in.) tubing extending from the packer to the top of the borehole. A Lynes transducer probe was lowered inside the 4.5 in. tubing below the water level for test 1711.2P. The transducer probe assembly is the same as described as part of the HTT. For test 1709.2D, the sensor carrier was removed from the tubing string and water levels were measured in the open borehole.

3.2 Testing Methods

Hydraulic testing methods are described in detail in Grisak et al. (1985) and only brief accounts of the various methods used in the Riniken borehole will be given here.

Several different configurations of the testing equipment were used during the drilling and testing phase according to the purpose and the time allocated for each interval. All of the hydraulic tests were configured in terms of either (1) single packer tests, (2) double packer tests, or (3) open borehole tests.

Single packer tests are typically used during the drilling phase to isolate the bottom section of the borehole, thus only one packer is required. These tests are typically run in zones of higher hydraulic conductivity where high fluid losses during drilling are observed or where there is an indication of a change in formation pressure. Their primary use is to isolate an interval immediately after drilling to determine accurate formation pressures (in an acceptable time frame) in conjunction with other hydraulic parameters. The isolated interval of a single packer test may also be used for geochemical sampling. Single packer tests conducted during drilling are typically short in duration in order not to delay the continuation of drilling. In the Riniken borehole, 10 of the 22 successful tests were conducted with a single packer HTT configuration. Two of the 10 single packer configured tests were pumping withdrawal tests.

Double packer tests use an upper and lower packer to isolate specific intervals within the borehole. These tests are typically completed after drilling in order to assess or re-assess an interval. Within the Riniken borehole, 12 double packer configured intervals were tested. Seven of these tests were run during one of the reconnaissance phases after completing the borehole to interim depths of 397.7 m and 1618.30 m. The remainder were completed during the drilling phase or as re-tests within perforated casing of zones showing anomalous formation pressures.

The three test types (single packer, double packer and open borehole) typically use one or more of the following hydraulic test methodologies at each test interval:

- Slug tests;
- Pulse tests;
- Drill-stem tests (DST); and
- Pumping tests.

In a slug test, a volume of water is quickly introduced to (slug injection test) or removed from (slug withdrawal test) the test interval. The rate of water-level recovery back to equilibrium provides an indication of the hydraulic conductivity of the interval. In the Riniken borehole, using the HTT equipment, slug withdrawal tests were completed by removing fluid from the tubing string (i.e., lowering the water level) with the shut-in valve closed, then opening the valve and allowing fluid in the test interval to flow to the tubing string. The pressure in the test interval was monitored. The pressure above and below the test interval was also monitored by the pressure transducers in the sensor carrier. For slug injection tests, an overpressure is introduced to the test zone by opening the shut-in valve with a column of water in the tubing. The tubing fluid is allowed to flow into the interval formation and the corresponding pressure response is monitored.

A pulse test is completed in a manner similar to the slug test. In a pulse withdrawal test, after the removal of fluid from the tubing string, the test interval is underpressured by opening the shut-in valve momentarily and then rapidly closing the shut-in valve. In pulse injection test, the shut-in valve is opened and the test interval is pressurized using a pump to force fluid into the interval. The shut-in valve is then quickly closed to trap the pressure pulse in the test zone. In very low permeability intervals, the

pressure recovery in the test zone is attributed primarily to the compressibility of the formation and the compressibility of the fluid in the borehole and in the formation.

A drill-stem test (DST) is a testing technique used extensively in the petroleum industry to assess formation permeability. The method is essentially a combination of the slug and pulse tests described above. In a DST, the test interval is first underpressured as in a slug withdrawal test. After a period of monitoring the flow recovery (referred to as the DST flow period), the shut-in valve is closed to isolate the test zone and induce a more rapid pressure recovery, as in a pulse withdrawal test (referred to as the DST shut-in or build-up period).

In a pumping test, an interval of relatively high hydraulic conductivity can be isolated using either double packers or, if the interval is at the bottom of the borehole, a single packer. If the entire drilled section of the borehole is to be tested, pumping can be conducted in the open borehole. The test interval is pumped using a submersible pump placed within the tubing string or open borehole below the static fluid level. The pressure response of the formation is monitored for the duration of the pumping. After the pumping period, the pressure recovery back to equilibrium can also be monitored.

The pressure or water-level response measured during testing is analyzed to obtain representative formation parameters (formation pressure, hydraulic conductivity, and specific storage) where possible.

4. INTERPRETATION METHODS

The purpose of this section is to provide a description of the methods used to interpret the hydraulic tests in the Riniken borehole. The interested reader is directed to Grisak et al. (1985) for detailed information on the theoretical development of hydraulic test analysis.

4.1 Definition of Formation and Fluid Properties

The hydraulic test interpretation methods for the Riniken borehole require the definition or estimation of the physical properties of the rock formation and the formation and borehole fluids. A number of these physical properties are required as basic input parameters to solve the flow equations which describe the testing response and yet have not been specifically determined by measurements in the field at the borehole. These parameters such as the fluid density, compressibility, viscosity, thermal expansion, formation compressibility, and porosity must be estimated based on the best available information and, in some cases, corrected for borehole conditions such as temperature and pressure. Other physical properties such as hydraulic conductivity, hydraulic head and specific storage are dependent on accurately simulating, with mathematical models, the pressure response in the formation during testing. On suitably modeling the field response, the formation pressure and formation compressibility are used in the calculation of hydraulic head and specific storage, respectively.

This section provides a definition of properties related to the hydraulic system under study and a discussion of the reasonable property values for the rock formation and borehole and formation fluids that are used in hydraulic test interpretations. In addition, a brief discussion of the methods and sources of information that are used to determine each parameter is provided.

4.1.1 Formation Compressibility

The reader is referred to Section 4.2.3 of Grisak et al. (1985) for a more complete discussion of formation compressibility. The following discussion provides an overview of the approach taken in the borehole test interpretation. The formation compressibility (C_R) can be defined as the change in volume of the formation under an applied stress, and can be written as follows:

$$C_R = - \frac{dV_T/V_T}{d\sigma_e} = \frac{d\epsilon}{d\sigma_e} \qquad (4.1\text{-}1)$$

where V_T = total volume of the rock, L^3;
dV_T = change in total volume, L^3;
$d\sigma_e$ = change in effective stress, $ML^{-1}t^{-2}$;
$d\epsilon$ = change in strain, dimensionless.

The total volume of the formation is the sum of the volume of the solids (V_S) plus the volume of the voids (V_V). The compressibility of the solids is generally considered to be negligible and therefore the change in volume of the solids is essentially zero and the total change in volume of the formation is equal to the change in volume of the voids and the pore fluid. Both the medium and the pore fluid are assumed to be compressible.

For the case of three-dimensional loading with equal stress in all directions, the formation compressibility can be written as:

$$C_R = \frac{3\ (1-2\mu)}{E} \qquad (4.1\text{-}2)$$

where E = Young's modulus or modulus of elasticity, $ML^{-1}t^{-2}$;

μ = Poisson's ratio.

Young's modulus is the ratio of stress to one-dimensional strain. Poisson's ratio defines the ratio of the strain in directions normal to the applied stress to the strain in the direction of the applied stress.

Using Equation 4.1-2, the formation compressibility can be defined based solely on Poisson's ratio and Young's modulus. For the hydraulic testing in the Riniken borehole, a suitable value of formation compressibility was determined based on a literature review of Young's modulus and Poisson's ratio. Touloukian et al. (1981) provide values of Young's modulus and Poisson's ratio for uniaxial compressive loading for various types of sedimentary rock. Young's modulus values range from 2.48 to 62.74 GPa and Poisson's ratio values range from 0.04 to 0.42 for the rock types, limestone, shale, sandstone, and quartzite, which describe the major lithologies intersected by the borehole. Each major lithology was assigned a reasonable value or range of values for Young's modulus and Poisson's ratio from which rock compressibility could be determined using equation 4.1-2. For limestone and dolomitic limestone, Young's modulus ranged from 2.48 to 8.69 GPa and Poisson's ratio from 0.04 to 0.12. Shale was described by a Young's modulus of 13.79 GPa and Poisson's ratio of 0.07. Sandstone was described by a greater range of Young's modulus from 10.34 to 16.41 GPa and Poisson's ratio from 0.23 to 0.42. Quartzite was assigned values of 37.60 to 62.74 GPa for Young's modulus and 0.12 to 0.22 for Poisson's ratio. The range of values for each parameter results from recognizing different confining pressures for each test interval and choosing an experimental value measured at or close to that confining pressure. For the interpretation of the hydraulic tests, the range of rock compressibility determined for limestone, based on reasonable

values for Young's modulus and Poisson's ratio, is 2.3E-11 to 3.2E-11 Pa^{-1}, for shale, a single value of 1.6E-10 Pa^{-1}, for sandstone, the range was 9.0E-11 to 7.95E-10 Pa^{-1}, and for quartzite, 9.0E-11 to 9.0E-10 Pa^{-1}. The compressibility of the rock within a test zone may also be affected by structure such as fracturing and jointing. In the test zones where the rock contains a significant number of fractures or other structural features, the compressibility may have been increased by an order of magnitude to compensate for these features. For determining reasonable variability of rock compressibility for a sensitivity study in specific storage, adjustments of one order of magnitude above and below this value were considered reasonable. One exception to this approach is for test 1378.9D where, because of the reported brecciation in the core, the rock compressibility was increased by more than one order of magnitude to compensate for rock structure.

4.1.2 Porosity

Porosity is a measure of the interstitial space in a porous or fractured rock. It is defined as the ratio of the volume of the voids to the total volume of the rock. Porosity may be classified into primary or secondary porosity. Primary porosity results from the original formation of the rock and includes all pore space between grains in a sedimentary rock or between crystals in a chemical precipitate such as a carbonate rock. Secondary porosity is developed after the formation of the rock mass by such mechanisms as solution weathering and fracturing. The total porosity includes both primary and secondary porosities. In the case of a fractured rock the total porosity is the sum of the matrix porosity (i.e., primary) and the fracture porosity (i.e., secondary).

The sedimentary rocks intersected by the Riniken borehole have been described in this report with a range of total porosities from 3 percent to 15 percent. The fractures

(e.g., secondary porosity) in the rock could be expected to contribute as much as one percent to the total porosity of a unit volume of rock. Therefore, this range of porosity used in the interpretation of the hydraulic tests represents the primary or matrix porosity of the rock. The effective porosity assigned to the rock in each test zone represents value obtained from a review of the literature and is considered representative.

4.1.3 Fluid Compressibility

For a fluid such as water, the compressibility (C_w) in terms of a volume change is defined as:

$$C_w = - \frac{dV_w/V_w}{dP} \qquad (4.1\text{-}3)$$

where V_w = volume of water, L^3;
dV_w = change in volume of water, L^3;
dP = change in fluid pressure, $ML^{-1}t^{-2}$.

For a given mass of water the compressibility can also be written in terms of a density change as follows:

$$C_w = \frac{d\rho/\rho}{dP} \qquad (4.1\text{-}4)$$

where ρ = fluid density, ML^{-3};
$d\rho$ = change in fluid density, ML^{-3}.

Water changes volume or density in a linear fashion with changes in pressure. Because fluid density is temperature dependent, the compressibility is also influenced by the fluid temperature.

For the purposes of hydraulic test analysis, a value of fluid compressibility (C_w) was taken from Figure 4.1 which illustrates the variation of fluid (pure-water)

compressibility with changes in pressure and temperature. To provide a fluid compressibility typical of a Riniken test interval, values were chosen from Figure 4.1 using an in-situ pressure and formation fluid temperature which were estimated based on the field data. [Note: the fluid property curves for compressibility, density, viscosity, and thermal expansion as shown in Figures 4.1, 4.2, 4.3, and 4.4, respectively, are based on data presented in Dorsey (1968)].

In a discussion of fluid compressibility in hydraulic testing it is also worthwhile to consider the interpretation of the test system compressibility and the observed compressibility. The test system compressibility (C_{TS}) includes the compressibility of water and the deformation of components of the hydraulic testing equipment. The system deformation is due to a certain amount of non-rigidity or compliance in the equipment, resulting from packer deformation or readjustment, entrapped air in the equipment or machined tolerances on the seating and positioning of various steel components and O-ring or other seals, should be considered if the information is available. System compliance enhances the compressibility within the test interval.

Most of the system compressibility for the Lynes equipment used in the testing of the Riniken borehole is represented by the packer compliance. The packer compliance or packer readjustment is a continuing process throughout a hydraulic test in response to the pressure differential between the test interval, the packer pressure and the pressure above and below the test interval. A discussion of packer compliance effects with respect to hydraulic tests is provided in Grisak et al. (1985).

While it is recognized that the test system compressibility may be greater than the compressibility of fluid only in the test zone, there has not been sufficient evaluation of the Lynes test equipment to estimate a value of C_{TS} a priori. In

laboratory and field testing using other systems (Neuzil, 1982; Forster and Gale, 1980, 1981; and Hsieh et al., 1983) the test system compressibility was found to be between a factor of 2 to 6 greater than the compressibility of water. None of these systems, however, are comparable to the Lynes system to allow a direct extrapolation to tests completed in the Riniken borehole. In fact, the Lynes system is considered to be more rigid than these systems and therefore in our opinion, the system compressibility is probably not more than a factor of 2 or 3 greater than water.

Another method of estimating the system compressibility is to measure the test interval pressure change after an instantaneous injection of a known volume of water and calculate an observed compressibility, as described by Neuzil (1982). This type of testing requires the condition that only a small fraction of the water pumped into the test interval flows out into the formation during pressurization of the interval. Alternatively, the test zone compressibility could be derived by pressurizing a representative test interval in blank casing using a test tool assembly identical to the borehole testing equipment. While these methods may provide a more appropriate measurement of system compressibility, it cannot be used in the hydraulic testing in the Riniken borehole because the injected volume was not measured during the testing phase.

4.1.4 Fluid Density

The fluid density is defined as the mass per unit volume of fluid and is a function of temperature and pressure, dissolved and suspended solids, and dissolved free gas. For use in hydraulic test analysis the fluid density represents in-situ conditions. To estimate an appropriate fluid density, a pure-water density was assumed, adjusted for in-situ temperature and pressure, and then corrected for salinity as explained in Sections 4.1.8 and 4.4.1. The

formation temperature was selected based on measured temperatures of the borehole fluid as reported in the interval reports. The in-situ pressure was derived from the measured pressure at the end of the shut-in period of a hydraulic testing sequence.

The variation of density of deionized water with changes in temperature and pressure is given in tabular form on Table 4.1 and graphically on Figure 4.2. Figure 4.2 illustrates the nonlinear dependence of density on temperature and pressure. The ranges of temperature and pressure given include the formation temperatures and pressures observed at the Riniken borehole. The density values were derived from the compressibility data and specific volume/pressure derivatives reported in Dorsey (1968). Compared to other sources of density data reported at one atmosphere (Weast, 1982), the derived densities do not exactly agree for the temperatures listed. Of relevance to the preparation of instrumentation uncertainty, the purpose of the density data is to generate correction terms where the of primary interest is in the difference between the density at a specific temperature and pressure and the density at a reference temperature (usually 20°C) and pressure (1 atmosphere). For one atmosphere and temperatures greater than 20°C, the average relative error of the correction term is less than 2 percent, indicating that the predicted density is accurate to within 0.002 percent for the pure-water case.

4.1.5 Fluid Viscosity

The internal resistance of a fluid to motion is known as its viscosity. Viscosity is greatly influenced by temperature while changes in pressure have only a negligible effect. The variation of viscosity with changes in temperature is given in Figure 4.3.

The viscosity of the fluid in the test zone and formation must be corrected for temperature for use in hydraulic test analysis. The average temperature is estimated based on the measured temperature transducer response during the interval testing. The viscosity is estimated based on a comparison to Figure 4.3.

4.1.6 Fluid Thermal Expansion Coefficient

Pressure changes within a shut-in test zone can occur as a result of temperature changes of the shut-in borehole fluid. If the borehole fluid is at a different temperature from the formation fluid, due to mixing within the borehole or the introduction of drilling fluids, expansion or contraction of the fluid will result in a fluid volume change which will result in a corresponding pressure change. The magnitude of pressure change is a function of the thermal expansion coefficient which is temperature dependent and, to a lesser extent, pressure dependent. At constant pressure, the thermal expansion of pure water can be expressed as follows:

$$\beta = \frac{1}{V}\left[\frac{\Delta V}{\Delta T}\right]_P \qquad (4.1.5)$$

where β = thermal expansion coefficient, $°C^{-1}$;
V = volume of water, L^3;
ΔV = change in volume of water, L^3;
ΔT = change in temperature of water, °C.

For pure water, the variation of the thermal expansion coefficient with temperature and pressure is given in Figure 4.4. For temperature variations from 0° to 100°C, the thermal expansion coefficient varies from -3.9E-05 to 7.5E-04$°C^{-1}$.

In the analysis of the Riniken hydraulic tests, the thermal expansion coefficient was estimated by correcting the freshwater coefficient for borehole temperature and pressure

at the test zone. The thermal expansion coefficient was only required when the borehole fluid underwent a significant (i.e., greater than 0.2 - 0.3°C) temperature change during the build up period of a hydraulic test. The borehole temperature was estimated from the responses of the temperature transducers. The pressure was estimated based on the average shut-in pressure response in the hydraulic test sequence. The average temperature and pressure were then applied to Figure 4.4 to determine the corrected thermal expansion coefficient of the test interval fluid.

4.1.7 Formation Pressure and Annulus Pressure

The formation fluid pressure is the undisturbed static pressure of the formation beyond the influences of the borehole. When analyzing hydraulic test data to determine hydraulic conductivity, a formation pressure that is representative of undisturbed conditions must be estimated as an initial condition for the analysis method. Several different approaches were used to define undisturbed fluid pressure within the test interval including the Horner method of analysis. A detailed description of the approaches for selecting the initial value of formation pressure is given in Section 4.3.

The effect that borehole fluid pressure (i.e., annulus pressure) exerts on a test interval prior to testing can be important for test interpretation purposes. Annulus pressure was considered when simulating the pressure history of the test interval prior to testing. When the annulus pressure differs from the formation pressure and the test interval is exposed to annulus pressure for a significant period of time, the result is a pressure disturbance or transient around the borehole. The annulus pressure is estimated at the center of the test interval from the P3 transducer during the installation of the test tool, and prior to the start of

testing. At Riniken, the annulus pressure often corresponds to overflow conditions at the top of the borehole casing and therefore, in this instance, would be less than the static fluid pressure of the formations.

4.1.8 Hydraulic Head and Equivalent Freshwater Head

The concept of a hydraulic potential, developed by Hubbert (1940), was derived on the basis of energy relationships for a homogeneous fluid. The fluid potential (Φ) in a porous medium is defined as follows:

$$\Phi = gh \qquad (4.1\text{-}6)$$

where g = gravitational acceleration, Lt^{-2};
h = hydraulic head, L.

For situations dealing with homogeneous fluids (i.e., constant properties spatially and temporally), the hydraulic head (h) is related to pressure by the following equation:

$$h = z + \frac{P}{\rho g} \qquad (4.1\text{-}7)$$

where z = elevation head (distance from the measuring point to a reference datum), L;
P = pressure, $ML^{-1}t^{-2}$;
ρ = fluid density, ML^{-3}.

If the fluid density is assumed equal to the density of fresh water, then the head calculated from equation 4.1-7 is referred to as the equivalent freshwater head.

Equivalent freshwater head is useful in the comparison of formation pressures from intervals at the same depth with similar salinity. Throughout this report, equivalent freshwater head is reported at the center of an interval and

is therefore based on the formation pressure at the center of the interval. In the context of the hydraulic tests analyzed for the Riniken borehole, the formation pressure is derived either from transducer measured pressures or water levels. For a transducer monitored system, formation pressure is found by:

$$P_{fc} = P_{ft} + \rho g d_{ct} \qquad (4.1\text{-}8)$$

where P_{fc} = formation pressure at the center of the interval, $ML^{-1}t^{-2}$;

P_{ft} = formation pressure at transducer depth, $ML^{-1}t^{-2}$;

ρ = average borehole fluid density between the transducer and the center of the interval, ML^{-3};

d_{ct} = true vertical distance between the transducer and the center of the interval, L.

In the case where water levels are being measured in an open borehole such that the estimated undisturbed formation pressure is in the form of a static fluid level, the formation pressure at the center of the test interval is calculated using:

$$P_{fc} = \rho g d_{cs} + P_{atm} \qquad (4.1\text{-}9)$$

where ρ = borehole fluid density depth-integrated in temperature, pressure and salinity, ML^{-3};

d_{cs} = true vertical distance between the static water level and the center of the interval, L;

P_{atm} = barometric pressure, $ML^{-1}t^{-2}$.

The fluid density term in equations 4.1-8 and 4.1-9 is interpreted as the average density between the point of measurement and the interval center. For transducer-monitored tests, the distance between these points is normally short enough to justify a density estimate at the interval center only. The estimates are based on the temperature and pressure at the interval center and the total dissolved solids. To estimate total dissolved solids, it may be necessary to account for the drilling fluid used, swabs taken both before and during testing, and the composition of the in-situ formation fluid. For water-level tests, the distance between measuring points is often large enough that density variations due to changes of temperature, pressure, and salinity with depth are significant. To average these effects, a depth-integration scheme for density, such as described in Section 4.4.1 below, can be used.

For the hydraulic testing program being conducted by Nagra, the datum for reporting equivalent freshwater head is sea-level. Using the formation pressures at interval center, the application of equation 4.1.7 specializes to:

$$H = \left(\frac{P_{fc} - P_{atm}}{\rho_f g}\right) - d_c + Z \qquad (4.1\text{-}10)$$

where H = equivalent freshwater head (m ASL), L;
ρ_f = reference density of freshwater, ML^{-3};
d_c = true vertical depth to the center of the interval, L;
Z = borehole surface elevation (m ASL), L.

The values reported for equivalent freshwater head are based on best estimates of the variables appearing in equations 4.1-8 to 4.1-10. There can be uncertainties surrounding the best-estimate values due to data interpretation, operator error, undetected equipment failure, and accuracy and

resolution specifications of the monitoring devices used. An assessment of the uncertainty of the freshwater head values due primarily to instrument accuracy specifications is presented as part of the results in this report. The uncertain variables and the statistical techniques used are discussed in Section 4.4.

4.1.9 Hydraulic Conductivity

The basis of ground water flow lies in the development of Darcy's Law which relates the rate of ground water flow to a hydraulic gradient.

$$v = - K \frac{dh}{dl} \qquad (4.1\text{-}11)$$

where v = specific discharge, Lt^{-1};
K = hydraulic conductivity, Lt^{-1};
h = hydraulic head, L;
l = distance between head measurements, L;
dh/dl = hydraulic gradient, dimensionless.

In equation 4.1-11, K is a constant of proportionality and is a function of both the medium and the fluid. The hydraulic conductivity can be defined in terms of medium and fluid properties as:

$$K = \frac{k\rho g}{\mu} \qquad (4.1\text{-}12)$$

where k = intrinsic permeability, L^2;
ρ = fluid density, ML^{-3};
μ = fluid viscosity, $ML^{-1}t^{-1}$;
g = gravitational acceleration, Lt^{-2}.

The intrinsic permeability is a property of the medium alone, being a function of the grain size, sphericity and roundness

of the grains, the nature of their packing and degree of cementation and fracturation.

The hydraulic conductivity determined from the test interpretation is an equivalent rock mass hydraulic conductivity (K_{erm}) applied to the entire test interval. This results from the interpretation of a pressure-time record that represents the response of an isolated test interval. The K_{erm} is an average for the test interval and it is recognized that higher or lower hydraulic conductivity zones may be contained within the interval in the form of fractured or brecciated areas or separate permeable lithograhic units.

4.1.10 Specific Storage

The specific storage of a saturated geologic medium is defined as the volume of water that a unit volume of the medium releases from storage under a unit decline in hydraulic head. This volume of water released from storage is dependent upon the compressibility of the fluid and the medium. Specific storage (S_s) can be expressed:

$$S_s = g\rho\ (C_R + \theta\ C_W) \qquad (4.1\text{-}13)$$

where ρ = fluid density, ML^{-3};
g = gravitational acceleration, Lt^{-2};
C_R = rock or formation compressibility, $M^{-1}Lt^2$;
θ = effective porosity, dimensionless;
C_W = fluid compressibility, $M^{-1}Lt^2$.

The mathematical representation of the specific storage is dependent on the definition of the fluid and medium compressibilities. A detailed review of the various conventions for defining the formation compressibility is given by Narasimhan and Kanehiro (1980). The expression for specific storage noted above is based on a formation

compressibility definition utilizing a normalization with respect to the bulk volume of the sample being tested. This definition is consistent with the standard hydrogeologic approach.

The storage coefficient is equal to the product of the specific storage and the formation thickness. During the hydraulic testing, the full test interval length is usually chosen as the formation thickness because the portion of the test interval length most actively contributing to the pressure recovery is unknown.

As indicated by equation 4.1-13, specific storage is a function of the formation fluid density and compressibility, the rock compressibility, and the formation porosity. Of these parameters, rock compressibility and formation porosity are the least certain for any test interval. As discussed previously a range of porosity from 3 to 15 percent was assumed for the sedimentary rock and compressibility was calculated from literature values of Young's modulus and Poisson's ratio that were considered to be representative of the rock types encountered at Riniken.

Regarding the sensitivity of the average hydraulic conductivity of a test interval to variations in specific storage, a summary of the results of sensitivity studies for several test intervals is provided in Section 4.3.4.

4.2 Hydraulic Test Interpretation Methods

4.2.1 Analytical Solutions

The pressure response during hydraulic tests varies with time, depending on the hydraulic properties of the formation being tested. Under ideal test conditions, hydraulic tests can typically be analyzed using analytical solutions of the transient radial flow equation. Each test type (i.e., slug,

pulse, drill stem or pump test) has had an appropriate analytical solution developed, which allows for the determination of transmissivity and in some cases formation pressure. The various test types and the literature references that provide the analytical solutions are listed as follows:

- Slug injection or withdrawal test - Cooper et al. (1967)
- Pulse injection or withdrawal test - Cooper et al. (1967)
  - Bredehoeft and Papadopulos (1980)
- Pulse test - Fractured Media approach - Wang et al. (1978)
  - Barker and Black (1983)
- Drill stem test - Matthews and Russell (1967)
  - Earlougher (1977)
- Pumping or Injection test - Theis (1935)
- Constant Drawdown Flow test - Jacob and Lohman (1952)

The reader interested in more details on the analytical solutions for individual hydraulic testing techniques is directed to the original references. A review of the theoretical aspects of borehole hydraulic testing methods is provided in Grisak et al. (1985). The analytical solutions generally use the confined porous media approach (except for the pulse test fractured media approach) for conceptualization of the flow regime during hydraulic testing of rock. Using a porous media conceptualization the following simplifying assumptions are adopted:

(1) The aquifer (test interval) is confined, infinite in a real extent and constant in thickness;
(2) The aquifer is homogeneous;
(3) Areal flow in the aquifer is negligible;
(4) Initially, constant head exists across the aquifer;
(5) No vertical component of flow exists in the aquifer.

These assumptions have been universally applied in ground water problems in porous media to simplify the flow regime in

a manner that is conducive to analysis. A discussion of the validity of these assumptions as applied to hydraulic testing is given in Grisak et al. (1985).

The analytical solutions can be solved using a representative range of parameters to obtain a series of type curves. The type curves can be compared graphically to the field data to determine the hydraulic parameters. A discussion of this method is provided in numerous references treating groundwater resource evaluation, one of which is Freeze and Cherry (1979).

Type curves can provide an estimate of the hydraulic parameters, but in many cases because of the quality of the data or the non-representativeness of an analytic solution, the fit to the type curves is poor and the field data can be matched to various parts of several curves. This nonuniqueness of fit in the use of type curves can result in considerable uncertainty in the estimation of the formation parameters. It is also necessary to extrapolate between curves if an accurate match can not be obtained with the existing curves. Herein lies the advantage of implementing the analytic solutions in the form of computer models. In the computer implementation, the analytical solution is solved numerically using appropriate ranges of formation parameter values. Each computer simulation is compared to the field data until a best fit curve is found. The formation parameters for the field data are the same as those for the best-fit curve. The advantages of the computer implementation method are therefore: (1) sensitivity analyses can be conducted to assess the effects of parameter value variation on the simulated pressure or head responses, (2) the formation parameters can be more easily varied to determine a more accurate best-fit curve, and (3) errors due to extrapolation and matching to the wrong curve are reduced.

4.2.2 Graphical Analysis Method (Horner Analysis of Drill-Stem Tests)

Graphical analysis or "Horner plot" methods are frequently used for evaluation of drill-stem tests (DST) and are well documented in the petroleum engineering literature (e.g., Matthews and Russell, 1967; Earlougher, 1977; Lee, 1982). These methods allow determination of formation pressure and hydraulic conductivity of the tested formation. As will be discussed further in Section 4.3.2, the Horner method of analysis has been used to interpret both formation pressure and hydraulic conductivity in tests from the Riniken borehole where the DST pressure response has not been affected by history or changing temperature within the test interval.

4.2.3 Practical Considerations in Interpreting Hydraulic Tests

In most cases, analytical solution methods for interpretation are best applied when all or most of the theoretical assumptions (i.e., confined, infinite, homogeneous aquifer with constant thickness and initially constant head) can be achieved. For deep borehole testing, non-ideal conditions often exist during the testing procedure, which may reduce the ability of the analytical methods to represent the testing results.

The purpose of this section is to identify and evaluate the processes and factors which are important in the analysis and interpretation of borehole hydraulic tests. The factors which are of particular importance in evaluating low hydraulic conductivity formations include borehole pressure history, formation pressure and hydraulic head, thermally-induced pressure responses, borehole/formation skin effects, and non-homogeneous medium. A discussion of these factors is necessary in order to set the basis for the development of

the analysis technique - the Graph Theoretic Field Model (GTFM) described in Section 4.3 and used in the analysis of several of the Riniken hydraulic tests.

The following discussion is based on concepts presented by Grisak et al. (1985).

4.2.3.1 Borehole Pressure History

The pre-test borehole pressure is, in general, different from the in-situ formation pressure. This results from the hydrostatic pressure corresponding to the fluid level in the borehole during the pre-test period differing from the formation pressure at some depth in the formation. When the borehole is full and overflowing during the pre-test period this represents the maximum borehole pressure, assuming that the density of the fluid in the borehole remains constant. This pressure differential results in a pressure transient around the borehole at non-formation pressures which interferes with the pressure response during the testing period. The pre-test borehole pressure history may be further influenced by pressure differentials imposed on the interval during previous tests. The net effect of the pressure disturbance developed during the open borehole periods is the development of testing conditions that do not meet the constant head assumption involved in data analysis methods using analytical solutions. The pressure recovery in the interval will not be simply related to the recovery to static formation pressure from the pressure differential imposed at the start of the test. The analysis of packer tests using analytical solution methods could therefore yield incorrect hydraulic conductivity estimates under conditions where a pressure transient exists in the vicinity of the borehole rather than static formation pressure. Grisak et al. (1985) and Pickens et al. (1987) discuss several examples

of the variation in hydraulic test response dependent on the magnitude and duration of the annular pressure history for pulse and slug tests.

The determination of the magnitude of the pressures during history events represents the largest uncertainty associated with incorporating the pressure history into the analysis of the hydraulic tests. The annulus pressure is generally taken as the pressure associated with the height of the fluid column in the borehole from the transducer depth prior to inflating the test tool packers at the test zone. The annulus pressure may be uncertain if the casing outflow elevation or the borehole fluid density changes during the borehole pressure history period. The outflow elevation may vary by about 1.5 to 2.0 m depending on the configuration of the overflow valve with respect to the top of the tubing string and the drill rig floor elevation. Formation inflow into the borehole would result in mixing of the formation and borehole fluids resulting in a change in fluid density and annulus pressure. With the annulus pressure changing in time, the pressure measured at transducer P3 of the Lynes Hydrologic test tool prior to the start of testing may not be entirely representative of the annulus pressure during the history period.

The borehole pressure history may also include the differential pressure between annulus pressure and test-interval pressure, or pressure disturbances imposed on the interval during previous test sequences that included at least a part of the interval. However, in most cases these influences on the pressure history can be incorporated into the analysis at least in a simplified form.

4.2.3.2 Formation Pressure

One of Nagra's objectives in hydraulic testing is to determine static formation pressure at the test interval.

For the case where the test zone has been subjected to very little or no borehole history and thermal effects are not significant, this pressure can be measured by a transducer at the test interval either during the static recovery period at the beginning of a test sequence (sometimes referred to as the Pstat period) or by allowing a pressure test to recover completely to a steady pressure (i.e., monitoring a stabilized pressure for several hours). In the instance of a complete recovery, the formation pressure can simply be taken from the data record. If the conditions are such that a test interval may be recovering to a static formation pressure but the test is terminated before a complete recovery, then the approach can be taken to determine formation pressure (P_f) by matching the partial recovery curve with simulated pressures using a reasonably unique set of T, S and P_f. This constitutes a simple calibration of formation pressure.

If a significant pressure disturbance exists around the borehole at the test interval, then a stable recovery pressure can be biased by borehole history and in the case of a shut-in test, by changes in fluid temperature within the test zone. In cases with significant pressure histories and/or thermal effects, the recovery to a static formation pressure can take as long as several months. When pressure recovery in a test interval is influenced by a pressure disturbance around the borehole and/or thermal effects, if the analysis technique can simulate these effects accurately, then it is possible to determine a formation pressure from such a test response. Simulated pressures with history and thermal effects considered are fit to the portion of the pressure response that has been measured and providing that the fit is reasonably unique in P_f, then this value of formation pressure which has been used in simulating the pressure response, can be taken as P_f for the isolated zone. This approach constitutes a more sophisticated calibration and is discussed further in Section 4.3. In most instances

where pressure recovery is influenced significantly by history and thermal effects, the model of these effects is too uncertain to yield a unique formation pressure.

4.2.3.3 Thermally-Induced Borehole Pressure Response

During and subsequent to drilling a test interval, a temperature profile can develop into the formation in response to the differential temperatures between the borehole fluid and the rock. The net effect of the development of such a temperature profile into the formation is a variation in the borehole fluid temperature during the hydraulic testing period as the borehole fluid equilibrates with the formation temperature. These temperature variations may result in significant pressure changes during pulse testing (i.e., under shut-in conditions where the thermally-induced changes in fluid volume are confined between packers), especially in low hydraulic conductivity formations.

Thermally induced pressure effects should be included in the analysis technique if the hydraulic testing technique is a pulse test; if the temperature change in the test interval during any single pulse test is greater than 0.2°C; and if the expected hydraulic conductivity of the interval is less than 1.0E-10 ms^{-1}.

Examples which illustrate the potential importance of thermal effects on the measured pressure response during borehole hydraulic testing are given in Grisak et al. (1985) and Pickens et al. (1987).

Analysis methods (e.g., GTFM) have been developed and utilized to account for thermally-induced pressure effects and borehole history effects to allow for more accurate formation pressure and hydraulic conductivity estimates to be determined from the test data.

4.2.3.4 Borehole/Formation Skin Effects

As a result of the drilling of the borehole, the hydraulic conductivity of the formation at and immediately surrounding the borehole wall may be altered. This borehole/formation skin may have a significant effect on the measured pressure response during hydraulic testing, resulting in incorrect estimates of both formation pressure and hydraulic conductivity. This altered skin zone may have either a higher or lower hydraulic conductivity than the surrounding formation. A higher hydraulic conductivity skin zone may occur in cases where the borehole wall and adjacent formation are eroded to some extent. This erosion may occur within both intergranular porous media and fractures. In contrast, drilling fluids such as mud may invade the formation and build up a filter cake at the borehole wall, thus causing a lower hydraulic conductivity skin zone. In some cases, plugging of the pore spaces and fractures may result from reactions between the drilling fluid and minerals in the formation.

The magnitude of skin effects are difficult to quantify but are related to the radius of influence of the hydraulic pressure response during testing, the thickness of the skin zone and the hydraulic conductivity contrast between the skin zone and the formation. A model sensitivity study conducted by Faust and Mercer (1984) has illustrated the difficulty in assessing the presence of skin effects. The modified pressure response caused by a lower hydraulic conductivity skin during a hydraulic test has the same characteristic shape and response as for a lower hydraulic conductivity formation. In this case, the formation hydraulic conductivity could be seriously underestimated. When the skin is of a higher permeability than the formation, the effect on the measured pressure response (and estimated hydraulic conductivity) is much less significant.

In addition to the more obvious drilling induced skin features, it should be noted that other natural skins or boundaries may exist in the vicinity of the borehole such as heterogeneities within the rock or hydraulic boundaries located adjacent to the borehole. These features may also affect the pressure response and are equally as difficult to assess.

In summary, the presence and characteristics (i.e., thickness and hydraulic conductivity) of a skin zone surrounding a borehole are very difficult to establish. While their existence and effects must not be overlooked during interpretation of hydraulic tests, one must be careful not to include unsubstantiated skin effects in a simulation, for the sole purpose of obtaining an improved fit to the measured pressure response. For these reasons, skin effects were not included in the analyses described in this report.

4.2.3.5 Non-Homogeneous Medium

Standard analysis techniques make the assumption that the hydraulic tests are representative of a homogeneous medium of infinite extent. However, it is always possible that the formation is heterogeneous and that hydrogeologic boundaries may exist within close proximity of the borehole.

Heterogeneities in the formation being tested may include fault or shear zones, lithologic changes or changes in the fracture frequency and distribution. Unfortunately, in deep borehole testing, fracture characteristics such as frequency, length, aperture size and orientation are rarely described in sufficient detail in order to be incorporated into an analytical technique. Given the uncertainties associated with fracture characteristics, the homogeneous assumption along the test interval length provides the simplest and possibly the most practical approach to be used in analytical methods. Fractured media approaches and dual porosity models

are available for hydraulic test analysis, however their use is more successful in those cases where the fracture and porosity heterogeneities and their response to hydraulic tests are better understood.

The assumption of infinite extent is related to homogeneity in that changes in the formation close to the borehole could represent boundary conditions for the hydraulic tests. Again, fractures may play a controlling part in defining the extent of the tested formation. Test intervals may be bounded by permeable fractures which may represent relatively constant head boundaries or by permeable fractures of limited extent which may be considered as impermeable (no flow) boundaries. Each of these conditions are contrary to the assumption of infinite extent, and if present, the analysis method which assumes homogeneity may not accurately represent the formation response. In order to reduce the uncertainty, hydrogeologic boundaries, if they can be identified, can be included in the hydraulic test analysis. However, in the pressence of other possible pressure disturbances prior to and during testing, the type of boundary (no flow or constant head boundary) and the distance to the boundary may be difficult to determine. For simulation purposes, external boundary conditions were applied at radial distances sufficiently large to not effect the calculated pressure response in the test interval.

4.2.3.6 Evaluating Formation Parameter Uncertainty

The physical properties of the formation, estimated from literature values of similar rock types, cannot be considered unique. For example, porosity could vary by at least several percent and rock compressibility over several orders of magnitude and still be considered reasonable for the types of rock at Riniken considering the uncertainty in the fracturing and structure in the rock. One approach to determine the effect is to simulate the measured pressure-time data using a

reasonable range of specific storage with specific storage variability resulting from uncertain porosity and rock compressibility values for the test interval. The result is a range of hydraulic conductivities corresponding to the uncertainty range for specific storage. The hydraulic conductivity corresponding to an intermediate value of storage is then adopted as the base case value with the upper and lower limit on hydraulic conductivity used to qualify this value.

This approach to uncertainty is accomplished using a simulation code such as GTFM where sets of hydraulic parameters can be used in the calculation of pressure-time profiles. By graphically comparing the simulated pressure data with the measured data for a range of hydraulic conductivity with each hydraulic conductivity simulated at different values of specific storage, a range of best-fit hydraulic conductivities can be obtained to quantify the uncertainty.

4.2.4 Analysis Technique - Graph Theoretic Field Model (GTFM)

As has been noted in previous subsections, the use of analytical solutions based on the standard hydraulic testing procedures and equations is invalid under certain conditions and will yield incorrect estimates for the formation parameters. It is essential in the analysis of the hydraulic testing data, to incorporate all important parameters and test conditions.

The problem of quantitatively describing borehole pressure history, thermally-induced pressure responses, borehole/formation skin effects and other factors in hydraulic tests was approached by the development and application of a model to meet the following objectives: (1) assist in understanding of the relative importance of various parameters and conditions on the borehole pressure response

during hydraulic testing, and (2) provide an analytical capability for analysis of hydraulic tests which includes the important phenomena. In order to simulate the system behavior, it was first necessary to develop an appropriate mathematical model. Since the task at hand was to simulate system response to special testing conditions which are represented as mathematically complex boundary conditions, a numerical modeling approach was selected.

Prior to development of the numerical model, the modeled system specifications were developed. For the borehole simulation model, the conceptualization of the actual physical system was simplified by the following assumptions:

- the formation whose response is being simulated is homogeneous (vertically), is confined, has a constant thickness, and has a finite radius centered upon the borehole;

- the major influence on the formation behavior is the borehole and conditions imposed in the borehole;

- all flow is radially away from or towards the test interval of the borehole;

- the pressure in the formation is uniform and constant radially at the start of a drilling period or a test sequence; and

- the effects of fluid temperature changes in the formation may be neglected in comparison to any thermally-induced pressure changes in the borehole during testing.

Given the above assumptions, a numerical model of the physical system was developed using a generalized Graph Theoretic Field Model (GTFM) approach. The details of the mathematical model, GTFM, and its development, verification

and application is documented in Grisak et al. (1985) and Pickens et al. (1987). The interested reader is directed to the original references for more details on the approach and test cases. The following paragraphs provide an overview of the approach and capabilities of the model.

GTFM constitutes a generalized methodology for modeling the behavior of field or continuum type problems. GTFM is based upon linear graph theory, continuum mechanics and a spatial discretization procedure. Savage and Kesavan (1979) present generalized descriptions of the methodology. The GTFM methodology as applied to the physical system under consideration results in an identical set of algebraic equations as would be derived using finite-element or finite-difference methodologies.

The GTFM simulation model is capable of handling the following conditions:

- borehole pressure history;
- isothermal and non-isothermal fluid conditions in the borehole;
- fixed pressure, pumping, pulse test and slug test sequences;
- fixed-pressure or zero-flow outer boundary; and
- borehole/formation skin effects.

There are two physical boundaries in the modeled system: the internal boundary at the borehole and the external boundary at the outside radius of the formation. The boundary condition at the external boundary can be either constant pressure or zero flow. Boundary conditions at the internal boundary are a function of the type of test being simulated.

The model was designed to simulate tests consisting of multiple consecutive test sequences, where each test sequence is one of four types: pumping, history, slug or pulse. Pumping sequences correspond to a specified flow boundary condition applied at the borehole. A wellbore storage boundary condition can be incorporated with the specified flow. History sequences are intended to be used for including the effects of pre-test borehole history in a test. A history sequence is modeled as a fixed-pressure boundary condition at the borehole. Slug sequences model the response of the formation to an instantaneous pressure change in an open well or borehole or in an open tubing string connected to a packer-isolated test interval. Pulse sequences model the response of the formation to an instantaneous pressure change in a shut-in test interval. Pulse sequences can be isothermal or non-isothermal. For the latter, the effects of temperature changes in the shut-in section of the borehole are incorporated in the simulation.

Hydraulic testing of a borehole interval usually involves a sequence of tests, each of which affect the measured pressure response of subsequent tests. The model presented here can be used to simulate multiple tests (i.e., test sequences) by using the pressure value at each node of the model grid at the end of a test as the initial condition for the subsequent test.

4.3 Hydraulic Test Interpretation Approach

This section describes the approach used in interpreting the sequences of hydraulic tests conducted in the Riniken borehole. In general, the interpretation approach consists of estimating the borehole pressure history for the test zone during the drilling phase and between drilling and the start of testing, borehole temperature and the physical properties of the formation, fluid and test interval and then by selecting a range of values for hydraulic conductivity and

formation pressure, generate, using GTFM, a series of simulated pressure curves for each hydraulic test. Hydraulic properties are adjusted until a best-fit simulation is obtained. The hydraulic properties used in the simulations are meant to describe the test interval. Once a best-fit case has been established, sensitivity studies can be conducted to determine the influence of the more uncertain parameters on the interpreted hydraulic conductivity.

An example is presented which illustrates the various components of the analysis approach including the determination of the borehole pressure history and the temperature at the test interval, the selection of appropriate parameters and estimation of the formation hydraulic properties and calibration of formation pressure. The interval selected as an example is test 1100.2S which was conducted in the Riniken borehole at an apparent depth of 1093.60 m to 1106.70 m on 14 and 15 October, 1983. This test sequence is appropriate because it represents a complex interpretation involving borehole history effects, a temperature change during testing, hydraulic conductivity determination and formation pressure calibration.

The specifications and characteristics of the formation, the borehole and equipment configuration are given in Table 4.2. All of this information is obtained from borehole geological logs (i.e., rock type, fractures, drilling period, etc.), geophysical surveys (i.e., borehole diameter, true vertical depth) and field hydraulic test reports (i.e., equipment configuration, depth interval, borehole temperature and testing sequences). The testing sequence for 1100.2S is illustrated in Figure 4.5 and consisted of a slug withdrawal test (Sw01), two pulse withdrawal tests (Pw01 and Pw02), and a pulse injection test (Pi01). The slug withdrawal test was unsuitable for analysis because of its short duration and insignificant pressure response.

4.3.1 Initial Conditions

4.3.1.1 Borehole Pressure History

The borehole pressure history for test 1100.2S consists of three components: an open borehole period (i.e. at annulus pressure), a packer compliance period, and a shut-in period which occurred immediately prior to testing. The borehole pressure history is illustrated in Figure 4.6. The drilling of the test interval began on 13 October, 1983 at approximately 03:30 and continued until 12:00 on 13 October, 1983. The middle of the drilling period is estimated at 07:45 on 13 October. After drilling, the interval was exposed to open borehole or annulus pressure conditions. The annulus pressure was determined from the hydraulic test field reports using the P3 transducer reading (which measures annulus pressure) of 11580 kPa. The annulus pressure was imposed upon the test interval from the middle of the drilling period to the start of the equipment compliance, a period of 29 hours. The test interval was isolated between a single packer and the bottom of the borehole. Following packer inflation, the test interval was subjected to an equipment compliance period of about 1.5 hours. The interval was exposed to an average pressure of 10822 kPa during this period. The shut-in period which immediately preceded testing exposed the test interval to a pressure of 10915 kPa over a period of one hour.

The length and magnitude of these pressure conditions described above are input to GTFM in order to define the pressure disturbance surrounding the borehole (i.e., the pressure transient) prior to the start of testing.

4.3.1.2 Temperature Profile

During test 1100.2S, the temperature of the borehole fluid measured at transducers T1, T2, and T3 increased from 51.6 to

57.0°C. The temperature data for test 1100.2S is given in Figure 4.7 and illustrates the trend of the temperature change as discussed above. From a review of the temperature data of T1, T2 and T3, this warming trend was considered to be representative of the change in test interval temperature. In order to incorporate the temperature change in the analysis technique, the measured temperature data is simulated using either a polynomial or cubic spline approximation and the approximated (smoothed) temperature response is input to GTFM such that the simulated pressure response is corrected for, in this case, fluid thermal expansion resulting from the temperature increase with time.

4.3.1.3 Parameter Selection

The list of parameters chosen for the analysis of test 1100.2S are given in Table 4.3. The most representative formation compressibility was estimated to be 9.0E-11 Pa^{-1}. This value is based on a literature review of values of Young's modulus and Poisson's ratio for a sandstone material. The formation compressibility (and corresponding specific storage) reported in the table was used in simulating the measured pressure data.

The effective formation porosity was estimated to be 15 percent based on a literature review of reported values for sandstone and considering the presence of some breccia within the test zone which could increase porosity.

The fluid compressibility has been estimated by assuming a pure-water (deionized water) compressibility and correcting for temperature and pressure at the test interval (see Figure 4.1). In this case, the average fluid temperature in the interval of about 55.5°C and average pressure of 10525 kPa (105.3 bar) (i.e., approximate formation pressure) results in a fluid compressibility of 4.34E-10 Pa^{-1}.

In a similar fashion, the fluid density and thermal expansion coefficient are corrected for formation temperature and pressure to result in values of 989 kgm^{-3} and 4.8E-04$°C^{-1}$, respectively.

The specific storage can be calculated using the formation compressibility, porosity, fluid compressibility and fluid density to yield a value of 1.5E-06 m^{-1}.

The test interval length is the distance from the bottom of the single packer to the bottom of the borehole. The borehole diameter at the time of testing was taken as the drilled borehole diameter.

4.3.1.4 Sequential Test Set-Up and Simulation

Once the borehole pressure history and temperature profile have been determined and the fluid, formation, and test interval parameters have been measured or estimated, the hydraulic test sequence can be set-up. The packer tests to be interpreted at each interval must be analyzed in the sequence in which they were conducted. This is necessary as the pressure disturbance around the borehole is modified by each preceding test.

For the pulse tests conducted at 1100.2S, the initial pressure imparted to the test zone after overpressuring or underpressuring the tubing string is specified in GTFM as the starting pressure in the test interval. For example, test Pw01 shown in Figure 4.5 has a starting pressure of 8681 kPa, test Pw02 shows a starting pressure of 9331 kPa, and test Pi01 shows a starting pressure of 11523 kPa. The pressure record at the start of each test must be carefully examined to determine the true starting pressure. Fluctuation in the pressures at the start of a test can be caused by movement of the shut-in valve, equipment compliance and problems with the injection pump at ground surface. The early time of all

tests is examined for the start of a regular pressure response and this starting pressure is specified in the simulation model. The duration of each test is specified while assembling the test sequence and the nature of the transient time stepping through the test must be specified by the analyst. By correctly specifying the initial pressure of each test sequence in GTFM, the simulated hydraulic response can be more readily compared to the measured response for each hydraulic test.

As part of the set-up of a pulse test simulation in GTFM, the analyst needs to specify whether the fluid temperature within the test interval is constant or varying. On specifying a variable fluid temperature, as would be the case for the pulse test sequence of test 1100.2S, the temperature change of the borehole fluid described by the temperature curve for the period of the pulse testing is applied to the calculated borehole pressures to correct the rate of pressure change for a temperature change. An indication of the representativeness of the measured temperature change can be seen in the concordance of the simulated pressure curve with the measured data. A simulated pressure curve for a pulse test which does not show the same shape as its measured counterpart possibly indicates that the measured temperatures were not representative of the test interval.

4.3.2 Initial Estimation of Formation Pressure, Hydraulic Conductivity and Specific Storage

Using the GTFM approach or computer-implementation of an analytical solution for hydraulic test interpretation requires that an initial estimate of formation pressure, hydraulic conductivity and specific storage be specified to model a test. The initial estimate of formation pressure has been determined using four different approaches in Riniken. For tests completed in lower permeability zones where recovery to static was not obtained and where the history

period was significant, the fluid pressure in the formation was assumed equal to either the mud-filled annulus pressure or the recovery pressure from one of the hydraulic tests. This approach assumes that the pressure transient around the borehole at the start of testing, which results from the history pressure period, will dominate during the test recovery, an assumption which generally is valid when the pressure transient extends into the formation beyond the outer influence of the hydraulic test. Tests 234.0D, 325.4D, and 368.2S, to name several examples, were interpreted in this manner. Since these pressures represent a local condition around the borehole during testing and not a static formation pressure, then they are referred to as reference pressures in this report. Another approach to determining formation pressure is useful when the formation is of relatively high permeability and the history period is of short duration. Under these conditions, the formation pressure can be taken as the pressure which is used to obtain the most accurate simulation of the last part of the measured pressure recovery curve. This method is referred to as pressure calibration and is discussed further below. This approach provides the most accurate estimate of an undisturbed formation pressure. This approach is used in the interpretation of test 513.0D. If the testing conditions are such that a DST pressure recovery is not influenced by pressure history then a Horner-type graphical analysis of the pressure data can be used to determine static formation pressure. Horner analyses were used on tests 515.7S, and 965.5D. When an interval is located adjacent to or between intervals at which the static formation pressure has been accurately determined, then the formation pressure for this zone may be extrapolated or interpolated from the adjacent known values. The initial estimate of formation pressure for test 1389.1D was derived in this manner.

The average hydraulic conductivity of the test intervals of the Riniken borehole was determined using one or more of the following approaches. These include the Horner graphical approach, type curve graphical techniques, computer implementations of analytical solutions and the GTFM method. The first two techniques do not require initial estimates of hydraulic conductivity and can be solved directly using information from the pressure-time plot or using match-point information from a suite of type curves. For the computer-analytic and numerical techniques, initial estimates of K are required. It is often necessary to choose three or four values which are separated by one order of magnitude in order to provide a wide enough range for the simulated responses to bracket the measured pressure response. The measured recovery rate of the hydraulic test response for various test types can be used as a general indication of the required range of hydraulic conductivity values. For test intervals with hydraulic conductivities less than 1E-10 ms^{-1}, slug tests do not show an appreciable pressure recovery while for hydraulic conductivities greater than 1E-07 ms^{-1} pulse test recoveries are almost instantaneous. This is combined with an understanding of recovery rates for slug and pulse tests at various formation hydraulic conductivities. An example of a preliminary assessment of hydraulic conductivity for test 1100.2S would be using the Pw01 data which shows close to 90 percent pressure recovery in about 1.7 hours. From previous test interpretations, this rate of recovery would indicate a low hydraulic conductivity on the order of 2.0E-10 ms^{-1}. The initial range of hydraulic conductivity used to attempt to bracket the test response was 1.0E-10 ms^{-1} to 3.0E-10 ms^{-1}.

When required, the initial estimate of the formation specific storage is taken as the base case value calculated from the fluid compressibility, average porosity, and average rock compressibility. During the initial simulation of the

pressure-time data, to determine the bounding values of hydraulic conductivity, a single specific storage is specified.

4.3.3 Iterative Approach for Solving for Formation Pressure, Hydraulic Conductivity and Specific Storage

To start the test analysis using a simulator such as GTFM, the simulated pressure-time curves are generated for an initial value of formation pressure, specific storage and an estimated range of values for hydraulic conductivity which are intended to bracket the data. In this case the hydraulic conductivity is a variable parameter and the rest of the parameters (i.e., formation pressure, specific storage, etc.) are constant. The simulated pressure curves can be compared to the measured field data to determine if the shape of the hydraulic conductivity-dependent curves are similar to the field data and if the final pressures of the simulated curves are similar to the final pressures of the field data. If the shape of the pressure curves does not match the field data (i.e., simulated pressures are too high or too low) the hydraulic conductivity values need to be adjusted to provide a more suitable fit. By using a sufficiently wide range of initial values of hydraulic conductivity it is often possible to bracket the field data and then refine the hydraulic conductivity values to obtain a best-fit thus minimizing the number of iterations.

For those tests in permeable zones which are not influenced significantly by pressure history or thermal effects, the measured pressure approaching complete recovery should match the simulated response. Otherwise, the formation pressure needs to be adjusted to obtain this match. The formation pressure that is used to obtain the most representative simulation is called the calibrated formation pressure. Essentially, for the tests that can be calibrated, GTFM is being used as a technique for solving for static formation

pressure in partial test responses where, had the tests been allowed to recover completely, the recovery would have been to the static formation pressure.

Assuming that the borehole history, thermal response, and formation pressure are accurate, the analyst can vary hydraulic conductivity and specific storage in order to improve the simulated fit. Usually, varying specific storage by one order of magnitude above and below the base case value is reasonable to describe the natural variability in the porosity and rock compressibility of the formation. The formation specific storage value which provides the best fit to the measured data is reported in the summary table of formation and fluid parameters for each interval.

4.3.4 Sensitivity of Best-Fit Hydraulic Conductivity to Variation in Specific Storage

For several of the test intervals (i.e., 513.0D and 1358.9D) the sensitivity of the interpreted K to variability in specific storage was evaluated. This was not conducted for the remaining tests because in the earlier test interpretations completed by INTERA and reported to Nagra in July, 1984, of which the results are summarized in this report, the specific storage of the formation was not treated as an uncertain variable. The iterative approach to determining hydraulic conductivity, as discussed in Section 4.3.3, provides a best-estimate of this parameter based on a base-case value of specific storage determined from the literature. Given the probable heterogeneity of the formation adjacent to the borehole and the range of compressibility calculated from stress and strain data in the literature for a particular rock type, it is reasonable to assume that specific storage could vary by as much as two orders of magnitude. It was found that the interpreted hydraulic conductivity is relatively insensitive to specific storage variability for hydraulic conductivities greater than

1.0E-10 ms^{-1}. The effect of varying specific storage for hydraulic conductivity less than 1.0E-10 ms^{-1} can be significant with uncertainty in hydraulic conductivity up to one order of magnitude depending on the choice of the specific storage for the interval.

4.4 Propagation of Instrumentation Uncertainties in the Determination of Equivalent Freshwater Head

The two primary formation properties obtained from the borehole tests described above are formation pressure and hydraulic conductivity. Equivalent freshwater head can be computed by substituting formation pressure and appropriate measured or estimated values into equations 4.1-8 to 4.1-10. For the most part these measured or estimated values have a quantifiable degree of uncertainty which can be used to generate corresponding uncertainty surrounding reported head values. Determination of hydraulic conductivity involves more complex data fitting with use of tools such as GTFM. The uncertainties involved in this data-fitting interpretation process are not as readily quantified and are beyond the scope of the current effort. Thus, this section only addresses the uncertainty in freshwater head calculations.

Typically, equivalent freshwater head is determined from equation 4.1-10 by substituting best-estimate values for the input variables appearing on the right hand side of the equation. These best-estimates are based either directly or indirectly on measured quantities. The objective of the uncertainty analysis presented in this report is to quantify the uncertainty surrounding the reported head values arising from the measurement errors that could be present in the best-estimates.

Accuracy and resolution specifications for measuring instruments are used whenever possible to determine uncertainty ranges for the input variables. Input variables are then assigned probability distributions that cover their uncertainty range. Section 4.4.1 describes the assumptions made for each input variable.

The approach taken to propagate input variable uncertainties to uncertainty in freshwater head involves statistical sampling and multiple evaluations of equations 4.1-8 to 4.1-10. The statistical properties of the resulting distribution of head values can be examined and those input variables contributing most to the uncertainty in head can be identified. The procedures used are discussed in Section 4.4.2 and the results are presented in Section 6.

4.4.1 Independent Variables

This section quantifies the uncertainties that can be attributed to measurement errors for the variables of equations 4.1-8 to 4.1-10. The order of the discussion in terms of variable symbols is: d_{ct}, P_{atm}, ρ_f, Z, d_c (and d_{cs}), g, P_{ft}, and ρ. Pressure at formation center, P_{fc}, is not on the list since equations 4.1-8 and 4.1-9 can be substituted into equation 4.1-10 thereby eliminating P_{fc}. In practice, however, equations 4.1-8 and 4.1-9 are evaluated separately and pressure at formation center is reported as the second output variable (after equivalent freshwater head). Further, as will be seen, gravity is treated as a function of surface elevation, depth, and average rock density from surface to depth. Thus, gravity is also reported as an output variable and rock density, ρ_r, is treated as an input variable.

The first variable examined is d_{ct}, the true vertical distance between the transducer and the center of the interval. Variable d_{ct} is used whenever equation 4.1-8 is applicable and is found by subtracting the apparent vertical

depth to the transducer from the apparent vertical depth to the interval center. Since this is a relatively short distance, any cumulative deviation from vertical at one depth should be approximately the same as at the other. Thus, by subtraction, deviation errors will tend to cancel. Further, since tubing stretch can be accurately predicted (Baker, 1985) and is accounted for in reported apparent depths, that potential source of uncertainty need not be addressed. Therefore, d_{ct} is considered a known, fixed value for the uncertainty analysis.

The second variable is P_{atm}, the barometric pressure. For the transducer monitored tests, formation pressure is normally calibrated during shut-in conditions. Under those conditions, changes in atmospheric pressure have little affect on downhole pressure measurements. For water level tests, water levels are converted to pressures and a fixed value for P_{atm} is added (equation 4.1-9) prior to calibration with GTFM. The same fixed value is then subtracted in equation 4.1-10. Thus, changes in barometric pressure with time are not treated for water level tests. For these reasons, the average fixed value reported for each test is not varied in the uncertainty analysis.

The third variable is ρ_f, a reference density for fresh water. Since the only purpose of ρ_f is to establish a convention for reporting head values, any reasonable value can be used. Earlougher (1977) reports 999.014 kgm^{-3} at 15.56°C. Other pure water densities that could be used are 998.23 kgm^{-3} (at "standard conditions", one atmosphere pressure and 20°C), 999.87 kgm^{-3} (at standard temperature and pressure, one atmosphere and 0°C), or 1000 kgm^{-3} (at one atmosphere and 3.98°C) (Weast, 1982). This report adopts 1000 kgm^{-3} primarily to be consistent with other reports describing interval hydraulic testing and long-term monitoring in the Boettstein, Weiach, and Leuggern boreholes.

The fourth variable is Z, the height above sea-level of the top of the borehole. Surface elevations are assumed to be accurate to ±10 cm (±.10 m). Thus, for the Riniken borehole, the true surface elevation is in the range 384.97 m to 385.17 m. In the absence of any detailed data on the behavior of the measurement error, these extremes are considered to be the 0.1 and 99.9 percentiles of a normal distribution. The percentiles are labeled on Figure 4.8 along with the mean, Z, and one standard deviation.

The fifth variable is d_c, the true vertical depth from the borehole surface to the interval center. Also discussed here is d_{cs}, the true vertical length of the water column. Variable d_{cs} is found by subtracting the measured water level depth below surface from d_c. Since the water levels are near-surface and since the water-level measurement errors are assumed to be small, uncertainty in d_{cs} is approximately equal to that of d_c.

True vertical depth is derived from apparent vertical depth using a gyro or similar survey as described in Section 2. Uncertainties in true depth can arise from at least three sources,

- uncertainties in the apparent depth,
- the measurement gradation with depth in the borehole and resulting interpolation of deviation angles to predict true depth, and
- instrumentation accuracy.

The apparent depth is based on cumulative tubing length adjusted for tubing stretch. As stated above for variable d_{ct}, the uncertainty analysis assumes that insignificant errors are introduced in the prediction of tubing stretch. Thus, uncertainty in apparent depth is based on measurement error for individual tubes and inconsistent joining of the tubes. As indicated by the Riniken field reports, tubing lengths are measured to the nearest centimeter, suggesting a

±0.5 cm rounding error for each tube. Error in total tubing length can also be introduced at the joints. Although tubing is joined using a specified torque, the connections are not necessarily subject to the same threading overlap. Reducing the measurement error by a factor of two (to account for the probable error cancellation caused by summing rounded numbers), and assuming a ±0.1 cm per tube threading error, gives a total error in apparent depth of ±0.35 cm per tubing length. The error range, 0.7 cm/tube (0.00077 $m \cdot m^{-1}$ for an average 30-ft tube), is folded into the general error expression presented below.

The summary report for apparent versus true vertical depth for the Riniken borehole (Weber et al., 1986) is graded with 50 m intervals of apparent depth. Deviations between data points can contribute to uncertainty in the interpolations used to derive true vertical depth. For example, if the borehole is assumed to follow a straight line between two data points, the derived true vertical depth is smaller than the depth derived assuming the hole follows a true vertical direction for some distance then deviates. The extent of uncertainty can be as large as 0.5 cm/data interval or 0.0001 $m \cdot m^{-1}$. Accuracy and resolution of the instrument used to measure angular deviations also propagate through the interpolation scheme. A SHDT tool was used for deviation logging with a reported accuracy of ±0.2°. Applying this uncertainty band to a total effective straight-line deviation leads to 0.23 m uncertainty at 1800 m depth or 0.00013 $m \cdot m^{-1}$. If all 3 error ratios are added and applied linearly with depth, the error multiple used for the Riniken borehole is 0.001 $m \cdot m^{-1}$. At any depth the range of uncertainty is applied symmetrically about the depth as shown in Figure 4.9, where 0.0005 is one half the multiplier 0.001. The depth variable is assigned a uniform probability distribution so that values at the extremes of the range are sampled with the same frequency as those near the midpoint of the range.

The sixth variable is g, the acceleration due to gravity. It is generally considered constant at a given latitude. However, it varies with depth and is affected by earth tides and nearby large topographical features. The latitude at the Riniken borehole is 261,899.5 m north of 45°, which is approximately 47.36°. Using the International Gravity Standardization Net 1971, IGSN 71, (Tsuboi, 1983), the equation for g (cms^{-2}) at any latitude ϕ (degrees) is

$$g_\phi = 978.03185\ (1 + 5.3024 \times 10^{-3} \sin^2\phi - 5.9 \times 10^{-6} \sin^2 2\phi) \qquad (4.4\text{-}1)$$

Thus, at $\phi = 47.36°$, $g_\phi = 980.832$ cms^{-2} at sea level. The equation for g_ϕ is derived from an ellipsoidal fit of worldwide gravity data that is subject to refinement with time. Woollard (1979) states that IGSN 71 is in general accurate to within ±0.05 mgal (±0.00005 cms^{-2}), which does not affect the signifance of g_ϕ calculated above. Below land surface two corrections to g due to depth are considered. The first is a free-air correction and the second is the simple Bouguer reduction. In gravitational units (1 g.u. = 0.0001 cms^{-2}) these corrections are given by (Parasnis, 1972)

$$\Delta g = 3.086\ (d_c - Z) - 0.4191\ d_c\ \rho_r \qquad (4.4\text{-}2)$$

where Δg = total elevation correction (g.u.);
ρ_r = average rock density from surface to d_c (gcm^{-3}).

Earth tides can affect g by at most 3 g.u. and topographical features may reduce g by a few tens of g.u. However, for the depths examined at the Riniken borehole, the correction term in equation 4.4-2 is in thousands of g.u., implying that the effects of earth tides and topography can be ignored for this application. Therefore, the combined expression used for g (cms^{-2}) is

$$g = g_{\phi} + \Delta g/10^4 \qquad (4.4\text{-}3)$$

In this analysis Δg is uncertain since Z and d_c are uncertain as described above. Furthermore, the rock density factor, ρ_r, is a length-averaged density subject to uncertainty. Minimum and maximum densities for each rock-type (Touloukian et al., 1981) encountered from surface to depth are thickness-weighted to determine the total average rock density range. Thus, the range varies from test interval to test interval and only a generic representation for ρ_r can be shown (Figure 4.10). The minimum and maximum values found are treated as the 0.1 and 99.9 percentiles of a normal distribution.

The seventh variable is P_{ft}, the fluid pressure measured at the P2 transducer. The accuracy and resolution of the transducer can vary from test to test depending on the transducer model and tool used. For all tests for which uncertainty is examined, a HTT was used. Since transducer model numbers and specifications are not fully reported, obtaining the exact transducer specifications for each test is difficult. For this reason a generic set of specifications have been adopted for pressure transducers. Typical of such tools is an operating range of 0 - 6000 psi (0 - 41370 kPa), having full scale accuracy and resolution of ±3.0 psi (20.7 kPa) and ±0.3 psi (±2.07 kPa), respectively. Assuming that the accuracy bounds do not account for resolution error, the accuracy and resolution bounds are additive, so that any measured value may be in error by ±22.8 kPa. Errors in the pressure readings can also be caused by transducer drift. However, unless there is evidence to the contrary, such as large differences in the before and after test pressure readings, it is assumed that drift is included in the scale accuracy uncertainty. For the tests analyzed at the Riniken borehole, observed transducer drifts remained less than 10 kPa. The distribution on P_{ft} is therefore based only on performance specifications. It is assumed to be a

normal distribution with the 0.1 and 99.9 percentiles defined as P_2 - 22.8 and P_2 + 22.8, respectively, where P_2 is the reported pressure at transducer P2. This is equivalent to a normal distribution with mean P_2 and standard deviation 7.38 kPa as shown on Figure 4.11.

The eighth variable is ρ, the fluid density within the borehole, rather than the in-situ fluid density discussed in Section 4.1.4. For the purposes of equations 4.1-8 and 4.1-9, it should be the fluid density between the point of physical measurement and the interval center. For six of the tests (513.0D, 515.7S, 805.8S, 965.5D, 1100.2S, and 1262.2D) the point of physical measurement is the location of the transducer at P2. For the other two tests analyzed here (654.4PV and 1709.2D), the point of physical measurement is the top of the water column in the open borehole measured by the water level monitoring device. Estimation of the densities in the appropriate portion of the borehole requires information regarding temperature, pressure, and salinity of the resident fluid. The following list summarizes the mean densities used and the remainder of this section discusses the justification for each value:

Test Designation	Density kgm^{-3}
513.0D	995.5
515.7S	1057.2
654.4PV	1007.1
805.8S	996.2
965.5D	1226.7
1100.2S	1149.7
1262.2D	1047.0
1709.2D	990.3

Density at a given temperature, pressure, and salinity is determined by adding a correction term to the density measured at known temperature and pressure. The laboratory or on-site measurement is used to account for density due to dissolved solids. The correction term accounts for the affect of in-situ temperature and pressure on density and is developed using the freshwater densities of Table 4.1, as described in Section 4.1.4. If temperature and pressure at all depths are known, then the density correction term can be treated as a function of depth. Since the temperature of the actual fluid in a test interval is not typically measured, this analysis uses average temperature and pressure relationships with depth. Temperature is approximated using a gradient of 0.0394°C m^{-1} and a surface temperature of 17.3°C. This relationship is a least-squares fit of temperature data obtained from hydraulic tests and a high resolution temperature (HRT) log. The maximum differences between observed temperatures and those produced by the data-fit are used to define the ±2°C uncertainty band for temperatures at the Riniken borehole. Fitting pressure data as a linear function of depth yields a surface pressure of 3.7 atm and a gradient of 0.094 atm m^{-1}. The differences between predicted and observed pressures for depths between 500 m and 1700 m can be as large as ±6 atm. Since the prediction error for ±2°C (about ±1 kgm^{-3}) is nearly four times the prediction error for ±6 atm (about 0.26 kgm^{-3}), pressure effects are ignored in computing uncertainty bounds for density. However, pressure effects are accounted for in computing the mean density, as shown below.

For any depth, d, the temperature at d, T_d (°C), and the pressure at d, P_d (atm), are first estimated using the equations:

$$T_d = 0.0394d + 17.3 \qquad (4.4\text{-}4)$$

$$P_d = 0.094d + 3.7 \qquad (4.4\text{-}5)$$

Table 4.1 is then interpolated linearly to approximate the density of fresh water, ρ_{fd}, at T_d and P_d. Finally, if the density of a fluid sample taken at depth d, ρ_{cd}, has been measured at 20°C and one atmosphere, then the fluid density at d, ρ_d, is determined by:

$$\rho_d = \rho_{cd} - (998.00 - \rho_{fd}) \qquad (4.4\text{-}6)$$

Here, as indicated in Table 4.1, the density of freshwater at 20°C and one atmosphere is taken to be 998 kgm^{-3}. Uncertainty is folded into the density at d by interpolating ρ_{fd} at T_d ±2 and P_d from Table 4.1 to determine the correction term extremes.

The procedure described in the preceding paragraph is used to calculate fluid density at a point. For the six transducer monitored tests mentioned above, the point of interest is taken to be the true vertical depth to interval center. Since the distance between the interval center and transducer is relatively short (less than 30 m), the density at the transducer is considered equal to that at the interval center. For the two water-level tests, the density variation from near-surface to interval center is too large to be ignored. The variation is accounted for by averaging the density due to dissolved salts and using an average temperature- and pressure-correction term (depth-integrated density).

Theoretically, the depth-integrated freshwater density to depth d is an integral,

$$\rho_{fdi} = (1/d) \int_o^d \rho_{fz}\, dz \qquad (4.4\text{-}7)$$

The integral of equation 4.4-7 is approximated using the trapezoid rule (James et al., 1968) with 100-m subintervals. The density at depth z, ρ_{fz}, is determined using equations 4.4-4 and 4.4-5. Uncertainty is included in ρ_{fz} due to the temperature uncertainties mentioned above, giving rise to an

uncertainty range for ρ_{fdi}. To then take average salinity into account, ρ_{fdi} is substituted into equation 4.4-6 in place of ρ_{fd}.

The remaining uncertainty on density is the variation of concentration of total dissolved solids in the fluid during the test. For the eight tests analyzed here, the borehole fluids are composed of mixtures of drilling fluids (drilling mud or deionized water) and formation fluids. These compositions change with time due to swabbing, which can introduce formation fluid into the borehole. For some tests the estimated densities at the beginning and ending of the test are used to define uncertainty ranges. Whenever formation fluid densities are used to determine densities of mixed fluids, density measurements are taken from Pearson and Lolcama (1987). The available information does not indicate the type or precision of the hydrometer used to measure the densities reported in Pearson and Lolcama (1987). To ensure that density uncertainties are covered, accuracy specifications for a multi-purpose hydrometer (rather than a precision hydrometer) are adopted. Formation densities for fluid samples taken at the Riniken borehole are therefore assumed to be accurate to ± 1.5 kgm^{-3}.

Deionized water was used for pre-test flushing of the borehole and sometimes as drilling fluid. In practice, a borehole is assumed flushed if the electrical conductivity reading of the near-surface circulated fluid stabilizes in the range of 100 to 200 μScm^{-1}. To account for this slight salinity, the density of "deionized" water at 20°C and one atmosphere is chosen to be 998.3 kgm^{-3} throughout the uncertainty analysis. For the remaining part of this section densities due to salinity refer to density at 20°C and one atmosphere. Densities are subsequently adjusted to borehole temperature and pressure using the corrections above.

For the two water-level tests conducted at the Riniken borehole and analyzed here, the borehole was flushed with deionized water prior to testing. For the bottom hole test (1709.2D), the flow of formation fluid into the borehole interval is probably small enough to be ignored, so that the average density due to salinity is 998.3 kgm^{-3}. For the test 654.4PV, sufficient fluid was pumped to replace the deionized water in the borehole between the pump (located at a depth of about 180 m) and the Muschelkalk with fluid from the Muschelkalk. At its minimum, the water level in the borehole was 40 m above the pump. Thus, near the time of recovery, the fluid shows a deionized water/formation water ratio of about 6/94. Density of the upper Muschelkalk formation fluid has been measured at 1009.7 kgm^{-3} under laboratory conditions (Pearson and Lolcama, 1987). The salinity-averaged density is therefore 1008.5 kgm^{-3}. The depth-integrated temperature and pressure corrections are calculated to be -1.4 kgm^{-3} and -8.0 kgm^{-3} for 654.4PV and 1702.2D, respectively.

For uncertainty calculations, the ±2°C temperature uncertainty band is propagated through the depth-integration computations to provide a range around the mean values. In addition the density measurement of the Muschelkalk formation fluid (representing 94 percent of the fluid mix for the test 654.4PV) is assumed accurate to ±1.5 kgm^{-3}. Combining the uncertainties, the minimum densities obtained for 654.4PV and 1709.2D, ρmin, are 1005.6 and 989.4 kgm^{-3}, respectively. The maximums, ρmax, are 1008.7 and 991.2 kgm^{-3}. These bounds are used as the endpoints of a uniform distribution as shown in Figure 4.12.

The density due to salinity for the remaining six analyzed tests is for the most part not as straight forward. The intervals of interest most likely contain mixtures of the drilling fluid (mud or deionized water) and formation fluid. Prior to test 513.0D the borehole was flushed with deionized water. Testing commenced 0.5 days later so that the water in

the interval remained essentially unchanged. Test 805.8S began with near deionized water in the test interval since that was the drilling fluid used. Sufficient volume was swabbed during testing to remove the test-interval volume more than once. Thus, by test end the test-interval fluid density was close to the formation fluid density of 1006.1 kgm^{-3}, reported in Pearson and Lolcama (1987). Since the calibrated formation pressure was determined using data throughout the testing period, neither the starting or ending density appears to be more applicable. Thus, the midpoint density, 1002.2 kgm^{-3}, is adopted.

For the remaining 4 tests, density is assumed to be that of the drilling mud at the beginning of the test period. These densities are 1100.0, 1260.0, 1190.0, and 1100.0 kgm^{-3} for tests 515.7S, 965.5D, 1100.2S, and 1262.2D, respectively. For tests 515.7S and 965.5D, the density at the end of testing is taken to be that of the 3rd and 9th swabs, respectively, that were withdrawn during the borehole cleaning period. According to tubing string volume, these specific swabs should have produced fluid closely approximating the test interval fluid at the time of test end. The ending densities are 1020.0 and 1210.0 kgm^{-3} for these two tests. For tests 1100.2S and 1262.2D, densities during the post-test swabbing period are not available. Thus, density reductions similar to those of tests 515.7S and 965.5D are assumed. The ending densities used are 1130.0 and 1020.0 kgm^{-3} for tests 1100.2S and 1262.2D, respectively. Again since the formation pressure is calibrated using data across the testing period, use of the midpoint of the starting and ending densities for each test is indicated. These averages are 1060.0, 1235.0, 1160.0, and 1060.0 kgm^{-3} for tests 515.7S, 965.5D, 1100.2S, and 1262.2D, respectively.

Due to the relatively large density differences between drilling mud and formation fluid, the borehole fluid density can change during the testing period by as much as 7 percent.

So, even though the test interval is short for tests 515.7S, 965.5D, 1100.2S, and 1262.2D, the density uncertainty is large. In fact, such uncertainty is considerably larger than uncertainty caused by instrumentation accuracy or temperature uncertainty. This is true to a lesser extent for test 805.8S. Thus, the beginning and ending densities (temperature and pressure adjusted) are used to define the uncertainty band for tests 515.7S, 805.8S, 965.5D, 1100.2D, and 1262.2D. Test 513.0D has uncertainty in density only due to temperature uncertainty. The minimum and maximum values for density are treated as the endpoints of a uniform distribution as shown on Figure 4.12.

4.4.2 Statistical Approach

The five variables of the previous section that are considered uncertain are surface elevation, true vertical depth to interval center, average rock density to that depth, pressure at the P2 transducer, and fluid density. Each variable has an associated probability distribution. All variables are sampled n times prior to model execution (i.e., evaluation of equations 4.1-8 to 4.1-10) using Latin Hypercube Sampling (LHS) (Iman and Shortencarier, 1984). Here, n is the user-specified number of trials and is set to 100 for the analysis. Thus, on every trial a sampled value for each of the five variables is used either directly or indirectly to solve equations 4.1-8 to 4.1-10.

LHS was introduced into the literature in 1979 (McKay et al., 1979). The motivation for the development of LHS was to improve sampling efficiency over the widely used Monte Carlo approach. In general, LHS produces smaller mean-square-errors of estimators than does Monte Carlo for small sample sizes. Thus, the number of trials can be smaller when using LHS. The mechanics of LHS are as follows: Each variable has its probability distribution partitioned into n intervals of equal area. A value is sampled randomly within each interval

with respect to the density function in the interval. These two steps help ensure that the entire range of uncertainty is covered even for smaller sample sizes. The n sampled values are then mixed in a prescribed manner and are entered as a column in the sample matrix. Thus for trial k, the 5 entries in the k^{th} row of this array are used as the values for the 5 input variables mentioned above.

All five variables are assumed to be uncorrelated. The sampling scheme attacks this problem by forcing the correlations among the ranks of the variables to be small. In fact this is a special case of a mixing scheme to induce any valid rank correlation structure amongst sampled variables. The technique used in treating the ranks of variables, as opposed to the values of variables, has the following desirable properties (Iman and Conover, 1982):

1. It is distribution free. That is, it may be used with equal facility on all types of input distribution functions.
2. It is simple. No unusual mathematical techniques are required to implement the method.
3. It can be applied to any sampling scheme for which correlated input variables could logically be considered, while preserving the intent of the sampling scheme. That is, the same numbers originally selected as input values are retained; only their pairing is affected to achieve the desired rank correlation. This means that in LHS the integrity of the intervals is maintained. If some lattice structure is used for selection of values, that same structure is retained.
4. The marginal distributions remain intact.

The current thinking for the hydraulic tests at the Riniken borehole is that there is no justification for inducing any nonzero rank correlations amongst input variables. However,

the capability is in place if future analyses indicate the need. Further, the concept of rank correlation is used in the analysis of the output, as discussed below.

One measure of the relative importance of input variables (the 5 discussed above) is the size of the correlations between the input variables and the response variable (equivalent freshwater head). The concept of correlations is illustrated in Figure 4.13. There is more of a trend evident between variable 1 and the response variable than between variable 2 and the response variable. Apparently variable 1 has a higher degree of importance in computing the response variable than does variable 2. A commonly used measure of the relationship between two variables is the correlation coefficient. Simple correlation coefficients provide a relative measure (from -1 to +1) of how well the observed variation can be explained by a linear relationship between two variables. For problems having non-linear relationships simple correlations may not provide an adequate measure of importance.

In this analysis the concept of rank correlations is used. For computation of correlations, each variable has its n values replaced by their ranks; the smallest having rank 1 and the largest having rank n. By using the ranks of the variables, any monotonic relationship between variables is transformed to a linear relationship. Thus, simple correlations on ranks can have broader application and can be more meaningful in some situations.

The concept of linear rank correlations is taken one step further. Simple correlations explain the variation of output to input while ignoring the presence of other input variables. Partial correlations explain the variation of output to a given input variable by systematically eliminating the effects of the other variables. In theory this involves the computation of the differences of the

observed values from those predicted by fitting a variable to be eliminated; and finding the simple correlation between the residuals. In practice, partial correlations are computed using selected entries taken from the inverse of the simple correlation matrix. In this analysis partial correlations on the ranks of variables are used as the primary measure of variable importance.

The size of the uncertainty about the mean freshwater head value is measured by the sample standard deviation. The mean and one and three standard deviations are routinely reported. In addition a histogram is shown of the head distribution for each test interval. Symmetry of the distribution, or lack of symmetry, should be readily apparent from the figure. An example histogram appears in Figure 4.14. Histograms for head are generated with the horizontal plot limits being the nearest integers that encompass the range.

The results for each test interval show the uncertainty of freshwater head due to instrumentation error, for the conditions of the test. Given that any required data interpretations are correct, that there was no operator error, and that instrumentation has operated within specifications, the equivalent freshwater head value should be contained in the reported uncertainty range. In addition to the examination of each individual test, general statements can often be made that apply to all tests. The general accuracy of freshwater head values throughout the borehole may be significant in predicting regional flow. Important input variables for the borehole may suggest the need for further examination of documentation or of refined testing procedures.

5. EXAMPLE FORMAT OF APPLICATION OF THE INTERPRETATION METHODOLOGY

This chapter provides an illustration of the application of the interpretation methodology for hydraulic conductivity and formation pressure for a selected test zone (965.5D) as discussed in Belanger et al. (1988). Full details on the interpretation of the hydraulic testing in all other test zones are provided in the same report.

Test 965.5D (958.40 m to 972.50 m)

The hydraulic tests completed at the depth interval 958.40 m to 972.50 m in the Riniken borehole included two drill-stem tests (DST01 and DST02), one pulse withdrawal test (Pw01) and two slug withdrawal tests (Sw01 and Sw02). Table 5.1 provides a summary of the borehole condition and equipment configuration during testing. The pulse withdrawal test was judged unsuitable for analysis due to abrupt, unexplained changes in the pressure recovery. The magnitude of flow from the test interval during the two drill-stem test flow periods indicates that the interval is of relatively high hydraulic conductivity.

The assumed pre-test borehole pressure history prior to the start of DST01 is shown in Figure 5.1. The history sequence includes a 43 hour open borehole period at a mud-filled annulus pressure of 12098 kPa. Other pressure conditions of shorter duration were imposed on the borehole due to tool malfunctions prior to testing.

The measured pressure response for the test sequence and the initial and final pressure of each test are shown in Figure 5.2. Test Pw01 and the build-up periods of tests DST01 and DST02 recovered to 99 percent of the estimated formation

pressure determined by Horner type interpretation of test DST01. Pressure recovery during Sw01 and Sw02 was 33 and 23 percent, respectively.

The two drill-stem tests were analyzed using the Horner method as discussed in Matthews and Russell (1967), Earlougher (1977) and Lee (1982). A summary of Horner analysis calculations from DST01 and DST02 are given below.

Figure 5.3 shows the Horner plot of pressure versus

$$\frac{t^* + \Delta t}{\Delta t}$$

Extrapolation of

$$\frac{t^* + \Delta t}{\Delta t}$$

to 1 yields a formation pressure of 9310 kPa.

A hydraulic conductivity of the formation was calculated as 4.0E-09 ms^{-1}, also based on the Horner plot.

Using the hydraulic test data for DST02, extrapolation to

$$\frac{t^* + \Delta t}{\Delta t} = 1$$

on the Horner plot of pressure data for DST02, yields a formation pressure of 9300 kPa (Figure 5.4). Hydraulic conductivity was calculated as 5.0E-09 ms^{-1}, from the Horner plot.

In summary, hydraulic conductivities calculated from the slope of the lines found in Figures 5.3 and 5.4 yield values of 4.0E-09 ms^{-1} and 5.0E-09 ms^{-1} for DST01 and DST02, respectively. The formation pressure is estimated to be about 9310 kPa at the transducer P2 depth of 953.69 m.

To obtain additional estimates of formation hydraulic conductivity, the data of the two slug withdrawal tests was analyzed by comparison of the measured pressure response to calculated pressure responses using a computer implementation of the Cooper et al. (1967) analytical solution. This solution requires an estimated formation pressure which was chosen based on the pressure determined from the drill-stem tests. Model parameters for the analytic solution are found in Table 5.2.

A hydraulic conductivity of 5.0E-09 ms^{-1} provides a reasonable simulation of the measured pressure data for Sw01 (Figure 5.5). The Cooper et al. (1967) solution for a hydraulic conductivity of 3.0E-09 ms^{-1} provided the best simulation of the pressure-time data for test Sw02 (Figure 5.6). The hydraulic conductivities for tests Sw01 and Sw02 are in good agreement with the hydraulic conductivities determined by the Horner method.

The hydraulic conductivities from the individual tests are summarized below:

Test	Hydraulic Conductivity Estimate (ms^{-1})	Figure
DST01	4.0E-09	5.3
DST02	5.0E-09	5.4
Sw01	5.0E-09	5.5
Sw02	3.0E-09	5.6

The geometric mean hydraulic conductivity of 4.0E-09 ms^{-1} from the four tests is considered representative for the test interval.

A formation pressure of 9451 kPa was calculated for the center of the test interval using an estimated borehole fluid density between the transducer and test interval center of 1226.7 kgm^{-3}, the assumed formation pressure at transducer P2 (9310 kPa) and the true vertical depth between the P2 transducer and the center of the test interval. Based on a freshwater fluid density of 1000 kgm^{-3}, the corresponding equivalent freshwater head is 372.8 m ASL. The borehole fluid density was taken as the average of the assumed density at the start and end of hydraulic testing corrected for temperature and pressure at depth (see uncertainty discussion).

The uncertainty in predicted equivalent freshwater head is shown on Table 5.3. There is a standard deviation of 0.82 m ASL about the mean, 372.8 m ASL. The true vertical depth to interval center ranges from 964.87 m to 965.83 m. Fluid density ranges from drilling mud (1260 kgm^{-3}) to a sample taken from the 9th swab after testing (1210 kgm^{-3}). Applying temperature and pressure effects at interval center gives a density range of 1201.7 to 1251.7 kgm^{-3}. No transducer malfunction was observed, so we assume the transducer performed within accuracy specifications throughout testing. From the partial rank correlations it is evident that the dominant cause for uncertainty in equivalent freshwater head is the uncertainty in the fluid pressure measured by the transducer at P2. In fact, the standard deviation of the pressure distribution (7.38 kPa) can be used to predict a large part of the standard deviation of equivalent freshwater head. True vertical depth is the second most important variable. The impact of the large density uncertainty is mitigated somewhat since it is applied to a relatively short distance (11.76 m).

6. RESULTS

Hydrogeologic interpretations were attempted on each of the 22 tests completed in the Riniken borehole. Representative formation pressures were determined from 8 tests. Formation pressures from each of these testing intervals are reported as equivalent freshwater head corresponding to the center of the tested formation or the center of the test zone. An estimate of uncertainty in freshwater head was determined based on quantifiable equipment uncertainty. Hydraulic conductivities were estimated from 19 of the tests in the borehole. These 19 tests covered 17 unique zones with two re-tested zones. Formation pressure, equivalent freshwater head, and hydraulic conductivity were plotted in profile for the borehole from 217 m to 1800 m depth.

6.1 Formation Pressure and Equivalent Freshwater Head

Representative formation pressures and freshwater heads were determined from the following tests:

513.0D	Gansinger Dolomite, Schilfsandstein
515.7S	Gansinger Dolomite, Schilfsandstein
654.4PV	Upper Muschelkalk
805.8S	Buntsandstein
965.5D	Permian
1100.2S	Permian
1262.2D	Permian
1709.0D	Permian

The formation pressures and equivalent freshwater heads are presented in Table 6.1. The formation pressures are plotted in Figure 6.1 and the equivalent freshwater heads are plotted in Figure 6.2. All freshwater heads are derived from formation pressures using mean values for true vertical depth

and surface elevation and fixed values for barometric pressure (test specific), freshwater density (1000 kgm^{-3}), and gravitational acceleration (9.81 ms^{-2}).

The calculated equivalent freshwater heads for tests 513.0D and 515.7S are approximately 72 m and 75 m above surface datum, respectively. An equivalent freshwater head below surface datum was determined for test 654.4PV in the Upper Muschelkalk, for test 805.8S in the Buntsandstein and for tests 965.5D, 1100.2S, 1262.2D and 1709.2D in the Permian.

The important factors that may affect the interpretation of the in-situ formation pressure from the measured pressure response during testing include: borehole pressure history, thermally-induced pressure effects, testing procedures, fluid properties (i.e., density), and non-ideal formation conditions. The influence of borehole pressure history and thermal effects, along with other factors, have been discussed in Section 4.2. In general, it is possible to determine formation pressures in intervals which have high hydraulic conductivities and a short borehole history period between drilling and testing. In intervals of intermediate hydraulic conductivity, a formation pressure may be determined if the testing sequence includes a shut-in recovery period during which a stable test interval (1 day or more) pressure is observed and the test interval is no longer responding to a pressure disturbance around the borehole. For the tests from which formation pressures were determined, thermal effects were of weak to moderate importance and borehole history effects of weak importance, on the interpretation of the formation pressure. Thermally-induced pressure effects and borehole pressure history effects prevented the determination of representative formation pressures or hydraulic heads from the remainder of the hydraulic tests.

The formation pressure and equivalent freshwater head values determined from calibration of tests 1100.2S and 1262.2D may be more uncertain than can be quantified through instrument-related uncertainty. The intermediate hydraulic conductivity of both intervals suggests that the pressure disturbance around the borehole would be slow to dissipate and could affect the portion of the pressure recovery curve that is used to calibrate a formation pressure. In this instance the calibrated pressure will have an associated error resulting from differences between the actual pressure disturbance and the simulated pressure disturbance around the borehole. This results from the formation pressure being adjusted to obtain a match of the simulated to measured pressures during calibration. As mentioned above, the actual pressures on the test interval during the history period are often not known and therefore an estimate of these pressures are used in the simulation.

The estimated freshwater head for the bottom hole test (1709.2D) is considered to have uncertainty due to borehole history effects, uncertainty in the estimate of the depth-integrated average fluid density in the borehole and non-static water levels observed at the end of the monitoring period. An underestimate of the average borehole fluid density would result in an underestimate of the calculated freshwater head. Since the measured water levels at the end of the monitoring period were continuing to increase, a true formation pressure and freshwater head higher than estimated, based on the last measured water level data, is indicated.

6.2 Instrumentation Uncertainties

Each equivalent freshwater head value reported in Table 6.1 has a degree of uncertainty due to instrumentation errors. The uncertainty is displayed graphically for each test with the histograms in Figure 6.3a-h. Also provided are the mean and standard deviation of the head distributions. If the

uncertainty band is defined as two standard deviations about the mean, the average band-width is 3.1 m. The shape of the histograms have the same general appearance as the histogram for the most important input variable for the test. This is true because each test has a dominant input variable, as discussed below. Of the eight tests interpreted, six used downhole transducers to measure pressure and two used water-level measurements. The six tests are referred to as group 1 tests and the two tests as group 2 tests.

The partial rank correlations for the group 1 tests all show measured pressure as the most important input variable. The range used for uncertainty of pressure is based on the accuracy and resolution of a typical transducer. The endpoints of the range (measured value ±22.8 kPa) are used as the 0.1 and 99.9 percentiles of a normal distribution. This is equivalent to a normal distribution with the measured value being the mean and having a standard deviation of 7.38 kPa. On average, the standard deviation for pressure represents 90 percent of the standard deviation for equivalent freshwater head. The importance of the pressure variable relative to the other input variables could be reduced given tighter accuracy specifications for the transducer. Using the model numbers and the operating specifications of the actual transducers, one could generate a narrower uncertainty band for each test. However, similar to the assumption made for the generic specifications, one would still have to assume that the crystal performed downhole the same way it did in the laboratory.

The second most important input variable for the group 1 tests is generally true vertical depth. As discussed in Section 4.4, uncertainty in depth increases with depth by a simple fractional multiplier. Best judgement for the Riniken borehole indicated that a multiple of 0.001 is reasonable. A uniform distribution ranging from the interpolated depth minus/plus half the uncertainty was assigned to true vertical

depth. The standard deviation for the distribution is therefore a multiple (3E-04) of the depth. From 500 m to 1700 m the standard deviation increases from 0.15 m to 0.5 m. So, throughout the borehole this deviation is less than the standard deviation for transducer measured pressure (7.38 kPa) converted to meters of freshwater head (0.75 m). If in the future, transducer ranges are narrowed, the quantification of depth uncertainty would have increased importance and should be examined further.

The remaining three input variables (surface elevation, fluid density, and rock density) are of lesser or no importance to freshwater head uncertainty for the group 1 tests. The exception is fluid density for the 515.7S test. The uncertainty range for density (80 kgm^{-3}) causes significant uncertainty (16 kPa) when applied over the 20.44 m between transducer P2 and the formation center.

Recall that surface elevation, true vertical depth, and rock density are used to generate estimates of gravitational acceleration. Thus, gravity is an output variable, not input, and does not enter into correlation computations for equivalent freshwater head. However, examination shows that rock density is the dominant variable in evaluating gravity. Since rock density is always the least important variable for freshwater head (see Figure 6.3a-h), it follows that uncertainty in gravitational acceleration is not important for calculations of freshwater head. This also indicates that uncertainties for surface elevation and true vertical depth are propagated to uncertainty of freshwater head primarily via equation 4.1-10 rather than indirectly through the evaluation of gravitational acceleration.

The group 2 tests require calculation of freshwater head from a measured water level. To calculate freshwater head, a formation pressure at the interval center is determined using a depth-integrated density in equation 4.1-9, then freshwater

head is found using equation 4.1-10. The derived pressure is based on water level measurements and hence does not depend on transducer specifications. With that source of uncertainty eliminated, the most important variables are average fluid column density and surface elevation. It is understandable that density is important since its uncertainty is multiplied by the entire depth to interval center (rather than the distance from transducer P2 to the interval center as in the group 1 tests).

The frequency histograms for equivalent freshwater head take on more of a uniform appearance for the group 2 tests, rather than the bell-shaped appearance of the group 1 tests discussed earlier. This is primarily due to the uniform distribution assigned to borehole fluid density. Test 654.4PV shows the smallest uncertainty due to instrumentation errors of the eight tests and the bottom hole test (1709.2D) shows the second largest. To reduce the uncertainty for the bottom hole test, uncertainty in fluid density must be addressed. Since deionized water is the assumed borehole fluid, the density uncertainty is only based on the temperature uncertainty (±2°C) propagated through the depth-integration scheme for density. Thus, under this assumption, only a smaller temperature uncertainty can reduce the uncertainty in freshwater head.

For all eight tests, the uncertainty of average rock density dominates the uncertainty of gravitational acceleration. Although gravity is not an important variable for any given test, using a fixed average value over all tests could cause about a 4 kPa variation in computed pressures throughout the borehole. The uncertainty surrounding the pressure at interval center is dominated by the same variables as equivalent freshwater head. That is, pressure at transducer P2 for the group 1 tests and borehole fluid density for the group 2 tests are the dominant variables.

6.3 Formation Hydraulic Conductivity

An estimate of hydraulic conductivity of the formation was obtained for 19 of the 22 hydraulic tests in the Riniken borehole. Three of the 22 tests did not provide a representative hydraulic conductivity estimate. 17 of the 19 successfully interpreted tests covered different zones within the borehole. Table 6.2 summarizes the estimated hydraulic conductivity, estimated specific storage, and the borehole temperature at the end of testing, determined from the test intervals with analyzable hydraulic tests. The hydraulic conductivities are plotted in Figure 6.4.

Interpreted hydraulic conductivities ranged from 4.0E-14 ms^{-1} to 1.5E-06 ms^{-1}. Zones of higher hydraulic conductivity (greater than 1.0E-09 ms^{-1}) were observed at the following apparent vertical depths:

- 500.99 m - 530.50 m (515.7S)
- 617.30 m - 696.00 m (654.4PV)
- 793.00 m - 820.20 m (805.8S)
- 958.40 m - 1009.95 m (965.5D and 993.5D)

The important factors which may affect the testing interpretation for hydraulic conductivity include: borehole pressure history, thermal effects, testing procedures, estimation of formation pressure, estimation of specific storage, and non-ideal formation conditions. Most of these factors have been addressed previously in Section 4.2.

6.4 Formation Temperature

Temperatures measured at the end of testing in each interval were assumed to be representative of the tested interval. However, since the temperature transducers are located above

the packed-off interval they may measure the temperature in the local portion of the hydrologic test tool (i.e., sensor carrier) and not the temperature in the interval.

Representative formation temperatures were obtained from tests 515.7S, 805.8S and 965.5D. Due to the relatively high hydraulic conductivity of these zones, the rate of fluid flow from the formation at the borehole was likely sufficient enough to ensure that the borehole fluid temperatures, measured by the downhole temperature transducer in the hydrologic testing tool, were representative of formation conditions at the test interval depth. For these tests, the measured temperature response was increasing at the end of testing, therefore the temperatures reported underestimate the formation conditions but are likely within one to three degrees Celsius of the actual value. Some of the factors which prevented the determination of a representative formation temperature from the temperature transducers in the hydrologic tool for the majority of the hydraulic tests were temperature disequilibrium between the tool and borehole fluid during testing, temperature transducers not positioned near the test interval, and fluid movement past the sensor carrier during tool operation. A representative temperature data set was obtained from the Schlumberger high-resolution temperature (HRT) log taken on 28 February, 1984 for the interval from 1618 m to 1785 m below the surface datum.

A plot of the temperatures measured at the end of tests 515.7S, 805.8S and 965.5D and temperatures estimated from the HRT log at depths of 1650, 1700 and 1750 m is shown in Figure 6.5 along with a linear approximation through the temperature data. This temperature-depth relationship is considered to be a reasonable representation of the in-situ temperature profile. The slope of the temperature-depth approximation indicates a thermal gradient of approximately 3.9°C/100 m.

7. REFERENCES

Baker, 1985. Tech Facts. Technical Information for the Oil and Gas Well Specialist, Baker Service Tools, pp. 1-28.

Barker, J.A. and J.H. Black, 1983. Slug tests in fissured aquifers. Water Resources Research, Volume 19, No. 6, pp. 1558-1564.

Belanger, D.W., T.L. Cauffman, J.L. Lolcama, D.E. Longsine, and J.F. Pickens, 1988. Interpretation of Hydraulic Testing in the Sediments of the Riniken Borehole-Appendices Describing Test Analyses. Nagra Interner Bericht 87-15, 236 p.

Bredehoeft, J.D. and S.S. Papadopulos, 1980. A method for determining the hydraulic properties of tight formations. Water Resources Research, Volume 16, No. 1, pp. 233-238.

Cooper, H.H. Jr., J.D. Bredehoeft, and S.S. Papadopulos, 1967. Response of a finite-diameter well to an instantaneous charge of water. Water Resources Research, Volume 3, No. 1, pp. 263-269.

Dorsey, N.E., 1968. Properties of Ordinary Water-Substance in all its Phases. Water-Vapour, Water and all Ices, American Chemical Society Monograph Series, Hafner Publishing Company, @ 1940 (reprinted in 1968), pp. 243-245.

Earlougher, R.C., 1977. Pressure Buildup Testing. Advances in Well Test Analysis. Monograph Volume 5, Soc. of Petroleum Engineers of AIME, New York, 181 p.

Faust, C.R. and J.W. Mercer, 1984. Evaluation of slug tests in wells containing a finite-thickness skin. Water Resources Research, Volume 20, No. 4, pp. 504-506.

Forster, C.B. and J.E. Gale, 1980. A laboratory assessment of the use of borehole pressure transients to measure the permeability of fractured rock masses. Report 8674, Lawrence Berkeley Laboratory, University of California, Berkeley.

Forster, C.B. and J.E. Gale, 1981. Injection versus pressure pulse borehole tests in fractured crystalline rocks-Observations and recent experiences. in Proceedings of Third Invitational Well Testing Symposium, pp. 74-83, University of California Press, Berkeley.

Freeze, R.A., and J.A. Cherry, 1979. Groundwater. Prentice-Hall, Inc., 604 p.

Grisak, G.E., J.F. Pickens, D.W. Belanger, J.D. Avis, 1985. Hydrogeologic Testing of Crystalline Rocks During the Nagra Deep Drilling Program. Nagra Technischer Bericht 85-08, 194 p.

Hsieh, P.A., S.P. Neuman, and E.S. Simpson, 1983. Pressure testing of fractured rocks - A methodology employing three-dimensional cross-hole tests. Report NUREG/CR-2313, U.S. Nuclear Regulatory Commission, Washington, D.C.

Hubbert, M.K., 1940. The theory of ground-water motion. Journal of Geology, Volume 48, pp. 785-819.

Iman, R.L. and W.J. Conover, 1982. A distribution-free approach to inducing rank correlation among input variables. Communications in Statistics, B11(3), pp. 311-334.

Iman, R.L. and M.J. Shortencarier, 1984. A FORTRAN 77 Program and User's Guide for the Generation of Latin Hypercube and Random Samples for Use with Computer Models. NUREG/CR-3624 and SAND83-2365, Sandia National Laboratories.

Jacob, C.E. and S.W. Lohman, 1952. Nonsteady flow to a well of constant drawdown in an extensive aquifer. American Geophysical Union Transactions, Volume 33, pp. 559-569.

James, M.L., G.M. Smith, J.C. Wolford, 1968. Applied Numerical Methods for Digital Computation with FORTRAN, International Textbook Company, pp. 273-274.

Lee, J., 1982. Well Testing. SPE Textbook Series, Volume 1, Soc. of Petroleum Engineers of AIME, New York.

Leech, R.E.J., K.G. Kennedy, and D. Gevaert, 1985. Sondierbohrung Boettstein-Hydrogeological Testing of Crystalline Rocks. Nagra Technischer Bericht 85-09.

Matthews, C.S. and D.G. Russell, 1967. Pressure Buildup Analysis. Pressure Buildup and Flow Tests in Wells. Monograph Volume 1, Soc. of Petroleum Engineers of AIME, New York.

McKay, M.D., W.J. Conover, and R.J. Beckman, 1979. A comparison of three methods for selecting values of input variables in the analysis of output from a computer code. Technometrics, 21, pp. 239-245.

Narasimhan, T.N. and B.Y. Kanehiro, 1980. A note on the meaning of storage coefficient. Water Resources Research, Volume 16, No. 2, pp. 423-429.

Neuzil, C.E., 1982. On conducting the "modified slug test" in tight formations. Water Resources Research, Volume 18, No. 2, pp. 439-441.

Parasnis, D.S., 1972. Principles of Applied Geophysics, Chapman and Hall, 46 p.

Pearson, F.J. and J.L. Lolcama, 1987. Chemistry of Ground Waters in the Boettstein, Weiach, Riniken, Schafisheim, Kaisten and Leuggern Boreholes: A Hydrochemically Consistent Data Set. Nagra Technischer Bericht 86-19 (in preparation).

Pickens, J.F., G.E. Grisak, J.D. Avis, D.W. Belanger, and M. Thury, 1987. Analysis and interpretation of borehole hydraulic tests in deep boreholes: Principles, model development, and applications. Water Resources Research, Volume 23, No. 7, pp. 1341-1375.

Savage, G.J. and H.K. Kesavan, 1979. The graph theoretic field model - I. Modelling and formulations. Journal of the Franklin Institute, Volume 307, pp. 107-147.

Theis, C.V., 1935. The relation between the lowering of the piezometric surface and the rate and duration of discharge of a well using ground-water storage. American Geophysical Union Transactions, Volume 16, pp. 519-524.

Touloukian, Y.S., W.R. Judd, and R.F. Roy, 1981. Physical Properties of Rocks and Minerals; Data Series on Material Properties, Volume 11-2 McGraw Hill Book Company, New York, 548 p.

Tsuboi, C., 1983. Gravity. George Allen and Unwin Ltd., 65 p.

Van Golf-Racht, T.D., 1982. Fundamentals of Fractured Reservoir Engineering. Developments in Petroleum Science 12, Elsevier Publishing, 710 p.

Wang, J.S.Y., T.N. Narashimhan, C.F. Tsang, and P.A. Witherspoon, 1978. Transient flow in tight fractures. in Proceedings of the Invitational Well Testing Symposium, pp. 103-116, University of California Press, Berkeley.

Weast, R.C., 1982. Handbook of Chemistry and Physics, 62nd Edition, CRC Press Inc., D232-D233, F11 p.

Weber, H.P., G. Sattel, and C. Sprecher, 1986. Sondierbohrungen Weiach, Riniken, Schafisheim, Kaisten, Leuggern. Geophysikalische Daten Textband. Nagra Technischer Bericht 85-50.

Wollard, G.P., 1979. The New Gravity System - Changes in the International Gravity Base values and Anomaly Values, Geophysics, Volume 44, No. 8, pp. 1352-1366.

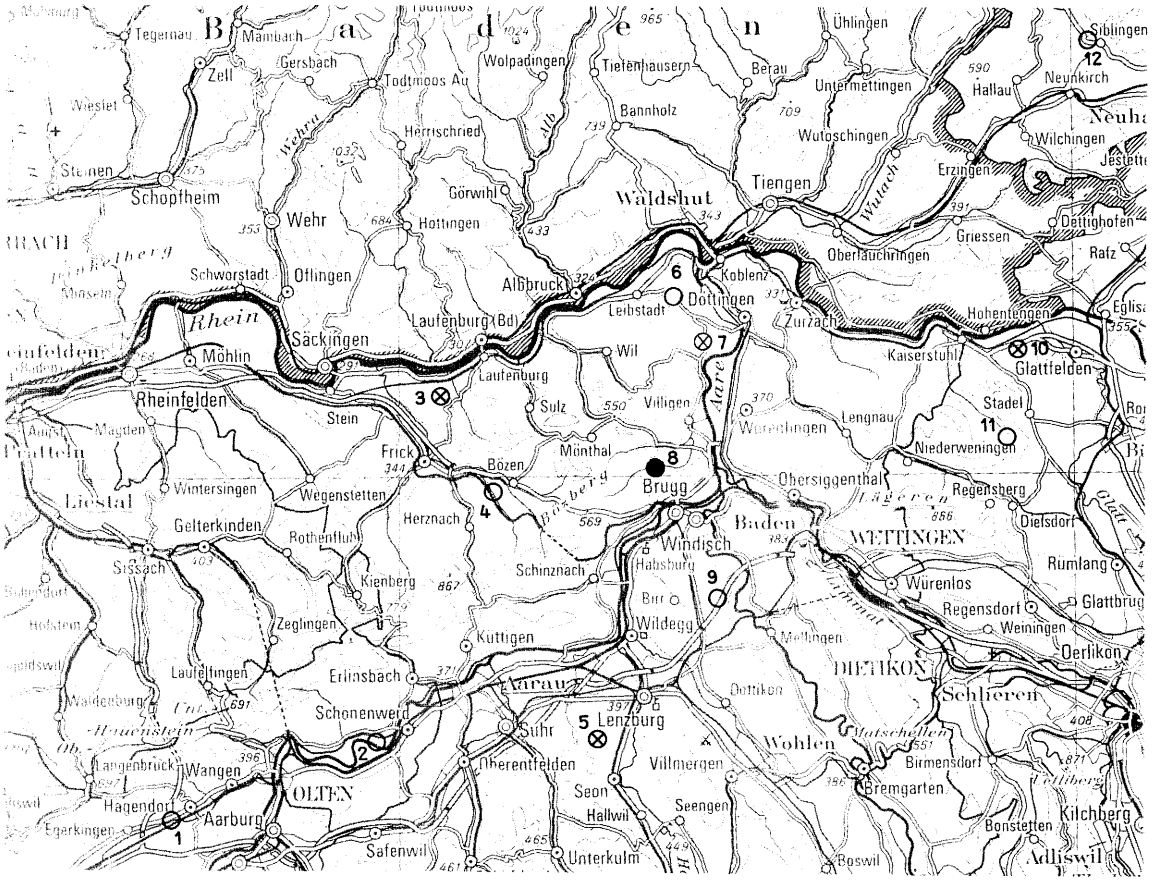

0 10 20 km

Reproduziert mit Bewilligung des Bundesamtes für Landestopographie vom 17. 7. 1981

Borehole		Depth
○ 1	HAEGENDORF	ca 2400 m
○ 2	NIEDERGOESGEN	ca 2250 m
⊗ 3	KAISTEN	1306 m
○ 4	HORNUSSEN	ca 1600 m
⊗ 5	SCHAFISHEIM	2006 m
○ 6	LEUGGERN	1689 m
⊗ 7	BOETTSTEIN	1501 m
● 8	RINIKEN	1801 m
○ 9	BIRRHARD	ca 2350 m
⊗ 10	WEIACH	2482 m
○ 11	STEINMAUR	ca 2500 m
○ 12	SIBLINGEN	ca 1450 m

LEGEND
○ Borehole
⊗ Borehole Completed

Figure 1.1 Riniken Borehole Location

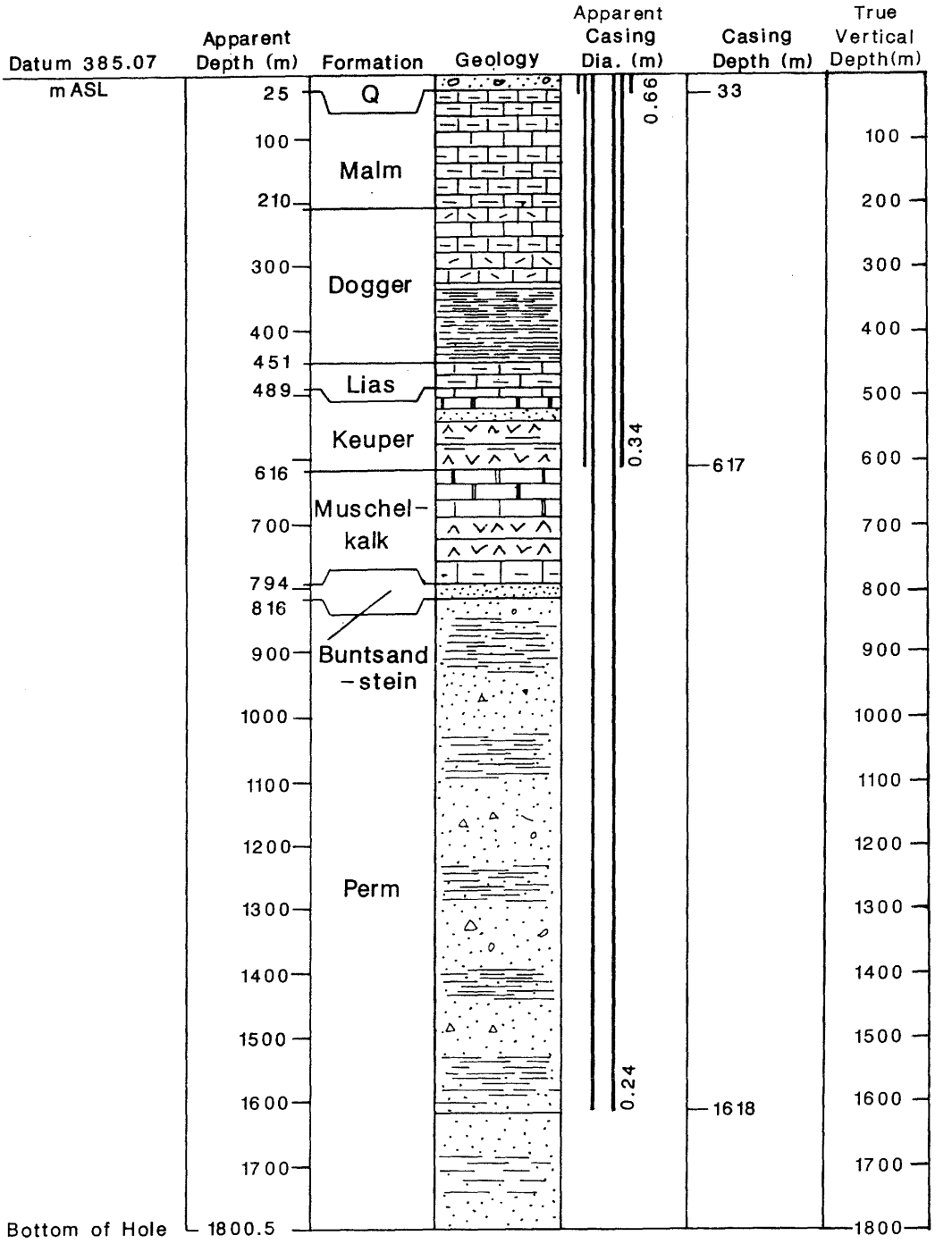

Figure 2.1 Riniken Borehole Geology

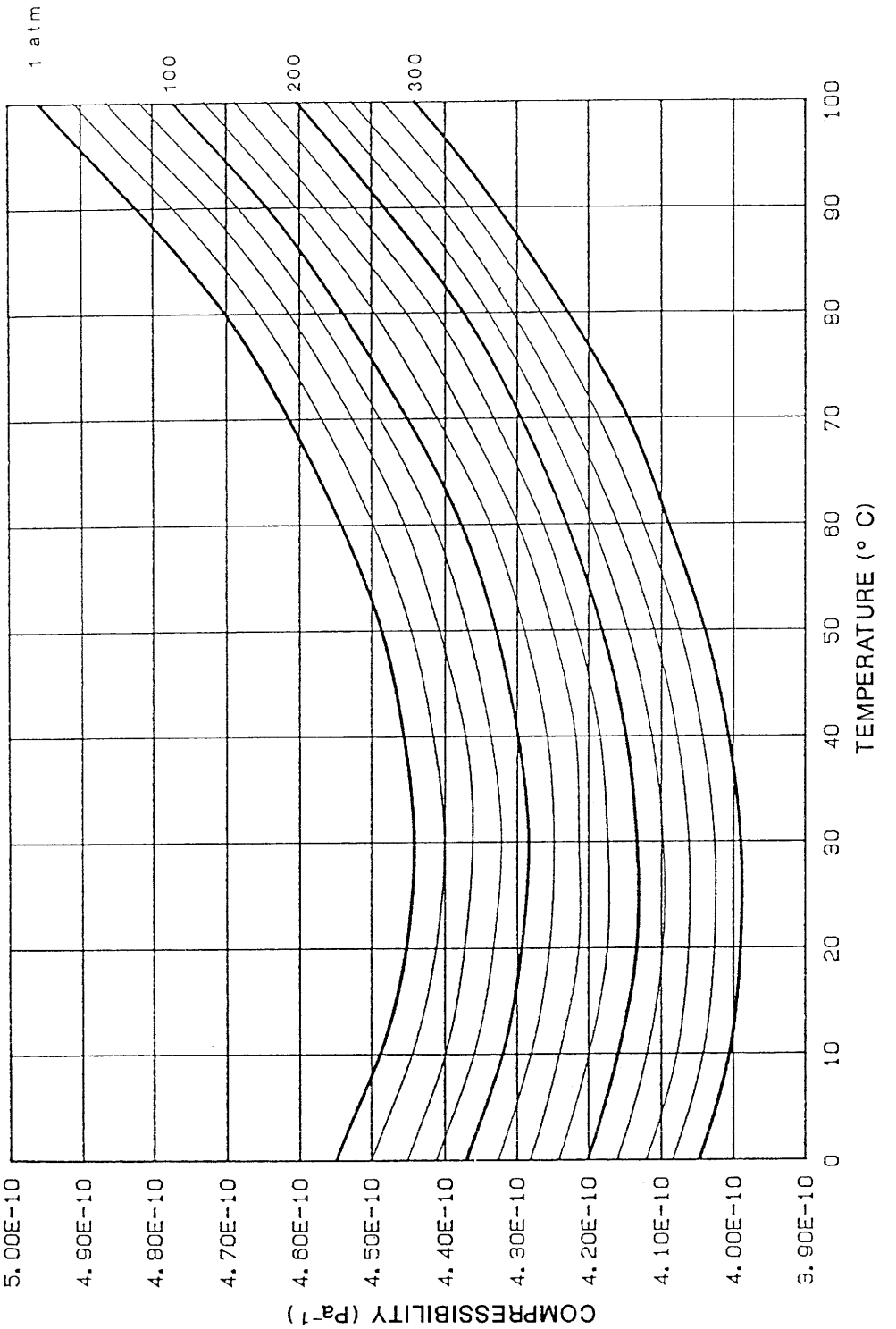

Figure 4.1 Fluid Compressibility: Variation with Temperature and Pressure

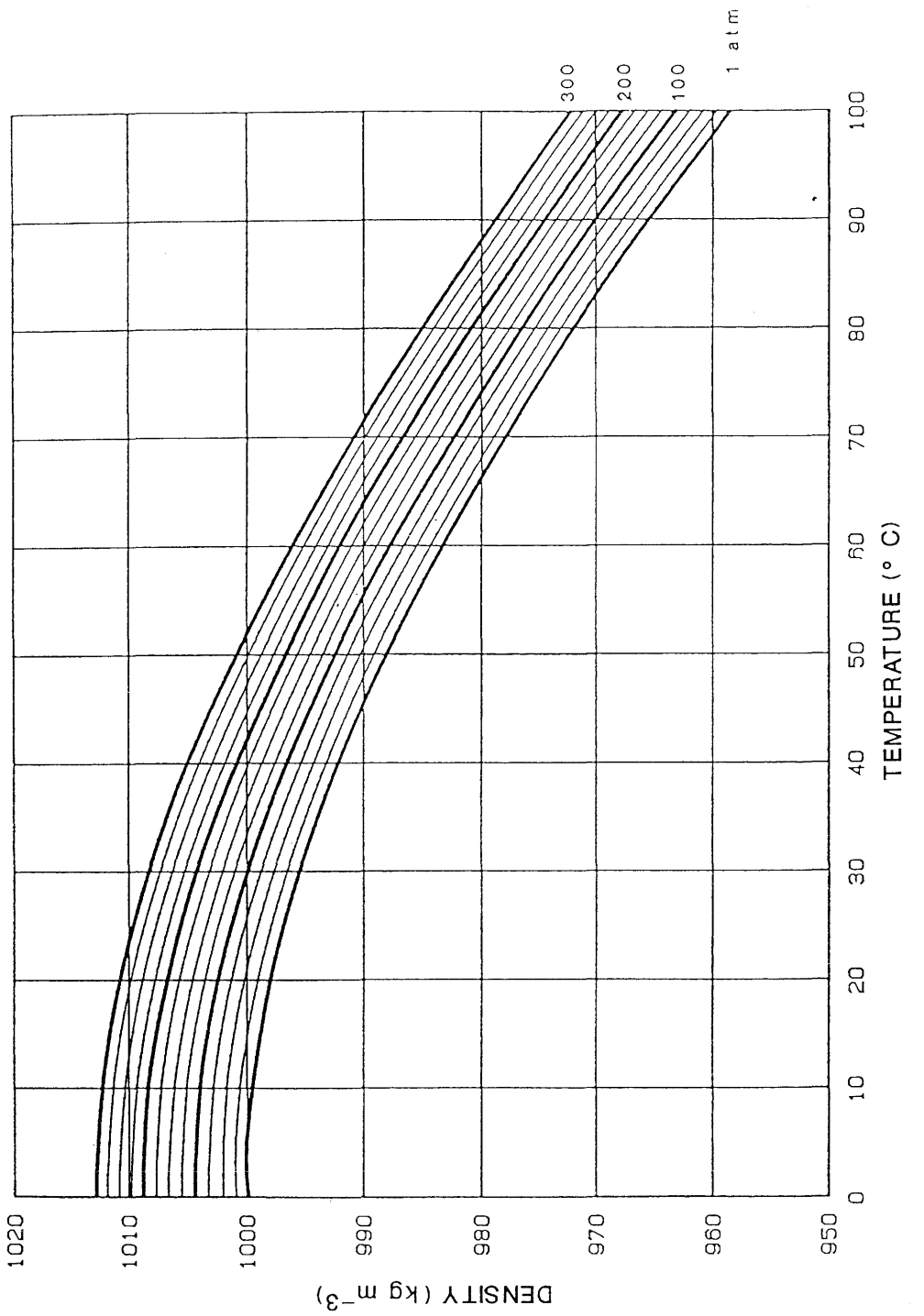

Figure 4.2 Deionized Fluid Density: Variation with Temperature and Pressure

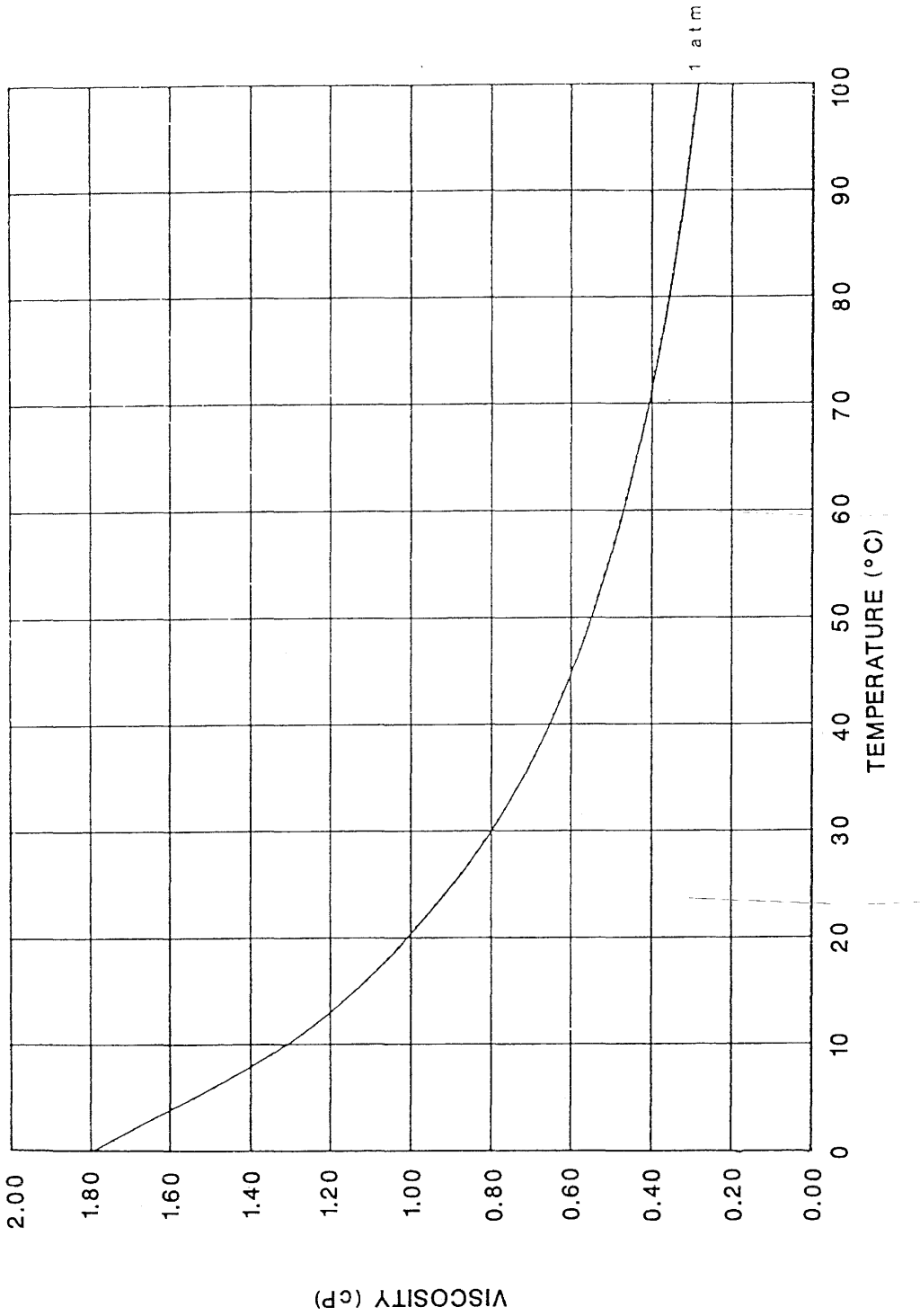

Figure 4.3 Fluid Viscosity: Variation with Temperature

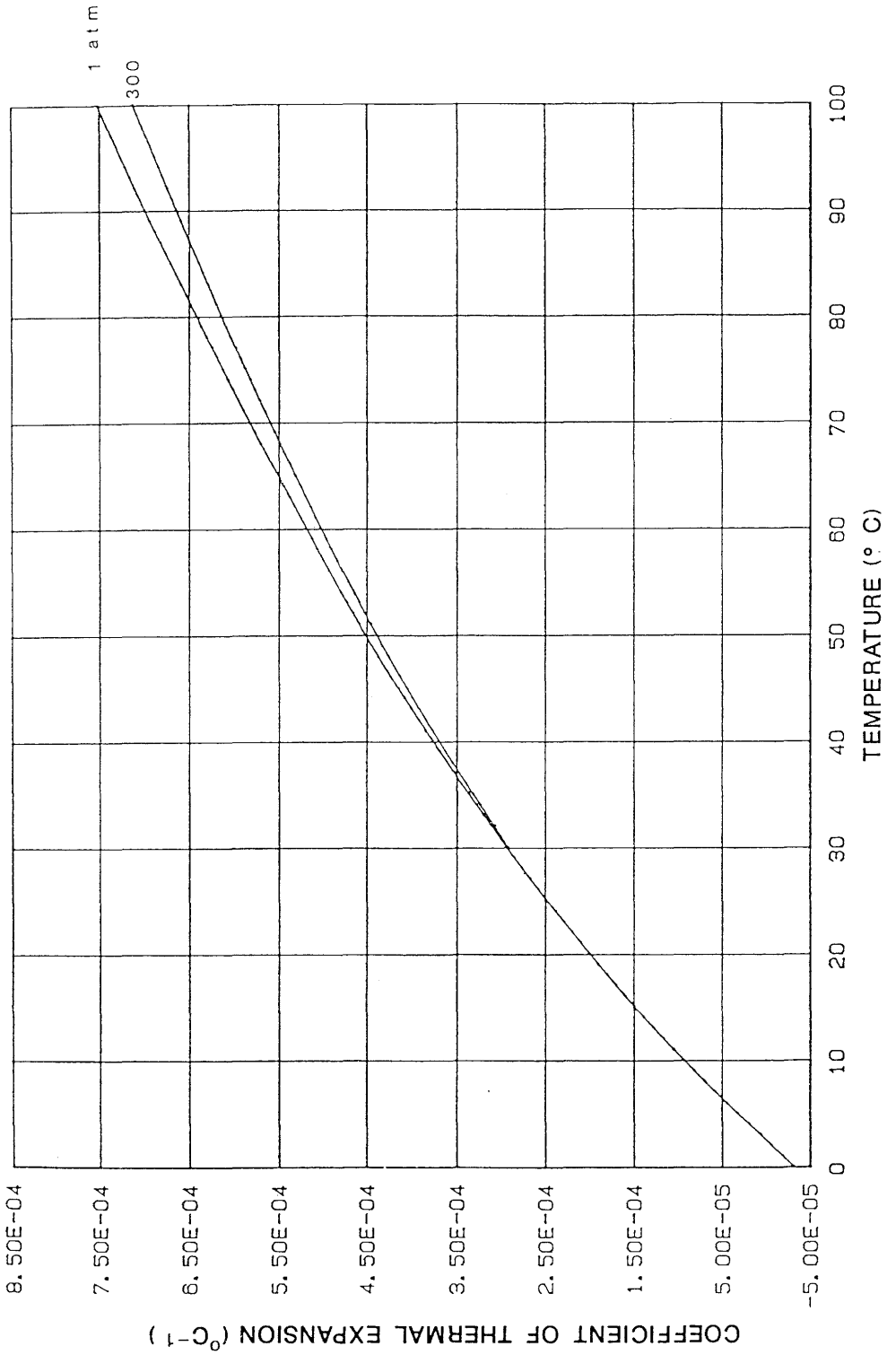

Figure 4.4 Fluid Coefficient of Thermal Expansion: Variation with Temperature and Pressure

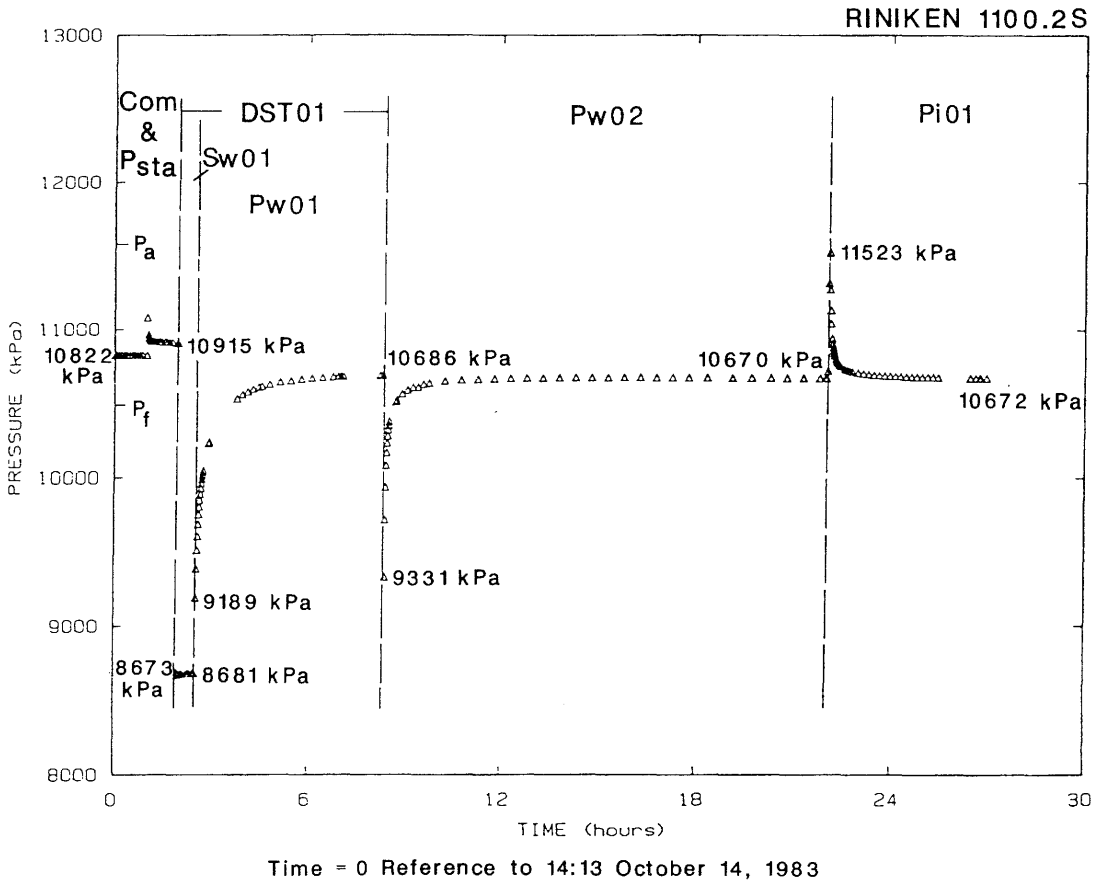

Figure 4.5 Measured Pressure Data for Test Interval 1100.2S, Test Sequence Designations, and Starting and Ending Pressures for Each Sequence

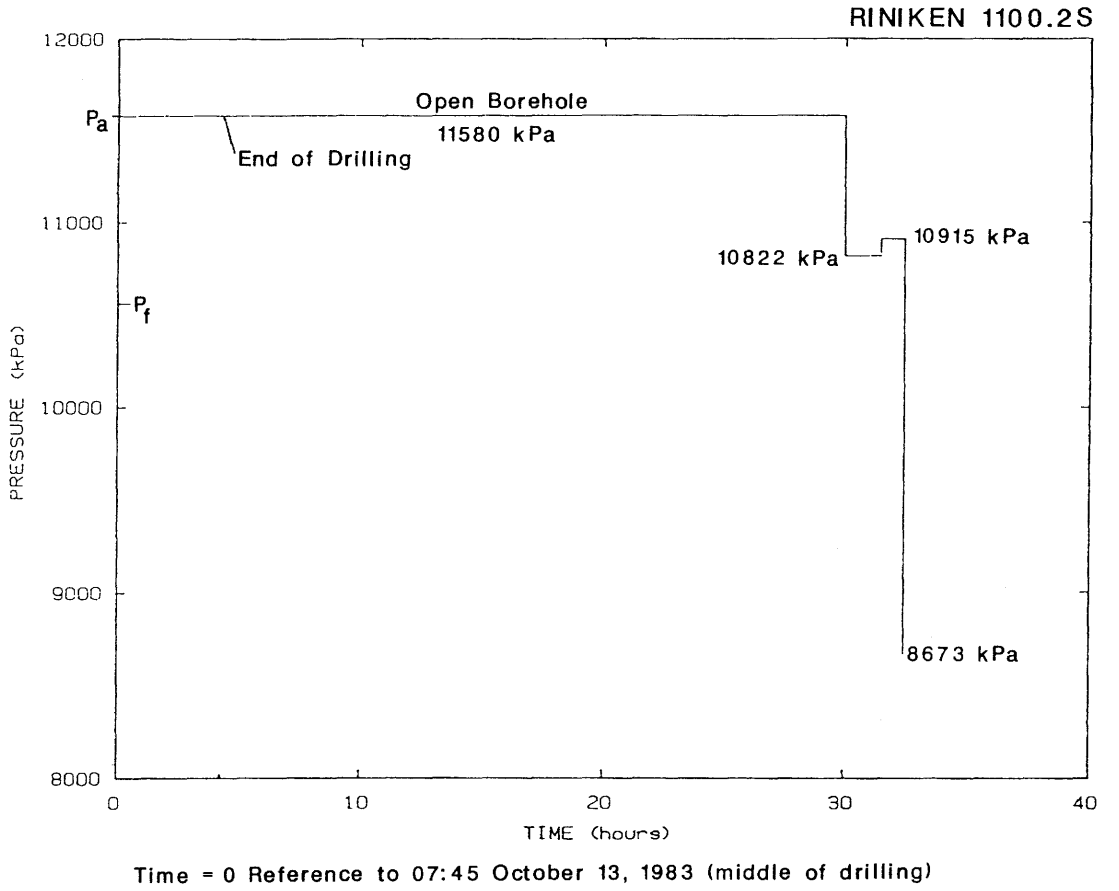

Figure 4.6 Assumed Pressure History on Test Interval 1100.2S

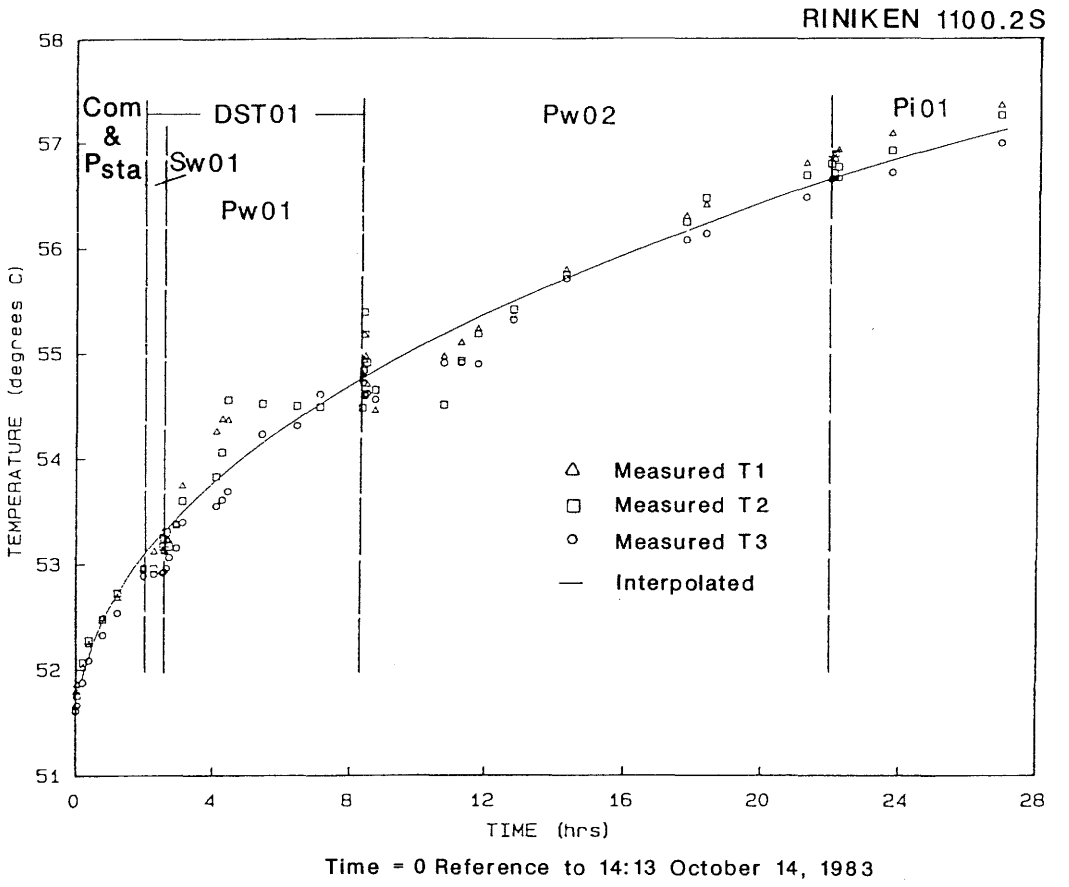

Figure 4.7 Measured Response and Best-Fit Interpolation of T1, T2 and T3 Temperature Transducers for Test 1100.2S

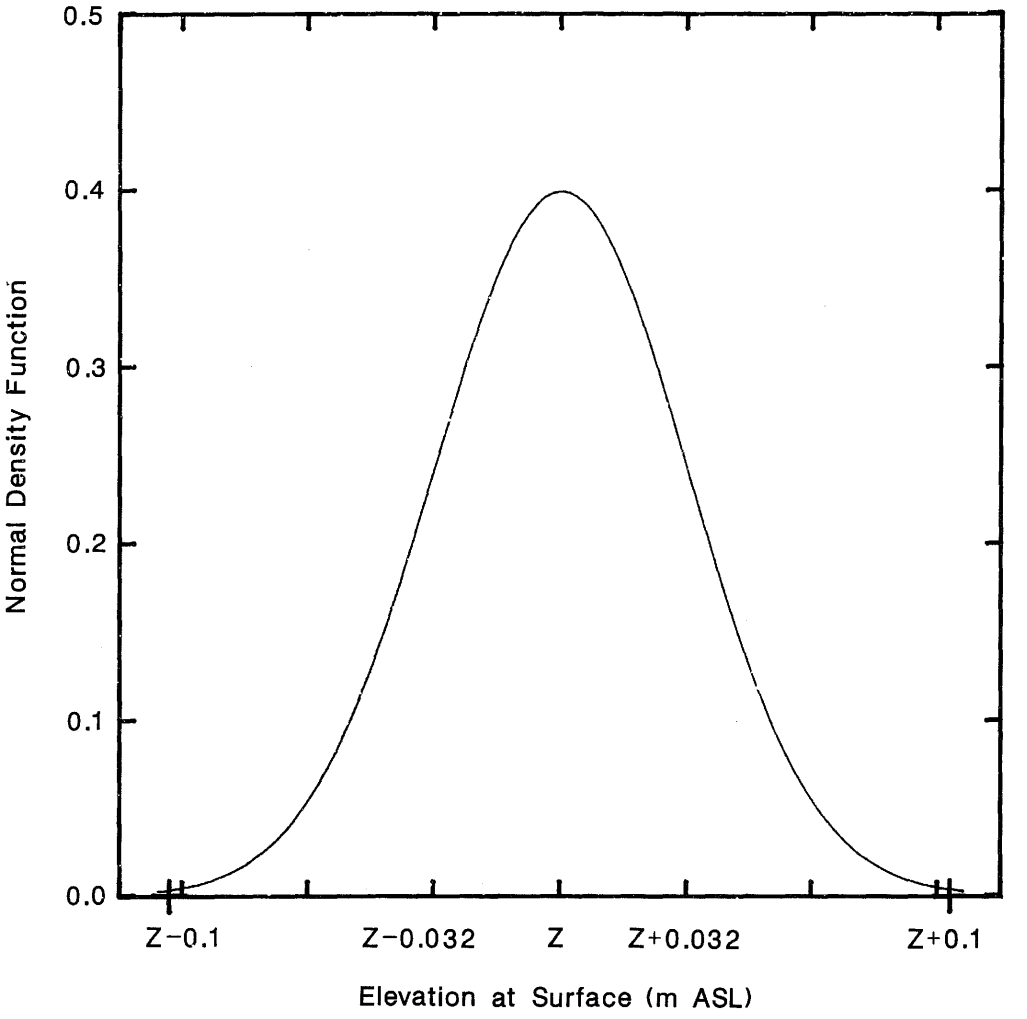

Figure 4.8 Probability Density Function for Elevation at Surface

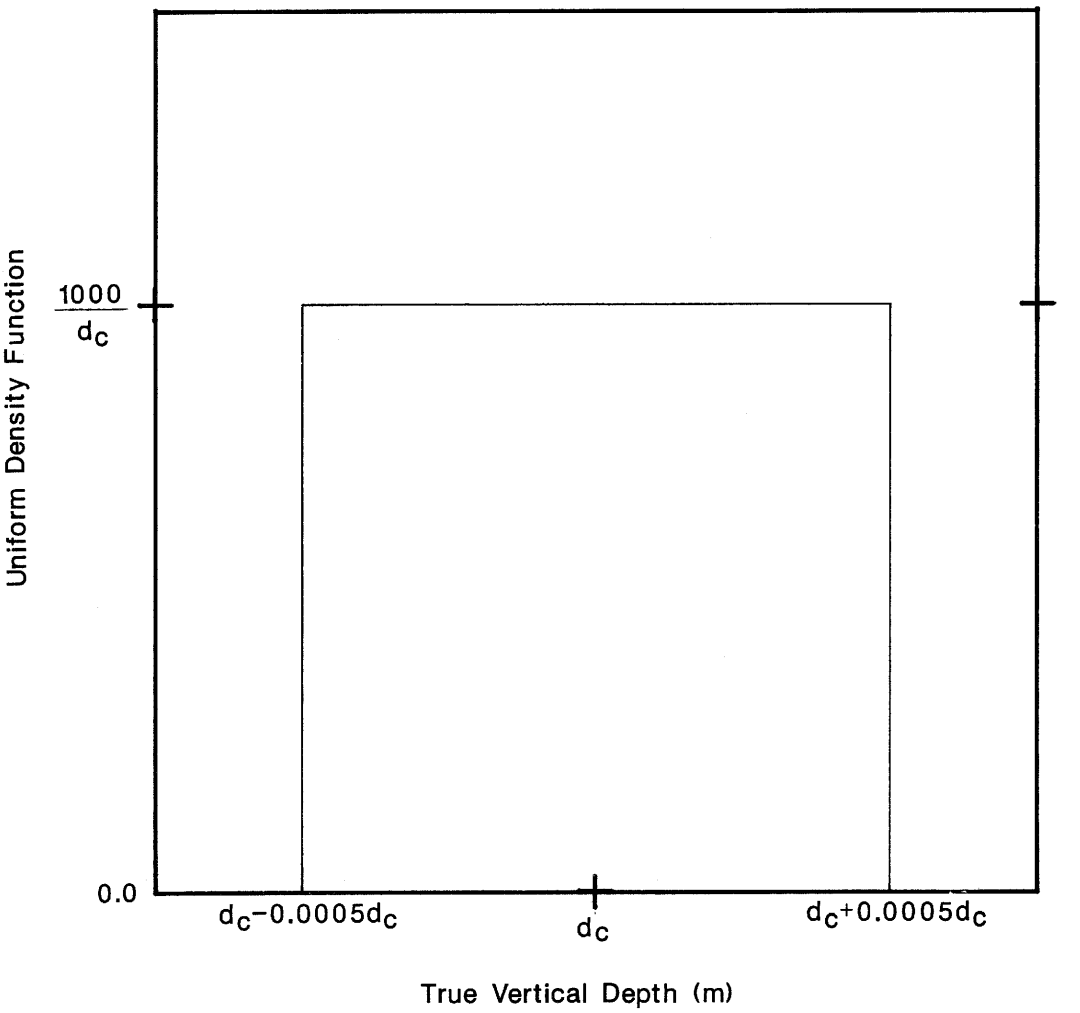

Figure 4.9 Probability Density Function for True Vertical Depth

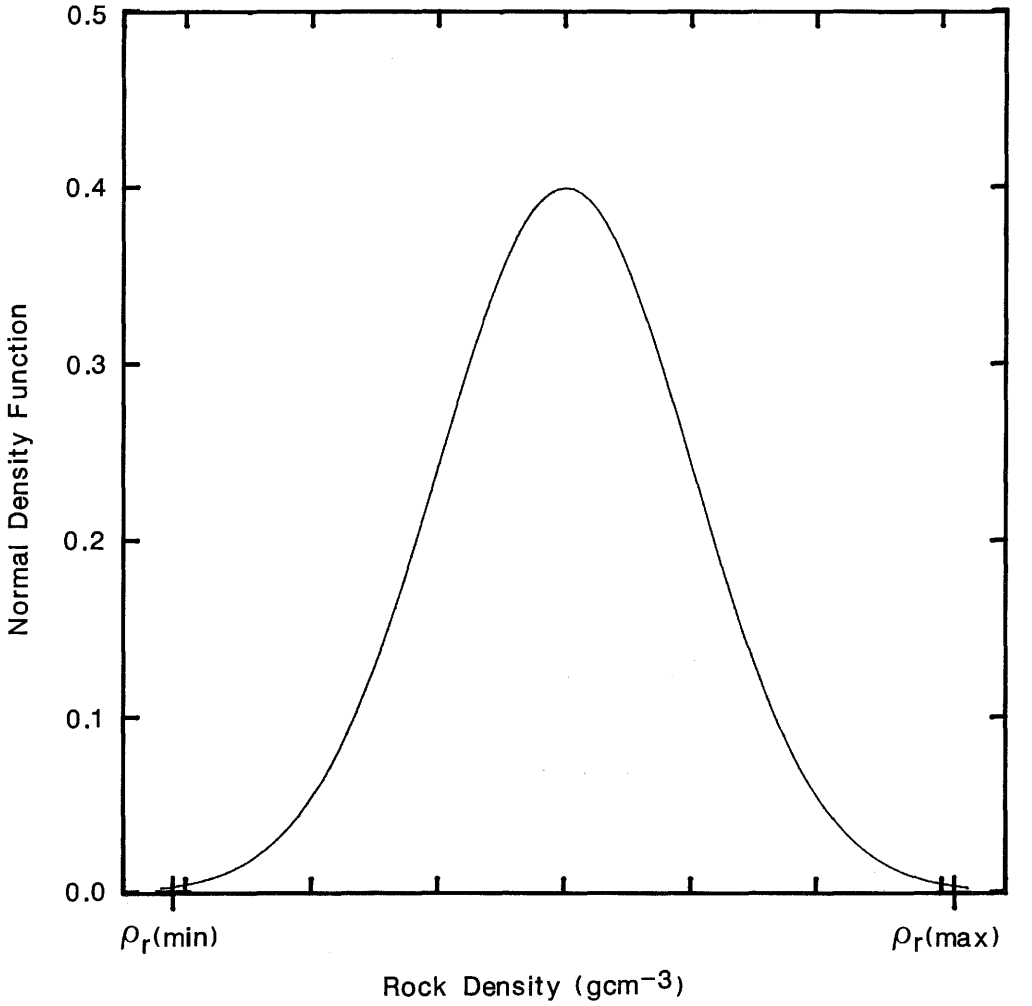

Figure 4.10 Probability Density Function for Rock Density

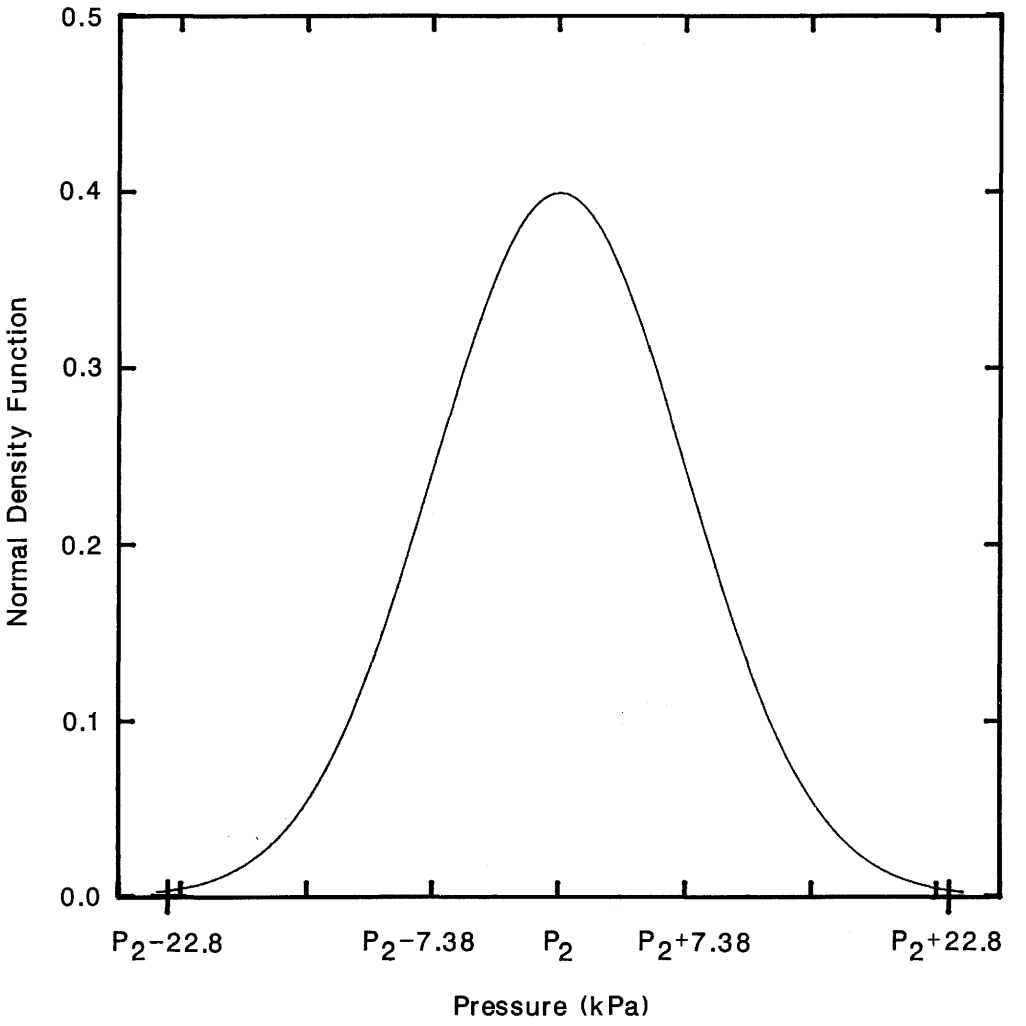

Figure 4.11 Probability Density Function for Pressure

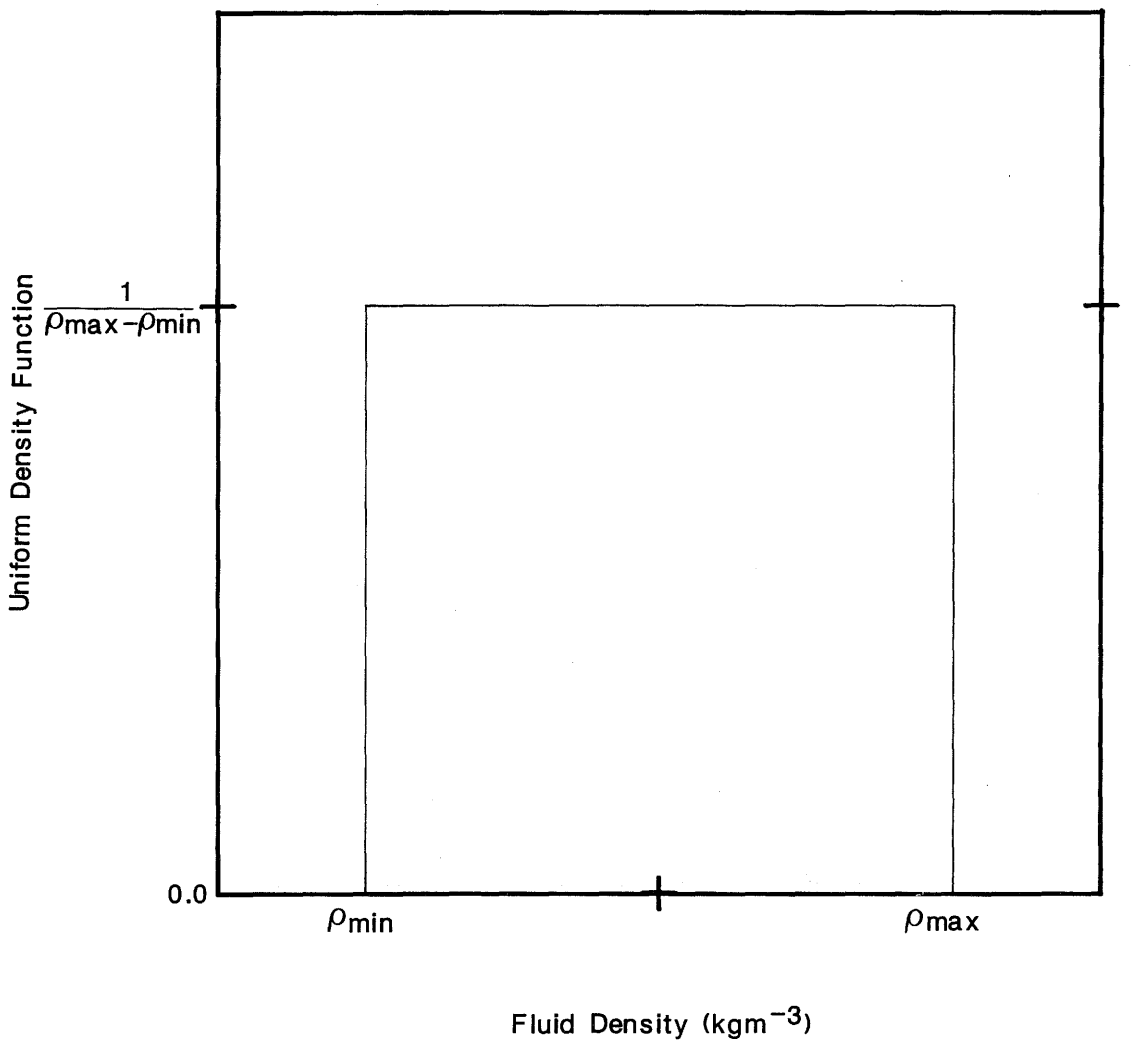

Figure 4.12 Probability Density Function for Fluid Density

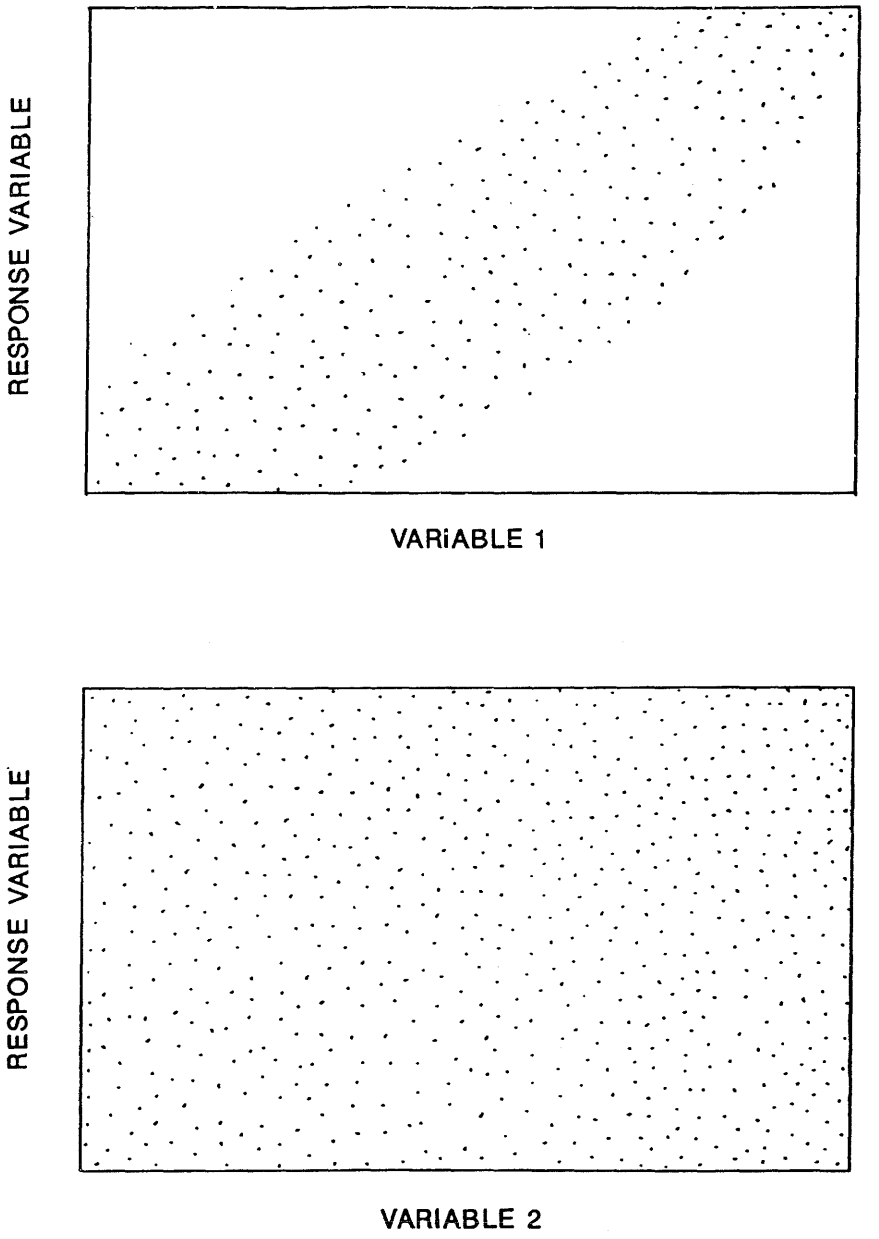

Figure 4.13 Example Scatter Plots of Input Variables 1 and 2 Versus a Response Variable

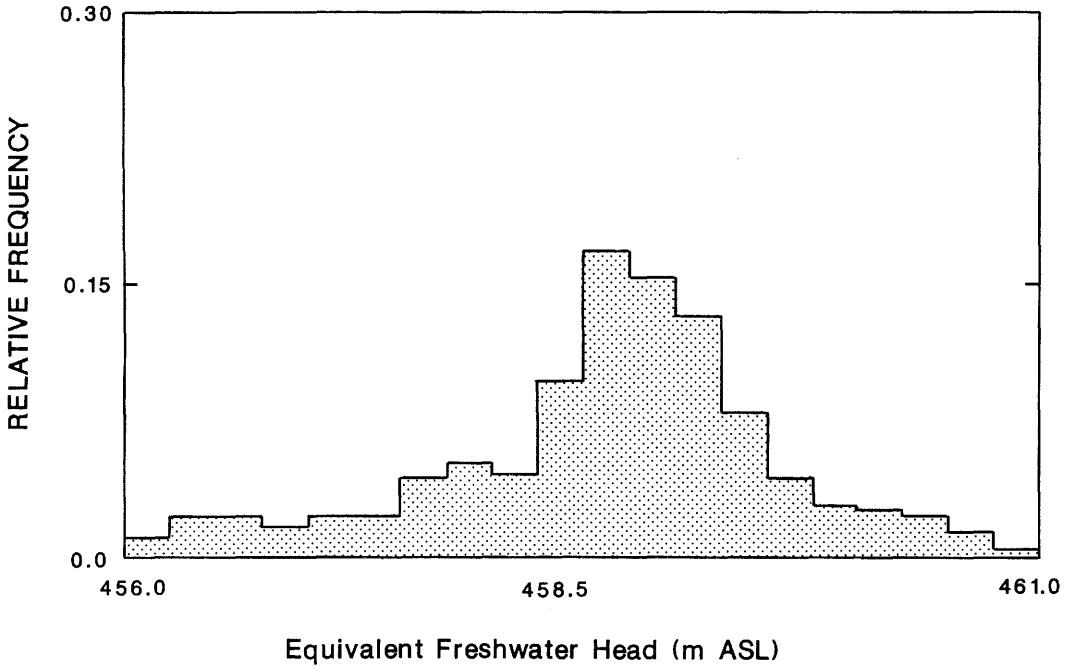

Figure 4.14 Example Histogram Showing Distribution of Equivalent Freshwater Head

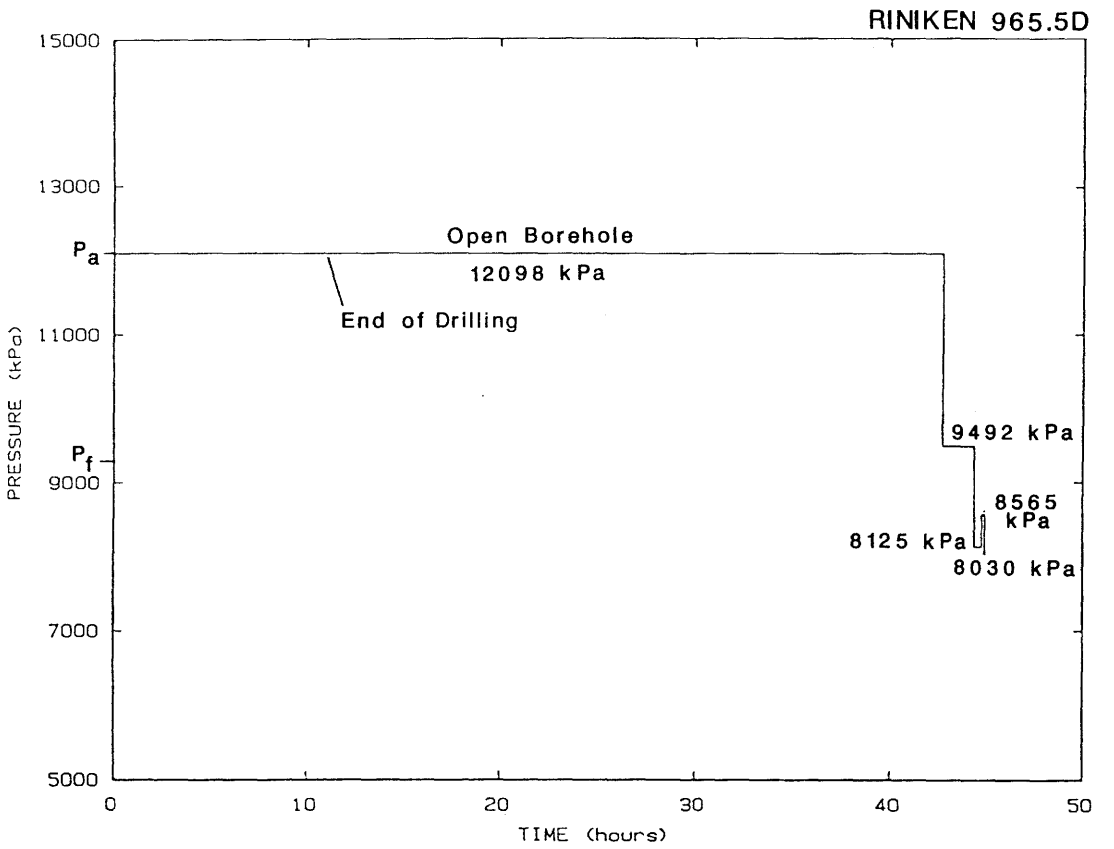

Figure 5.1 Assumed Pressure History on Test Interval 965.5D From Mid-Point of Drilling

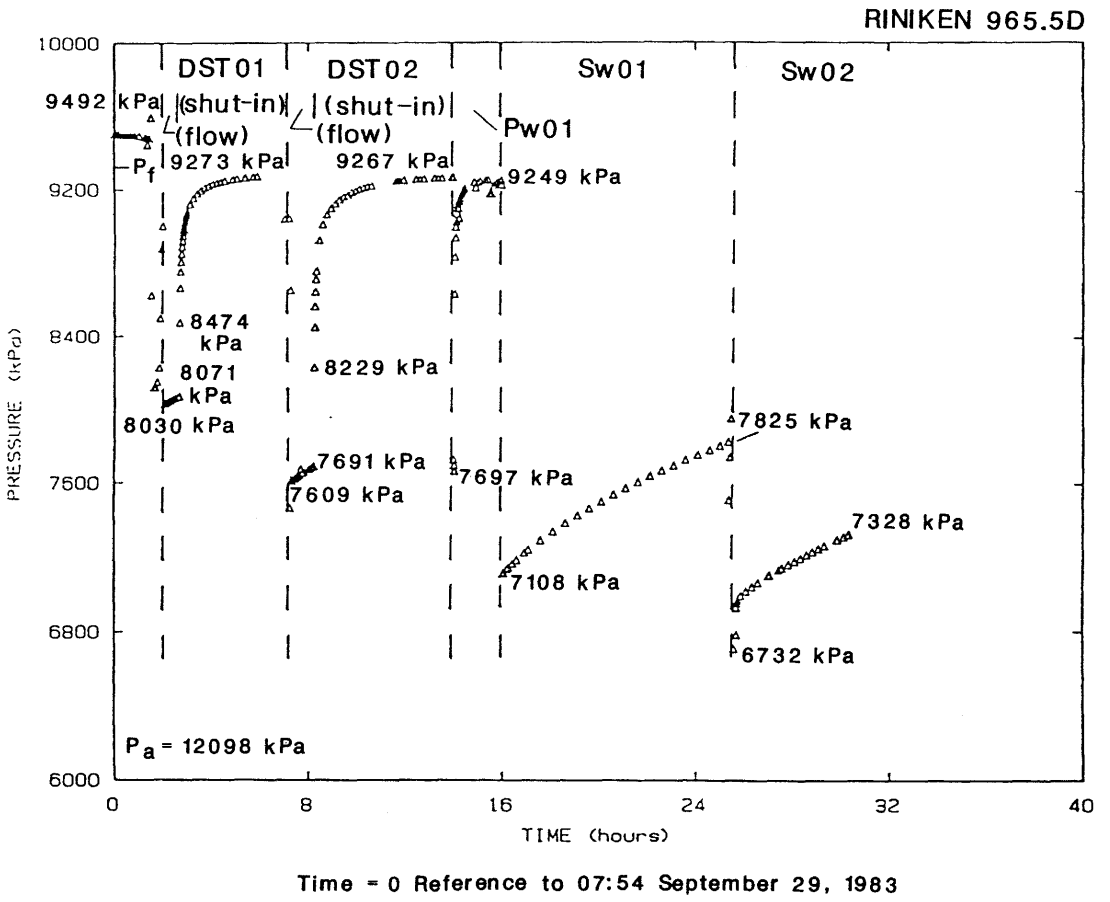

Figure 5.2 Measured Pressure Data for Test Interval 965.5D, Test Sequence Designations, and Starting and Ending Pressure for Each Sequence

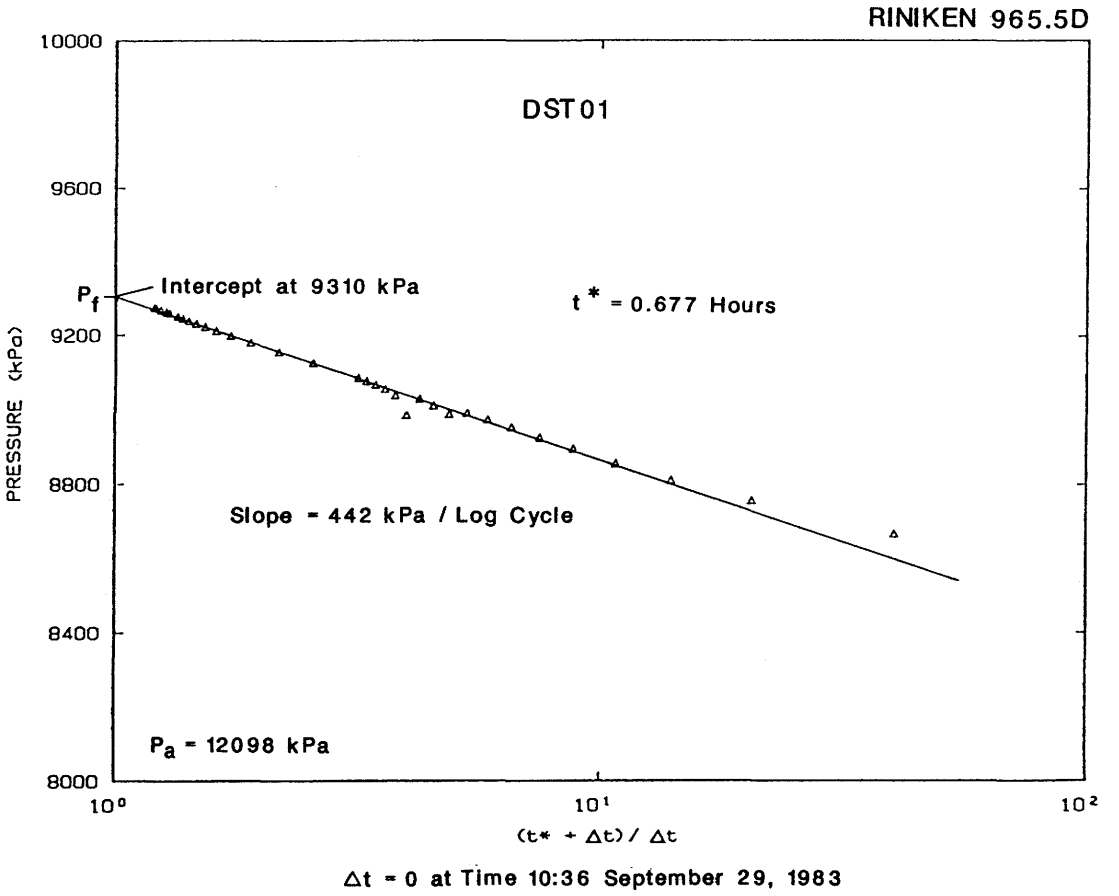

Figure 5.3 Horner Plot of Pressure Data for Test DST01 of 965.5D

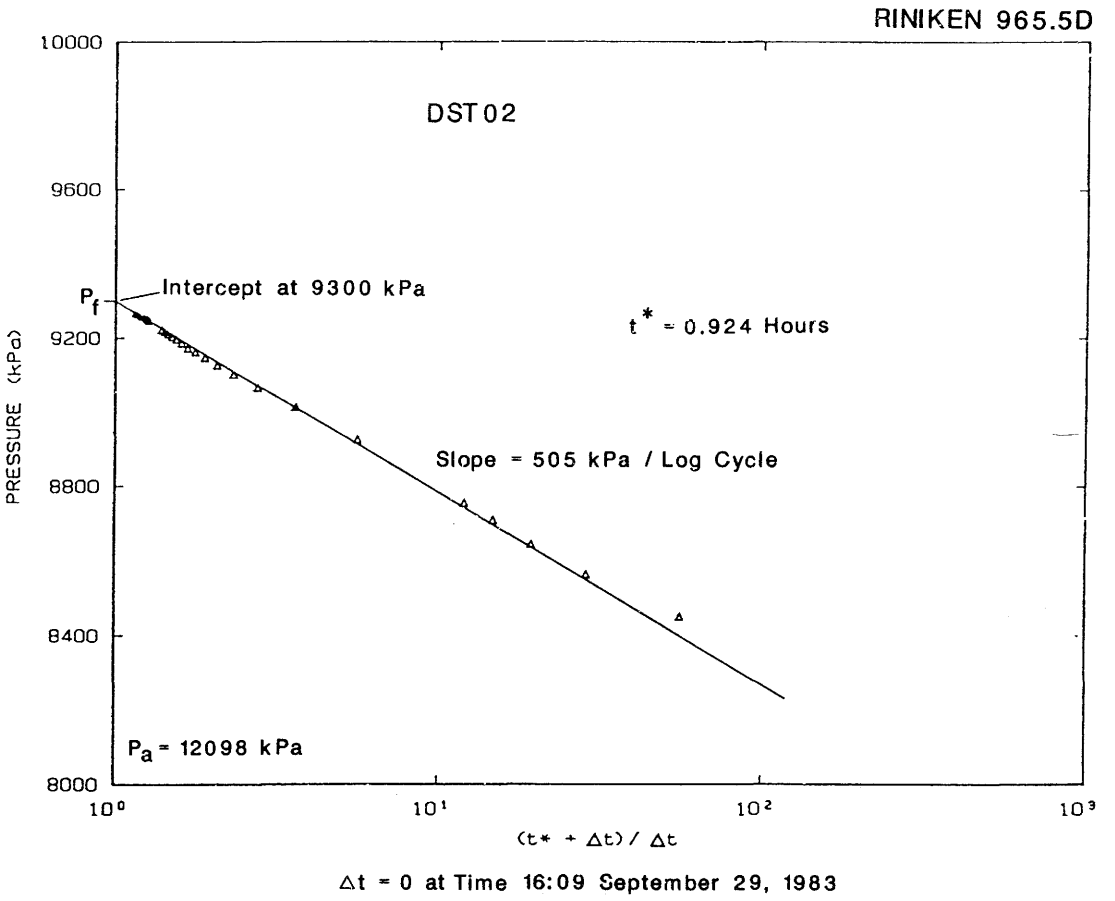

Figure 5.4 Horner Plot of Pressure Data for Test DST02 of 965.5D

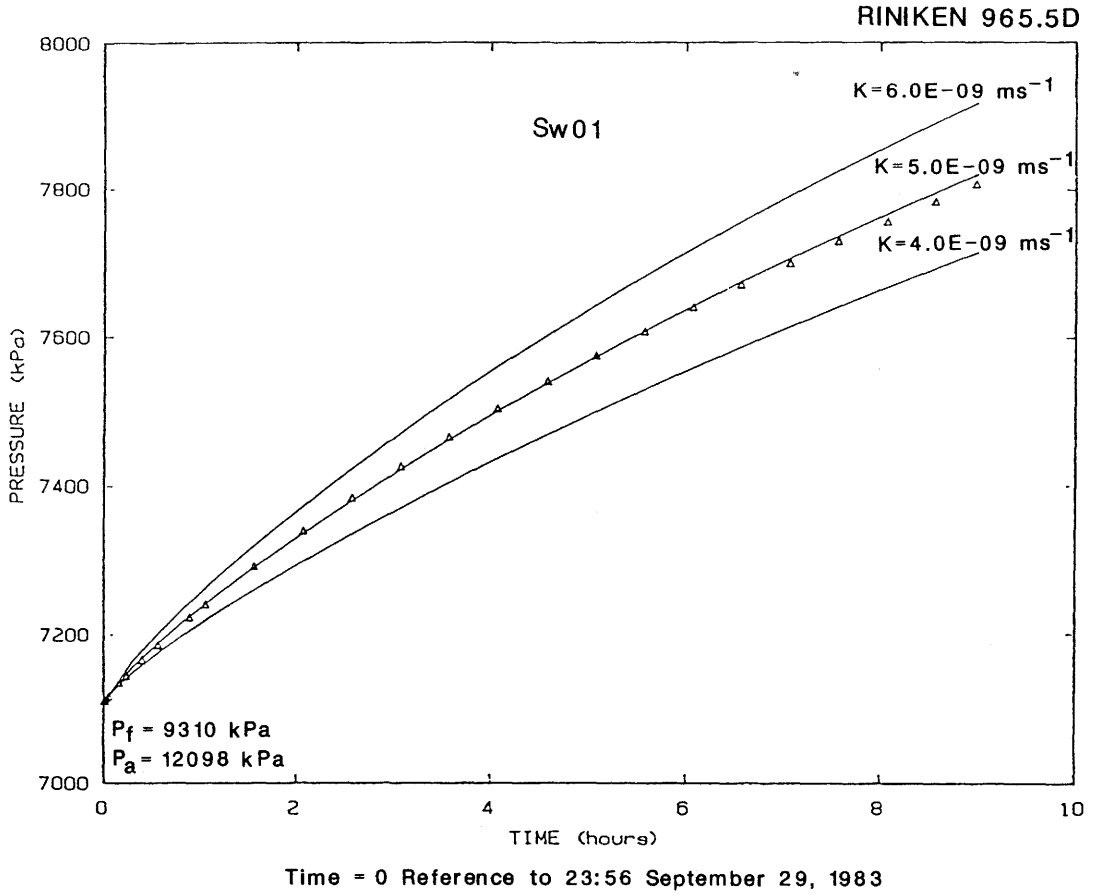

Figure 5.5 Measured (Δ) and Simulated Pressure Response for Test Sw01 of 965.5D

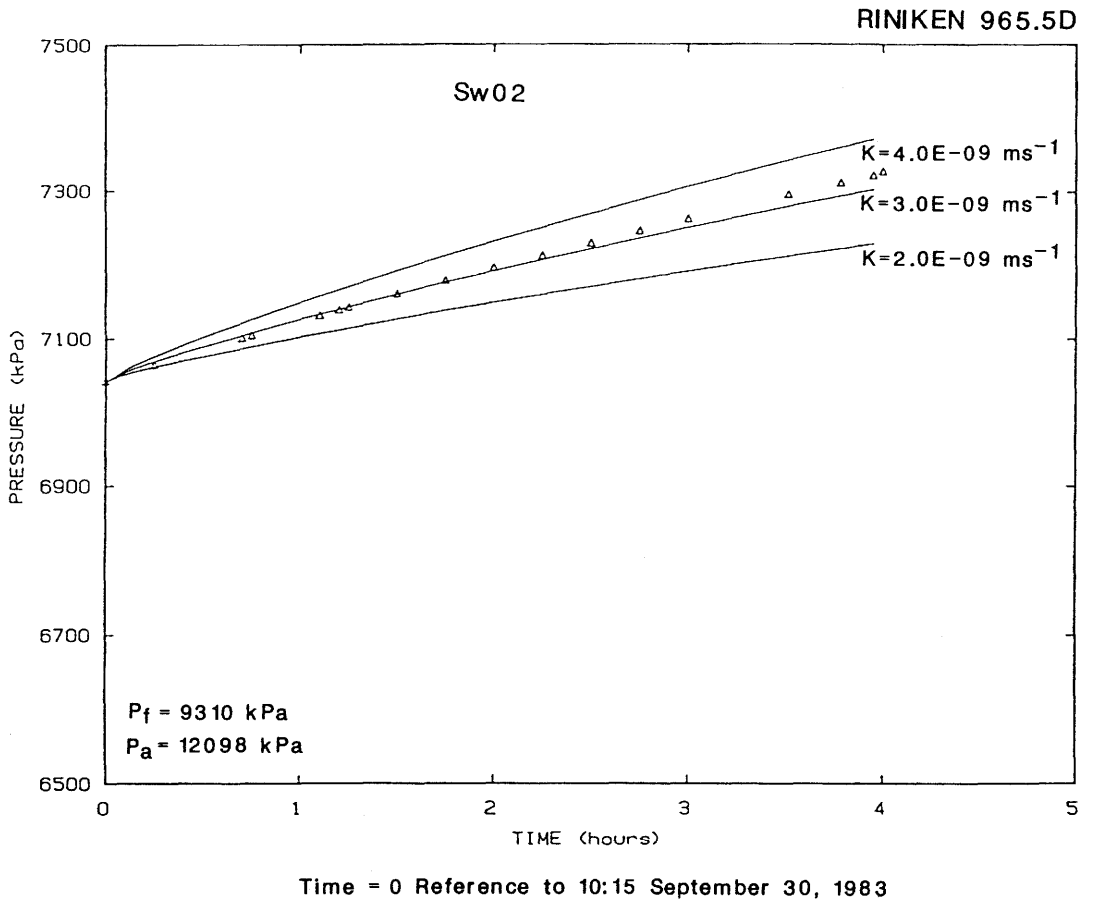

Figure 5.6 Measured (Δ) and Simulated Pressure Response for Test Sw02 of 965.5D

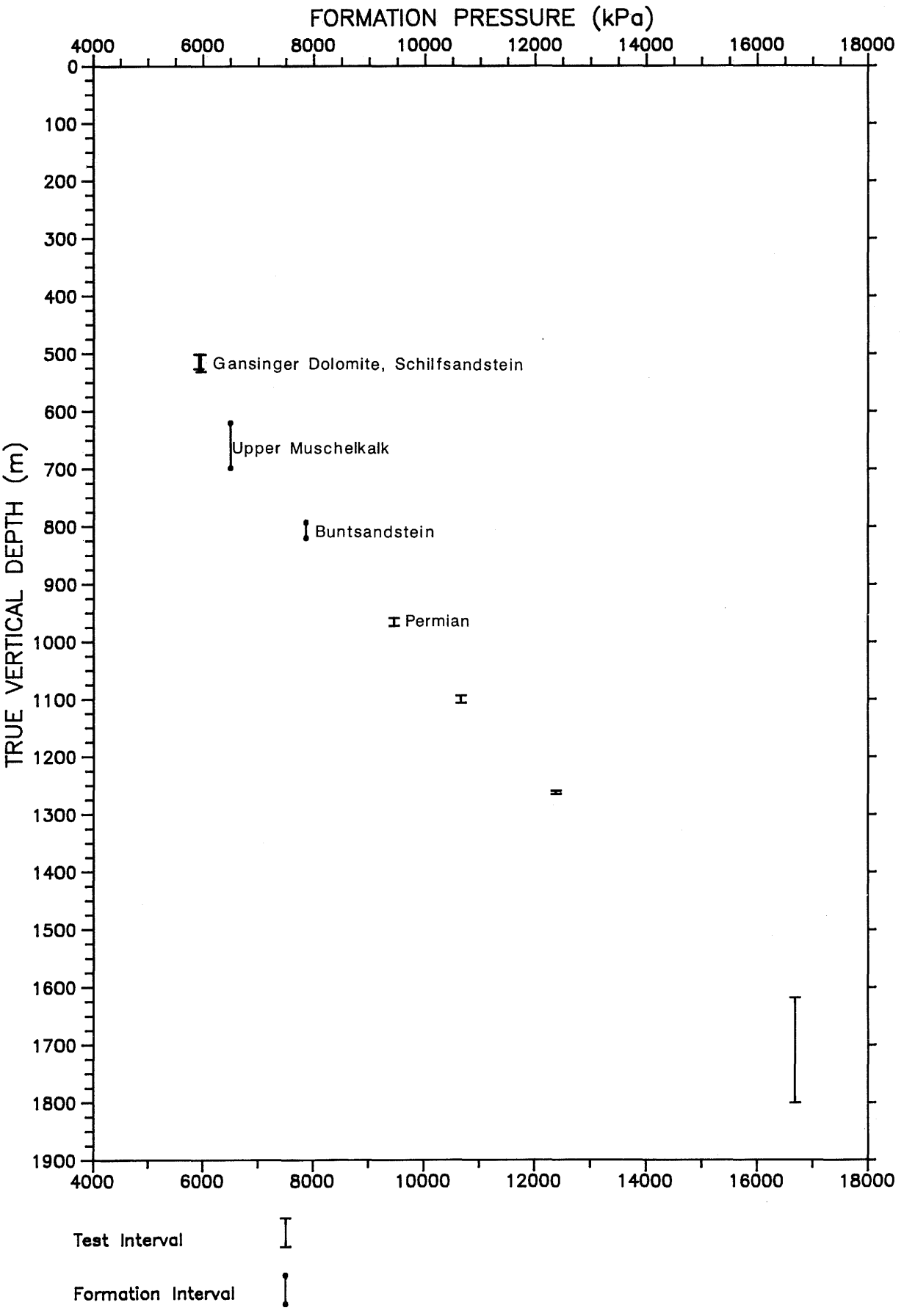

Figure 6.1 Estimated Formation Pressures from Hydraulic Testing at the Riniken Borehole

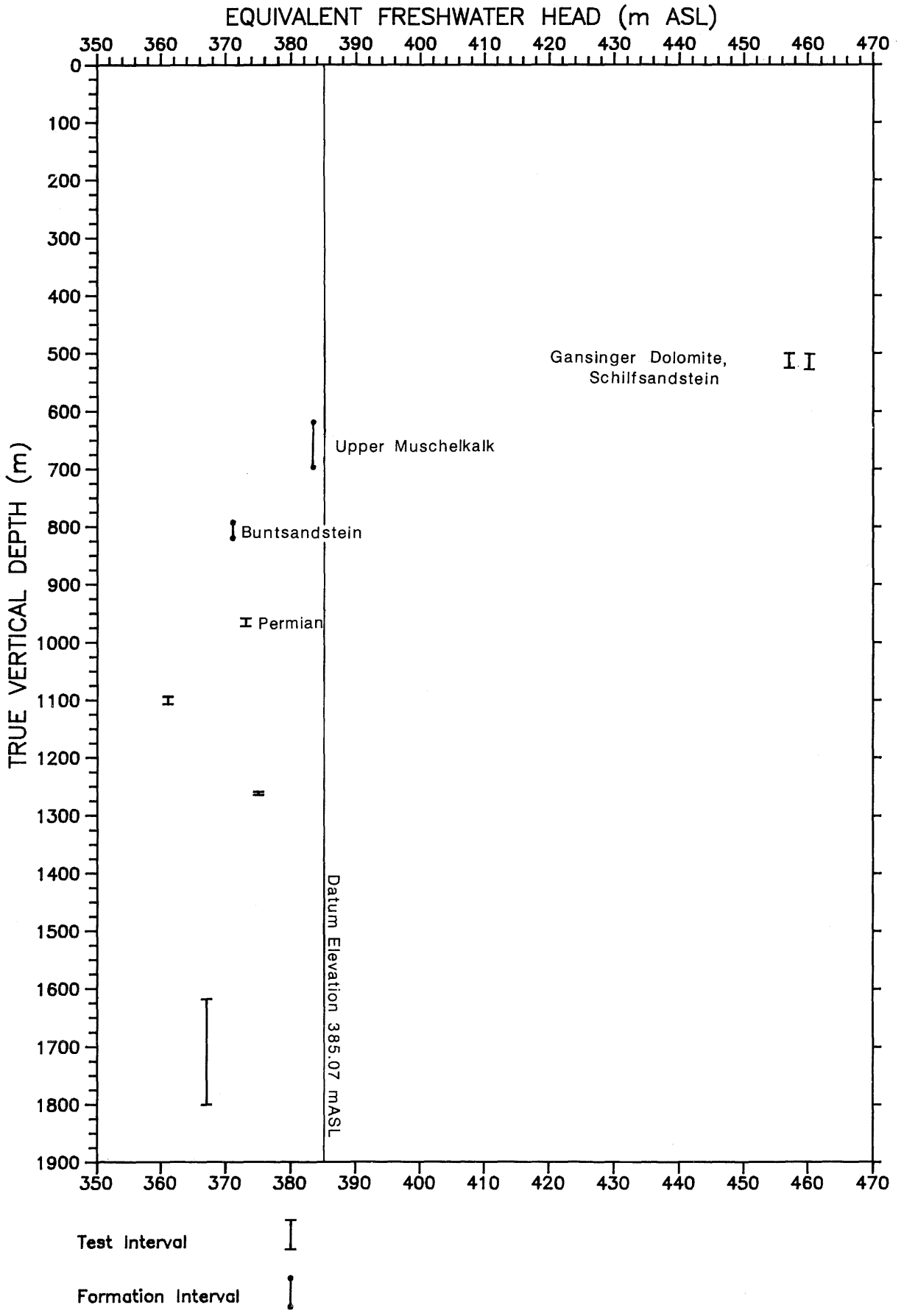

Figure 6.2 Estimated Equivalent Freshwater Heads from Hydraulic Testing at the Riniken Borehole

Test Type and Designation: **Double packer 513.0D**

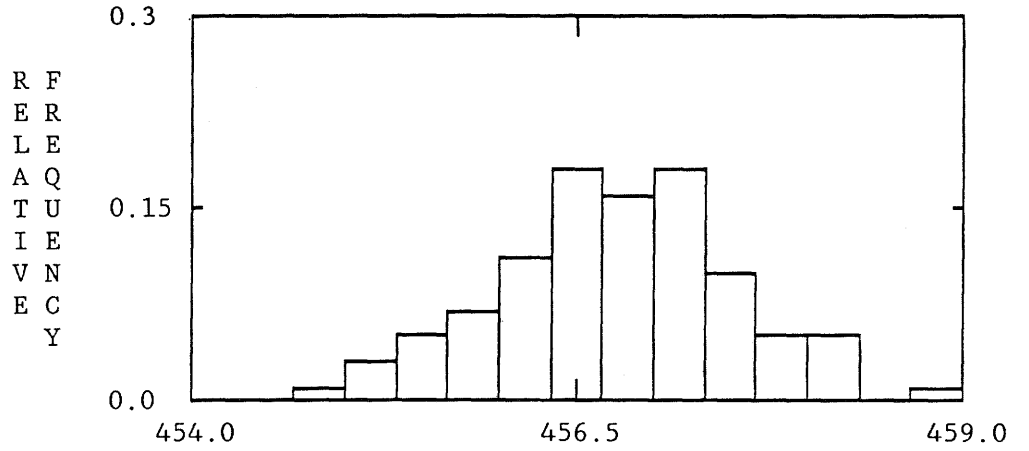

Sample Mean: μ = 456.7 (m ASL)
Sample Standard Deviation: σ = 0.77 (m ASL)
3σ = 2.30 (m ASL)
Width of Each Bin: 0.333 (m ASL)

VARIABLE RANGES

INPUT VARIABLES	MINIMUM	MAXIMUM
Elevation at Surface (m ASL)	384.99	385.17
Average Rock Density (g/cm^3)	2.03	2.54
Depth to Interval Center (m)	512.74	513.26
Pressure at P2 Transducer (kPa)	5647.4	5686.4
Fluid Density of Interval (g/cm^3)	0.995	0.996
OUTPUT VARIABLES		
Equivalent Freshwater Head (m ASL)	454.9	458.8
Pressure at Interval Center (kPa)	5816.9	5856.0
Gravitational Acceleration (cm/s^2)	980.817	980.828

PARTIAL RANK CORRELATIONS

VARIABLE	CORRELATION
Pressure at P2 Transducer	1.00
Depth to Interval Center	-0.93
Elevation at Surface	0.35
Fluid Density of Interval	0.05
Average Rock Density	-0.01

Figure 6.3a Uncertainty of Freshwater Head: Histogram, Statistics, Input, and Correlations

Test Type and Designation: **Single packer 515.7S**

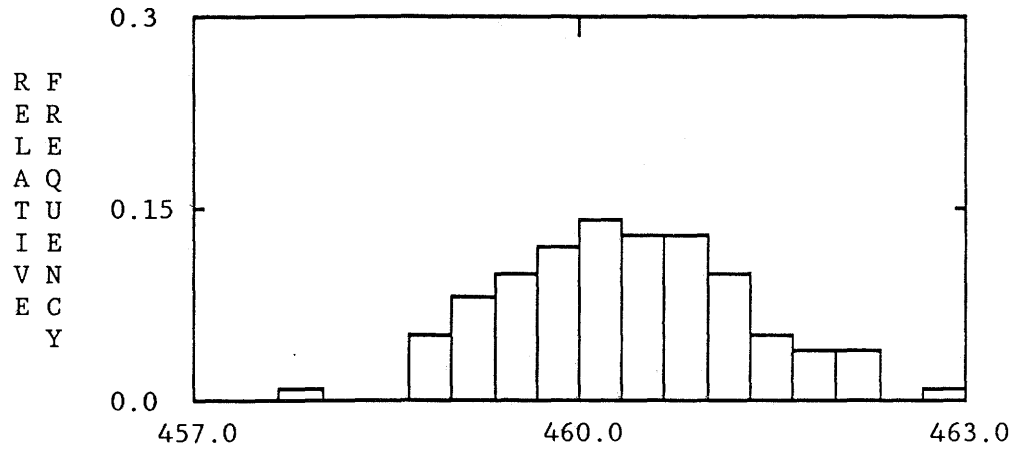

Sample Mean: μ = 460.4 (m ASL)
Sample Standard Deviation: σ = 0.91 (m ASL)
3σ = 2.72 (m ASL)
Width of Each Bin: 0.333 (m ASL)

VARIABLE RANGES

INPUT VARIABLES	MINIMUM	MAXIMUM
Elevation at Surface (m ASL)	384.99	385.17
Average Rock Density (g/cm^3)	2.03	2.54
Depth to Interval Center (m)	515.49	516.01
Pressure at P2 Transducer (kPa)	5669.4	5708.4
Fluid Density of Interval (g/cm^3)	1.017	1.096
OUTPUT VARIABLES		
Equivalent Freshwater Head (m ASL)	458.0	462.9
Pressure at Interval Center (kPa)	5876.0	5925.1
Gravitational Acceleration (cm/s^2)	980.818	980.829

PARTIAL RANK CORRELATIONS

VARIABLE	CORRELATION
Pressure at P2 Transducer	0.98
Fluid Density of Interval	0.95
Depth to Interval Center	-0.72
Elevation at Surface	0.31
Average Rock Density	0.21

Figure 6.3b Uncertainty of Freshwater Head: Histogram, Statistics, Input, and Correlations

Test Type and Designation: Pumping Test 654.4PV

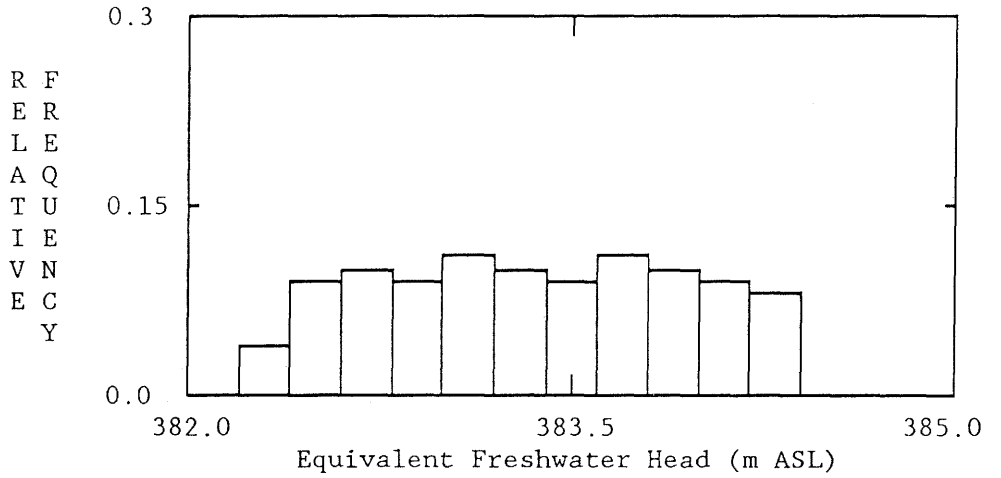

Sample Mean: μ = 383.3 (m ASL)
Sample Standard Deviation: σ = 0.59 (m ASL)
3σ = 1.76 (m ASL)
Width of Each Bin: 0.2 (m ASL)

VARIABLE RANGES

INPUT VARIABLES	MINIMUM	MAXIMUM
Elevation at Surface (m ASL)	384.98	385.15
Average Rock Density (g/cm^3)	2.10	2.60
Depth to Interval Center (m)	651.17	651.83
Fluid Density of Interval (g/cm^3)	1.006	1.009
OUTPUT VARIABLES		
Equivalent Freshwater Head (m ASL)	382.3	384.3
Pressure at Interval Center (kPa)	6464.8	6486.9
Gravitational Acceleration (cm/s^2)	980.844	980.857

PARTIAL RANK CORRELATIONS

VARIABLE	CORRELATION
Fluid Density of Interval	1.00
Elevation at Surface	0.85
Average Rock Density	-0.08
Depth to Interval Center	0.02

Figure 6.3c Uncertainty of Freshwater Head: Histogram, Statistics, Input, and Correlations

Test Type and Designation: **Single packer 805.8S**

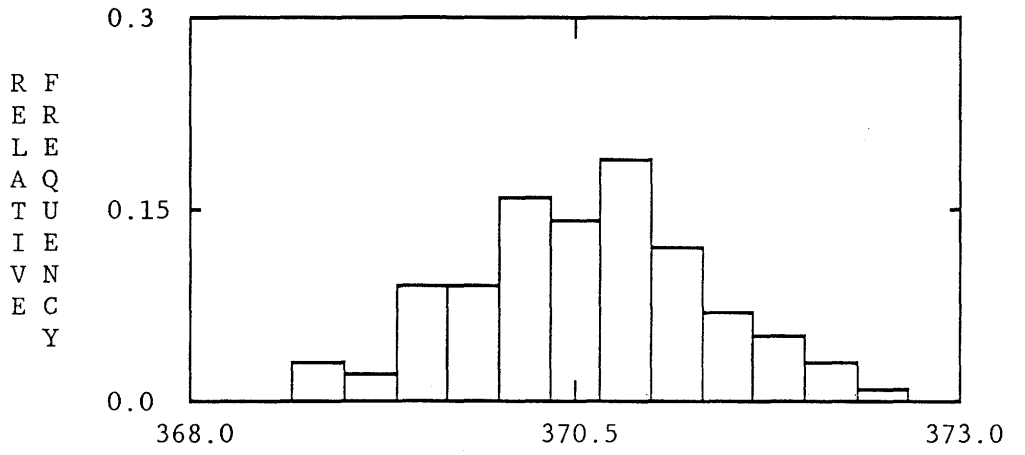

Sample Mean: μ = 370.6 (m ASL)
Sample Standard Deviation: σ = 0.79 (m ASL)
3σ = 2.37 (m ASL)
Width of Each Bin: 0.333 (m ASL)

VARIABLE RANGES

INPUT VARIABLES	MINIMUM	MAXIMUM
Elevation at Surface (m ASL)	384.99	385.17
Average Rock Density (g/cm^3)	2.24	2.66
Depth to Interval Center (m)	804.65	805.45
Pressure at P2 Transducer (kPa)	7648.4	7687.4
Fluid Density of Interval (g/cm^3)	0.992	1.000
OUTPUT VARIABLES		
Equivalent Freshwater Head (m ASL)	368.7	372.6
Pressure at Interval Center (kPa)	7838.8	7878.7
Gravitational Acceleration (cm/s^2)	980.872	980.887

PARTIAL RANK CORRELATIONS

VARIABLE	CORRELATION
Pressure at P2 Transducer	0.99
Depth to Interval Center	-0.94
Fluid Density of Interval	0.38
Elevation at Surface	0.31
Average Rock Density	0.08

Figure 6.3d Uncertainty of Freshwater Head: Histogram, Statistics, Input, and Correlations

Test Type and Designation: **Double packer 965.5D**

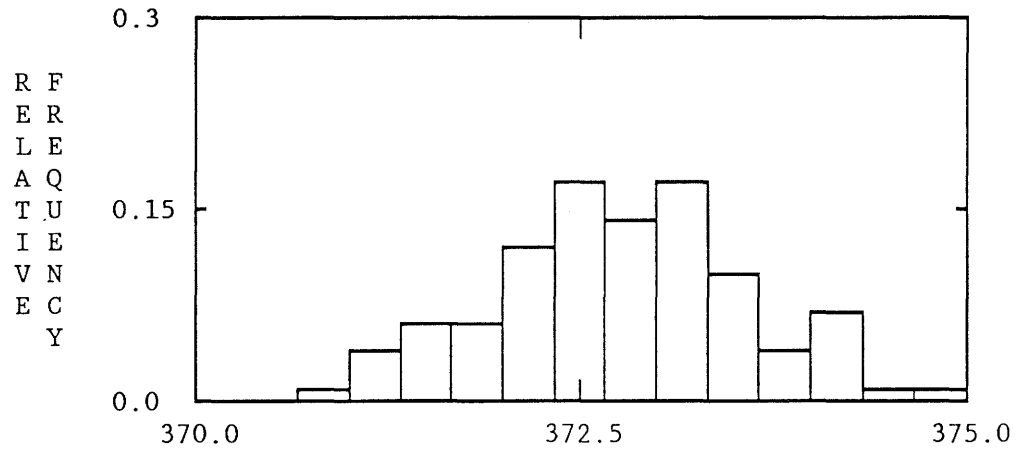

Sample Mean: μ = 372.8 (m ASL)
Sample Standard Deviation: σ = 0.82 (m ASL)
3σ = 2.47 (m ASL)
Width of Each Bin: 0.333 (m ASL)

VARIABLE RANGES

INPUT VARIABLES	MINIMUM	MAXIMUM
Elevation at Surface (m ASL)	384.99	385.17
Average Rock Density (g/cm^3)	2.26	2.66
Depth to Interval Center (m)	964.87	965.83
Pressure at P2 Transducer (kPa)	9292.4	9331.4
Fluid Density of Interval (g/cm^3)	1.202	1.251
OUTPUT VARIABLES		
Equivalent Freshwater Head (m ASL)	370.7	374.9
Pressure at Interval Center (kPa)	9432.0	9474.6
Gravitational Acceleration (cm/s^2)	980.904	980.920

PARTIAL RANK CORRELATIONS

VARIABLE	CORRELATION
Pressure at P2 Transducer	0.99
Depth to Interval Center	-0.93
Fluid Density of Interval	0.82
Elevation at Surface	0.23
Average Rock Density	0.16

Figure 6.3e Uncertainty of Freshwater Head: Histogram, Statistics, Input, and Correlations

Test Type and Designation: **Single packer 1100.2S**

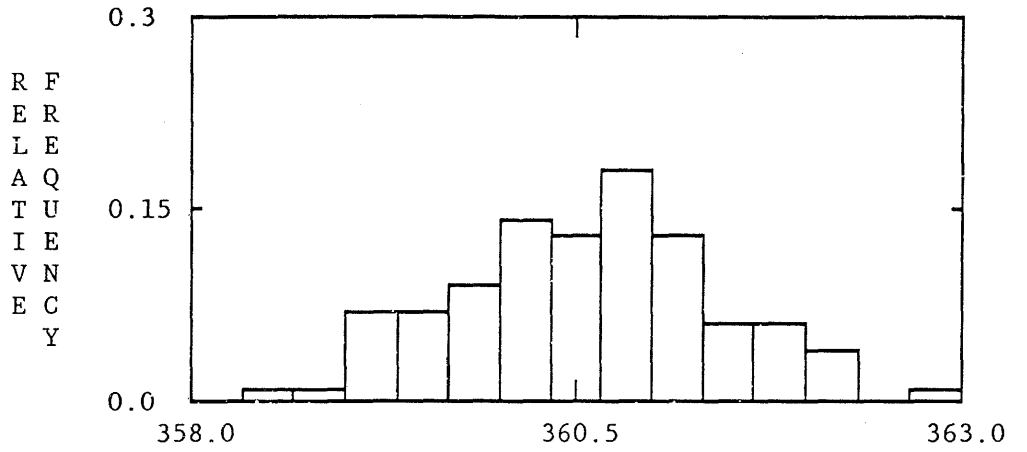

Sample Mean: μ = 360.6 (m ASL)
Sample Standard Deviation: σ = 0.84 (m ASL)
3σ = 2.53 (m ASL)
Width of Each Bin: 0.333 (m ASL)

VARIABLE RANGES

INPUT VARIABLES	MINIMUM	MAXIMUM
Elevation at Surface (m ASL)	384.99	385.17
Average Rock Density (g/cm^3)	2.27	2.67
Depth to Interval Center (m)	1099.40	1100.50
Pressure at P2 Transducer (kPa)	10507.4	10546.4
Fluid Density of Interval (g/cm^3)	1.120	1.179
OUTPUT VARIABLES		
Equivalent Freshwater Head (m ASL)	358.5	362.8
Pressure at Interval Center (kPa)	10632.7	10675.9
Gravitational Acceleration (cm/s^2)	980.930	980.949

PARTIAL RANK CORRELATIONS

VARIABLE	CORRELATION
Pressure at P2 Transducer	0.99
Depth to Interval Center	-0.94
Fluid Density of Interval	0.83
Elevation at Surface	0.23
Average Rock Density	0.19

Figure 6.3f Uncertainty of Freshwater Head: Histogram, Statistics, Input, and Correlations

Test Type and Designation: **Double packer 1262.2D**

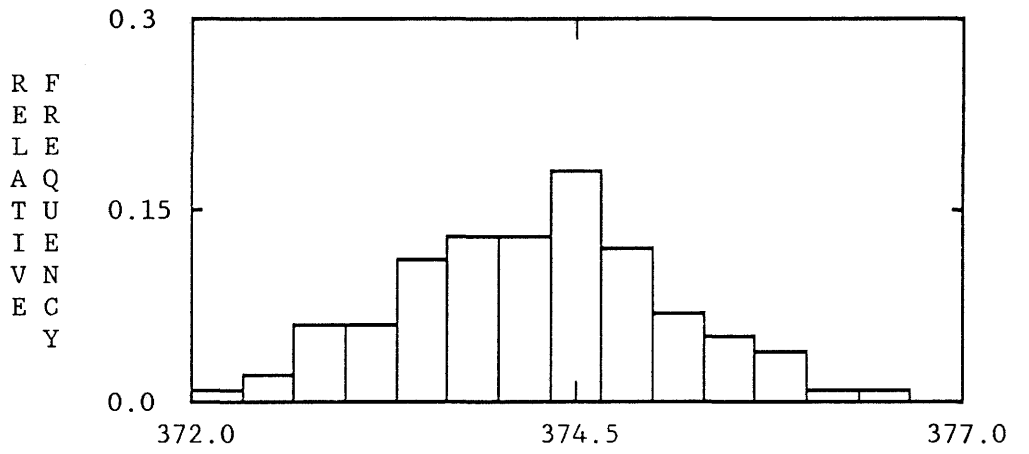

Sample Mean: μ = 374.3 (m ASL)
Sample Standard Deviation: σ = 0.86 (m ASL)
3σ = 2.57 (m ASL)
Width of Each Bin: 0.333 (m ASL)

VARIABLE RANGES

INPUT VARIABLES	MINIMUM	MAXIMUM
Elevation at Surface (m ASL)	384.99	385.17
Average Rock Density (g/cm^3)	2.27	2.67
Depth to Interval Center (m)	1261.37	1262.63
Pressure at P2 Transducer (kPa)	12282.4	12321.4
Fluid Density of Interval (g/cm^3)	1.007	1.086
OUTPUT VARIABLES		
Equivalent Freshwater Head (m ASL)	372.2	376.4
Pressure at Interval Center (kPa)	12357.7	12400.3
Gravitational Acceleration (cm/s^2)	980.962	980.983

PARTIAL RANK CORRELATIONS

VARIABLE	CORRELATION
Pressure at P2 Transducer	0.98
Depth to Interval Center	-0.95
Fluid Density of Interval	0.79
Elevation at Surface	0.24
Average Rock Density	0.15

Figure 6.3g Uncertainty of Freshwater Head: Histogram, Statistics, Input, and Correlations

Test Type and Designation: **Bottom hole 1709.2D**

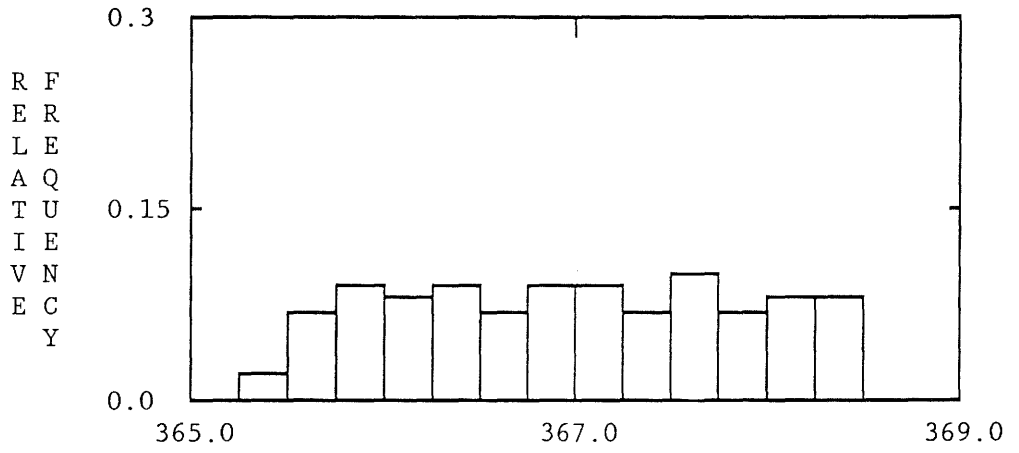

Sample Mean: μ = 367.0 (m ASL)
Sample Standard Deviation: σ = 0.89 (m ASL)
3σ = 2.68 (m ASL)
Width of Each Bin: 0.25 (m ASL)

VARIABLE RANGES

INPUT VARIABLES	MINIMUM	MAXIMUM
Elevation at Surface (m ASL)	384.98	385.15
Average Rock Density (g/cm^3)	2.24	2.66
Depth to Interval Center (m)	1708.08	1709.76
Fluid Density of Interval (g/cm^3)	0.989	0.991
OUTPUT VARIABLES		
Equivalent Freshwater Head (m ASL)	365.4	368.5
Pressure at Interval Center (kPa)	16671.4	16709.9
Gravitational Acceleration (cm/s^2)	981.050	981.081

PARTIAL RANK CORRELATIONS

VARIABLE	CORRELATION
Fluid Density of Interval	1.00
Elevation at Surface	0.72
Depth to Interval Center	-0.28
Average Rock Density	0.01

Figure 6.3h Uncertainty of Freshwater Head: Histogram, Statistics, Input, and Correlations

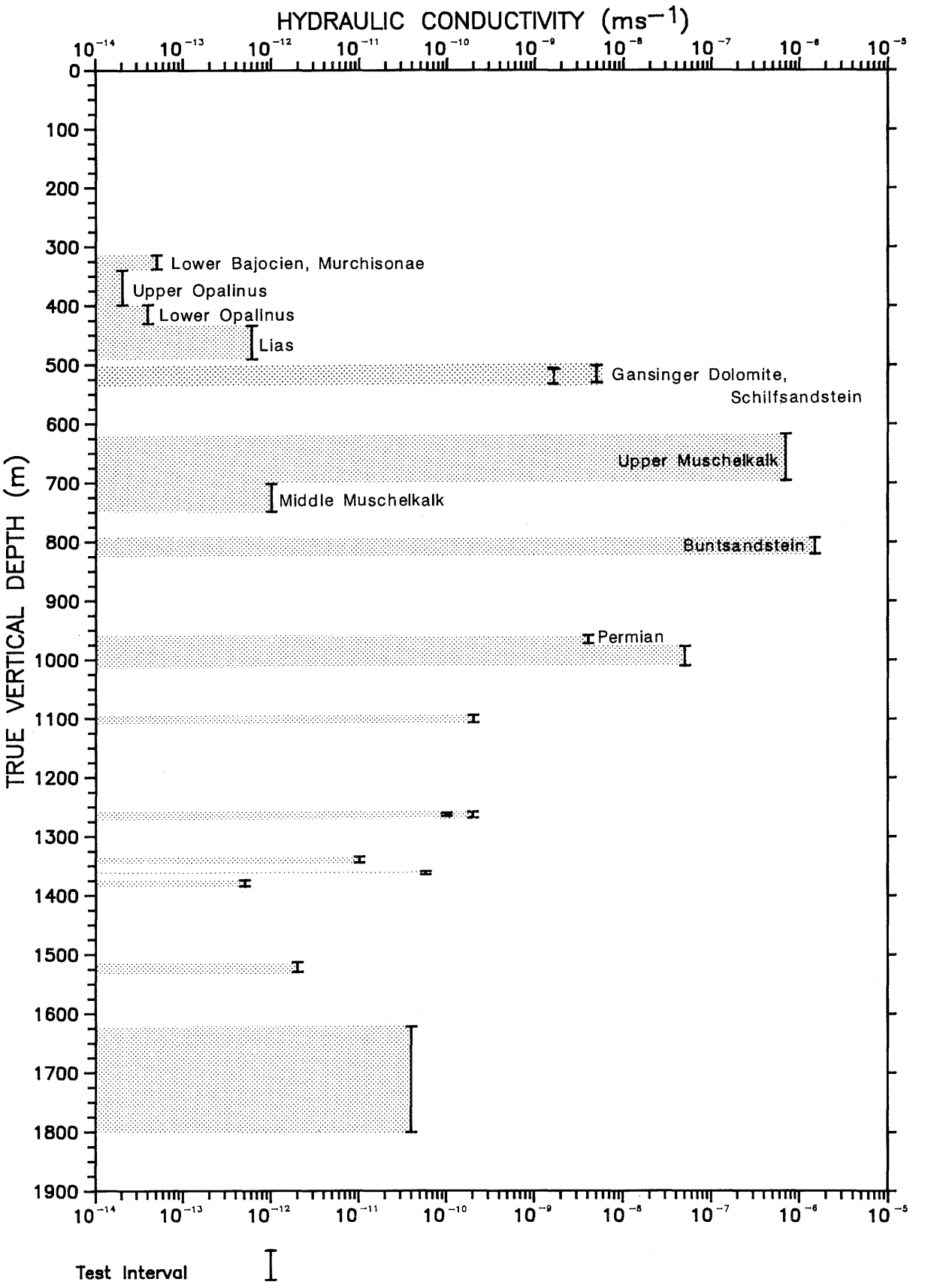

Figure 6.4 Estimated Hydraulic Conductivities from Hydraulic Testing at the Riniken Borehole

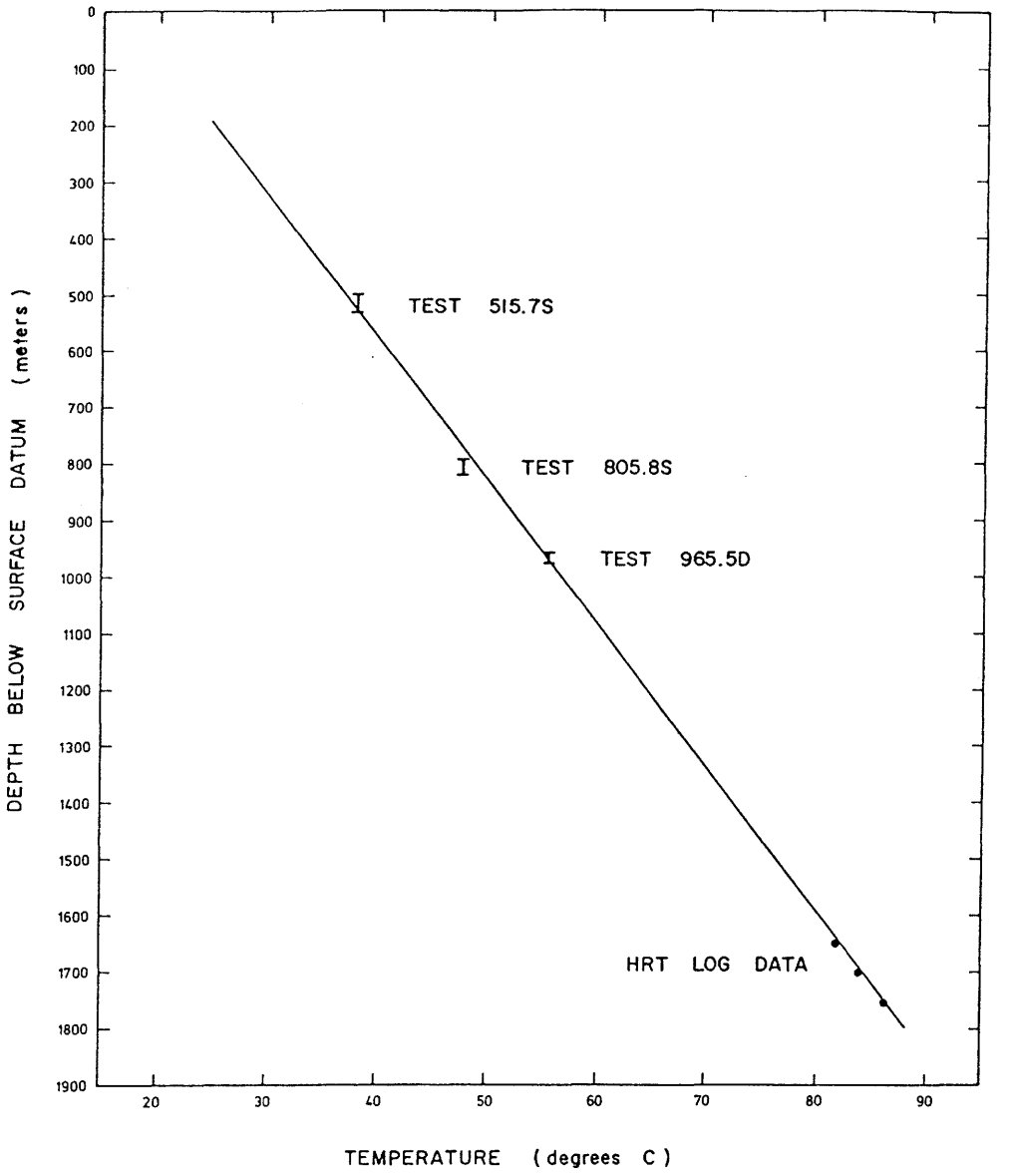

Figure 6.5 Representative Formation Temperatures for Riniken Borehole Obtained From Hydraulic Tests 515.7S, 805.8S and 965.5D and From a High-Resolution Thermometer (HRT) Log Below 1650 m Depth

FRESHWATER DENSITIES IN kgm^{-3} AT
TEMPERATURE (°C) AND PRESSURE (atm)

TEMP. / PRESS	0.	10.	20.	30.	40.	50.
1.	999.80	999.50	998.00	995.52	992.16	988.04
25.	1000.90	1000.60	999.10	996.61	993.25	989.12
50.	1002.00	1001.70	1000.20	997.71	994.33	990.30
75.	1003.21	1002.81	1001.30	998.80	995.42	991.38
100.	1004.32	1003.92	1002.41	999.90	996.61	992.46
125.	1005.43	1005.03	1003.51	1001.00	997.61	993.54
150.	1006.54	1006.04	1004.52	1002.00	998.70	994.63
175.	1007.56	1007.15	1005.63	1003.11	999.80	995.72
200.	1008.67	1008.27	1006.64	1004.22	1000.80	996.71
225.	1009.74	1009.29	1007.71	1005.23	1001.85	997.76
250.	1010.82	1010.31	1008.78	1006.24	1002.91	998.80

TEMP. / PRESS	60.	70.	80.	90.	100.
1.	983.28	977.90	971.91	965.44	958.41
25.	984.35	978.95	973.05	966.56	959.60
50.	985.51	980.10	974.18	967.68	960.80
75.	986.58	981.26	975.32	968.90	961.91
100.	987.75	982.32	976.47	970.03	963.11
125.	988.83	983.48	977.52	971.16	964.32
150.	989.90	984.54	978.67	972.29	965.44
175.	990.98	985.61	979.72	973.43	966.56
200.	992.06	986.68	980.87	974.47	967.68
225.	993.10	987.75	981.93	975.56	968.80
250.	994.13	988.83	982.99	976.66	969.93

Table 4.1 Temperature and Pressure Effects on Deionized Fluid Density (Calculated from Data in Dorsey, 1968)

Test Type and Designation: **Single packer 1100.2S**

Geology of test interval: Layered sandstone and breccia

Formation: Permian

Fractures: Core loss was 9 percent. Average 1.3 fractures per meter Fracture orientation varies from 10 to 60 degrees from vertical.

Borehole fluid: Drilling mud

Drilled borehole diameter in test interval: 216 mm

Average borehole diameter from caliper: not applicable

Test interval length 13.10 m

Apparent depth of test interval: 1093.60 m to 1106.70 m

True vertical depth of test interval: 1093.40 m to 1106.50 m

Apparent depth to center of test interval: 1100.15 m

True vertical depth to center of test interval: 1099.95 m

Apparent depth to pressure transducer P2: 1088.84 m

True vertical depth to pressure transducer P2: 1088.64 m

Datum elevation at ground surface: 385.07 m ASL

Barometric pressure: 103 kPa

Inside diameter of tubing string: 100.5 mm

Annulus pressure at transducer P3: 11580 kPa

Packer inflation pressure above annulus pressure: 8000 kPa

Drilling period of test interval (estimate):
03:30, 13 October, 1983 to 12:00, 13 October, 1983

Mid-Point: 07:45, 13 October, 1983

Testing Period: 14:00, 14 October, 1983 to 17:20, 15 October, 1983

Test designations and start times:

Sw01	16:11, 14 October, 1983	Pi01	12:17, 15 October, 1983
Pw01	16:46, 14 October, 1983		
Pw02	22:38, 14 October, 1983		

Time between middle of drilling and start of testing: 1.3 days

Temperature at probe: start of first test: 53.0°C
end of testing: 57.3°C

Table 4.2 Physical Description of the Geology and Testing Conditions at 1100.2S

Test Type and Designation: **Single packer 1100.2S**

Formation		
Compressibility	9.0E-11	Pa^{-1}
Porosity	0.15	
Specific Storage	1.5E-06	m^{-1}
Fluid		
Compressibility (at formation temperature and pressure)	4.34E-10	Pa^{-1}
Density (at formation temperature and pressure)	989	kgm^{-3}
Thermal Expansion Coefficient	4.8E-04	$^oC^{-1}$
Test Interval		
Length	13.1	m
Diameter	0.216	m
Annulus Pressure	11580	kPa
Formation Pressure (calibrated)	10525	kPa
Formation Pressure (assumed)	not applicable	
Conditions of Analysis		
Borehole Pre-Test Pressure History	yes	
Thermal Effects	yes	

Table 4.3 Parameters Used for Simulation of the Test Interval Pressure Response at 1100.2S

Test Type and Designation: **Double packer 965.5D**

Geology of test interval: Brecciated sandstone and siltstone

Formation: Permian

Fractures: Approximately 25 percent core loss. Mineral infilling was not observed in the one mapped fracture.

Borehole fluid: Drilling mud

Drilled borehole diameter in test interval: 216 mm

Average borehole diameter from caliper: not applicable

Test interval length 14.10 m

Apparent depth of test interval: 958.40 m to 972.50 m

True vertical depth of test interval: 958.30 m to 972.40 m

Apparent depth to center of test interval: 965.45 m

True vertical depth to center of test interval: 965.35 m

Apparent depth to pressure transducer P2: 953.69 m

True vertical depth to pressure transducer P2: 953.59 m

Datum elevation at ground surface: 385.07 m ASL

Barometric pressure: 103 kPa

Inside diameter of tubing string: 100.5 mm

Annulus pressure at transducer P3: 12098 kPa

Packer inflation pressure above annulus pressure: 6000 kPa

Drilling period of test interval (estimate):

02:00, 27 September, 1983 to 00:00, 28 September, 1983

Mid-Point: 13:00, 27 September, 1983

Testing Period: 07:38, 29 September, 1983 to 16:47, 05 October, 1983

Test designations and start times:

DST01 09:57, 29 September, 1983 Sw01 23:56, 29 September, 1983

DST02 15:13, 29 September, 1983 Sw02 09:35, 30 September, 1983

Pw01 21:53, 29 September, 1983

Time between middle of drilling and start of testing: 1.8 days

Temperature at probe: start of first test: 48.8°C

end of testing: 55.4°C

Table 5.1 Physical Description of the Geology and Testing Conditions for Test 965.5D

Test Type and Designation: **Double packer 965.5D**

Formation		
Compressibility	9.0E-11	Pa^{-1}
Porosity	0.15	
Specific Storage	1.5E-06	m^{-1}
Fluid		
Compressibility (at formation temperature and pressure)	4.3E-10	Pa^{-1}
Density (at formation temperature and pressure)	990	kgm^{-3}
Thermal Expansion Coefficient	not applicable	
Test Interval		
Length	14.1	m
Diameter	0.216	m
Annulus Pressure	12098	kPa
Formation Pressure (Horner plot)	9310	kPa
Formation Pressure (assumed)	not applicable	
Conditions of Analysis		
Borehole Pre-Test Pressure History	yes	
Thermal Effects	no	

Table 5.2 Parameters Used for Simulation of the Test Interval Pressure Response for Test 965.5D

Test Type and Designation: Double packer 965.5D

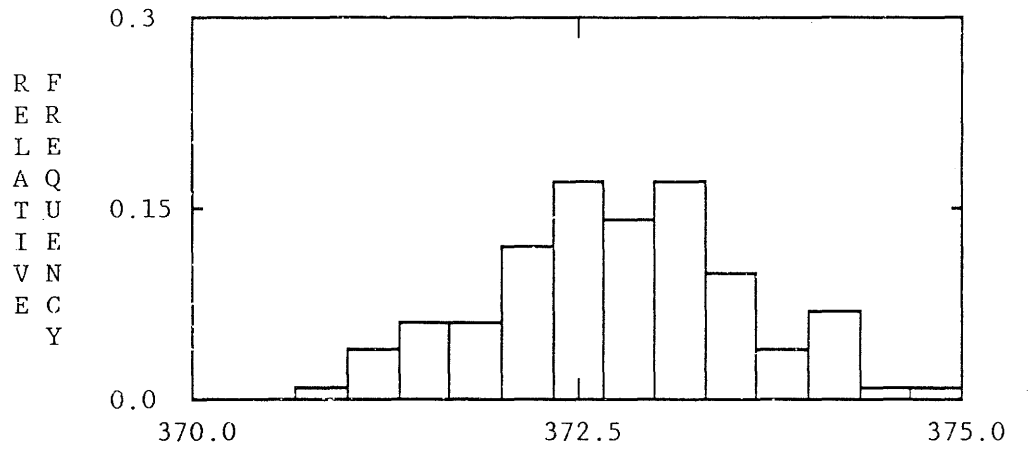

Sample Mean: μ = 372.8 (m ASL)
Sample Standard Deviation: σ = 0.82 (m ASL)
3σ = 2.47 (m ASL)
Width of Each Bin: 0.333 (m ASL)

VARIABLE RANGES

INPUT VARIABLES	MINIMUM	MAXIMUM
Elevation at Surface (m ASL)	384.99	385.17
Average Rock Density (g/cm^3)	2.26	2.66
Depth to Interval Center (m)	964.87	965.83
Pressure at P2 Transducer (kPa)	9292.4	9331.4
Fluid Density of Interval (g/cm^3)	1.202	1.251
OUTPUT VARIABLES		
Equivalent Freshwater Head (m ASL)	370.7	374.9
Pressure at Interval Center (kPa)	9432.0	9474.6
Gravitational Acceleration (cm/s^2)	980.904	980.920

PARTIAL RANK CORRELATIONS

VARIABLE	CORRELATION
Pressure at P2 Transducer	0.99
Depth to Interval Center	-0.93
Fluid Density of Interval	0.82
Elevation at Surface	0.23
Average Rock Density	0.16

Table 5.3 Uncertainty in Freshwater Head for Test 965.5D: Histogram, Statistics, Input, and Correlations

Table 6.1 Summary of Formation Pressures and Equivalent Freshwater Heads Determined From Hydraulic Testing in the Riniken Borehole

TEST DESIGNATION	STRATIGRAPHY	TRUE INTERVAL CENTER DEPTH (m)	FORMATION PRESSURE AT CENTER OF INTERVAL (kPa)	EQUIVALENT FRESHWATER HEAD (m ASL)	ESTIMATED HYDRAULIC CONDUCTIVITY (ms^{-1})	LENGTH OF BOREHOLE HISTORY PERIOD (Days)
513.0D	Gansinger Dolomite, Schilfsandstein	513.00	5835	457	1.4E-09	0.5*
515.7S	Gansinger Dolomite, Schilfsandstein	515.75	5899**	460	5.0E-09	0.7
654.4PV	Upper Muschelkalk	656.65	6476**	383	7.0E-07	10.0
805.8S	Buntsandstein	806.50	7857**	371	1.5E-06	1.0
965.5D	Permian	965.35	9451	373	4.0E-09	1.8
1100.2S	Permian	1099.95	10653	361	2.0E-10	1.3
1262.2D	Permian	1262.00	12377	375	1.0E-10	27.9
1709.2D	Permian	1708.92	16683	367	N.R.	21.0

* Length of time since casing perforation at interval depth.

** Interpreted formation pressure and corresponding depth are reported for the center of the formation (not center of the interval).

N.R. Determination of a representative value from this test is no

Table 6.2 Summary of Hydraulic Conductivities, Specific Storage, and Temperatures Determined From Hydraulic Testing in the Riniken Borehole

TEST DESIGNATION	TRUE INTERVAL TOP DEPTH (m)	TRUE INTERVAL BOTTOM DEPTH (m)	APPARENT INTERVAL TOP DEPTH (m)	APPARENT INTERVAL BOTTOM DEPTH (m)	INTERVAL LENGTH (m)	ESTIMATED HYDRAULIC CONDUCTIVITY (ms^{-1})	ESTIMATED SPECIFIC STORAGE (m^{-1})	TEMPERATURE AT END OF TESTING (deg. C)
234.0D	217.11	250.89	217.11	250.89	33.78	$\leq$1.0E-12	5.0E-07	22.1
325.4D	313.41	337.28	313.41	337.28	23.87	5.0E-14	4.4E-07	25.4
368.2S	338.65	397.70	338.65	397.70	59.05	2.0E-14	2.2E-06	26.6
413.9S	397.70	430.10	397.70	430.10	32.40	4.0E-14	2.2E-06	29.6
461.8S	433.42	490.20	433.42	490.20	56.78	6.0E-13	7.4E-07	32.6
513.0D	500.30	525.78	500.30	525.78	9.00*	1.4E-09	9.4E-06	37.5
515.7S	500.99	530.50	500.99	530.50	29.51	5.0E-09	1.2E-06	37.5
654.4PV	617.30	696.00	617.30	696.00	78.70	7.0E-07	N/A	--
725.0S	701.50	748.40	701.50	748.50	47.00	$\leq$1.0E-12	3.2E-07	42.9
805.8S	792.90	820.10	793.00	820.20	27.20	1.5E-06	1.5E-06	47.5
965.5D	958.30	972.40	958.40	972.50	14.10	4.0E-09	1.5E-06	55.4
993.5D	976.80	1009.75	977.00	1009.95	32.95	$\geq$5.0E-08	N/A	--
1100.2S	1093.40	1106.50	1093.60	1106.70	13.10	2.0E-10	1.5E-06	57.3
1252.7D	1247.40	1257.58	1247.60	1257.78	10.18	--	unsuccessful test	--

Table 6.2 Summary of Hydraulic Conductivities, Specific Storage, and Temperatures Determined From Hydraulic Testing in the Riniken Borehole

TEST DESIGNATION	TRUE INTERVAL TOP DEPTH (m)	TRUE INTERVAL BOTTOM DEPTH (m)	APPARENT INTERVAL TOP DEPTH (m)	APPARENT INTERVAL BOTTOM DEPTH (m)	INTERVAL LENGTH (m)	ESTIMATED HYDRAULIC CONDUCTIVITY (ms^{-1})	ESTIMATED SPECIFIC STORAGE (m^{-1})	TEMPERATURE AT END OF TESTING (deg. C)
1262.2D	1259.19	1264.80	1259.39	1265.00	5.61	1.0E-10	1.5E-06	63.2
1262.9D	1257.62	1267.80	1257.82	1268.00	10.18	2.0E-10	2.1E-06	57.2
1339.1D	1333.80	1343.98	1334.00	1344.18	10.18	1.0E-11	1.5E-06	58.3
1358.9D	1349.45	1360.70	1349.65	1360.90	3.90*	<6.0E-11	8.3E-06	69.1
1378.9D	1373.62	1383.80	1373.82	1384.00	10.18	5.0E-13	1.5E-06	58.9
1389.1D	1383.80	1393.98	1384.00	1394.18	10.18	≤1.0E-12	1.5E-06	57.3
1520.9D	1512.52	1528.80	1512.72	1529.00	16.28	2.0E-12	1.5E-06	62.7
1709.2D	1617.80	1800.30	1618.00	1800.50	182.50	N.R.	N/A	--
1711.2P	1621.75	1800.30	1621.95	1800.50	178.55	<4.0E-11	1.5E-06	38.0

N.R. Determination of a representative value for this test is not possible.

* Perforated length.

N/A Not applicable to interpretation method.

-- Not measured during testing.